Mean systemic filling pressure

From Guyton to the ICU, and back again

Per Werner Möller

Department of Anaesthesiology and Intensive Care Medicine
Institute of Clinical Sciences
Sahlgrenska Academy, University of Gothenburg

UNIVERSITY OF GOTHENBURG

Gothenburg 2019

Cover illustration: Gunilla Möller

Mean systemic filling pressure – From Guyton to the ICU, and back again

per.moller@vgregion.se

ISBN 978-91-7833-231-1 (PRINT)
ISBN 978-91-7833-232-8 (PDF)
http://hdl.handle.net/2077/57739

Printed in Gothenburg, Sweden 2019, by BrandFactory

To my extended family

Mean systemic filling pressure

From Guyton to the ICU, and back again

Per Werner Möller

Department of Anaesthesiology and Intensive Care Medicine

Institute of Clinical Sciences
Sahlgrenska Academy, University of Gothenburg
Gothenburg, Sweden

ABSTRACT

Introduction: Mean systemic filling pressure (MSFP) is the equilibrated vascular pressure at zero flow. Venous return (VR) driving pressure (VRdP) is the difference between MSFP and right atrial pressure (RAP). In clinical research, MSFP can be estimated: $MSFP_{insp\_hold}$ is the zero-flow extrapolation of RAP-cardiac output data-pairs from inspiratory hold maneuvers; $MSFP_a$ is a dynamic analogue computed from clinically available hemodynamics. However, results are controversial and fundamental concepts of VR physiology are questioned. We aimed to test experimentally the concept of VRdP in dynamic conditions and validate estimates of MSFP against zero-flow measurements.

Methods: We compared estimates of MSFP against zero-flow measurements from right atrial balloon occlusion ($MSFP_{RAO}$), or from intermittently paused venoarterial extracorporeal membrane oxygenation (ECMO), in three porcine models exposed to changing blood volumes and vasoconstriction.

Results: Changes in RAP resulted in immediate and directionally opposite changes in VR. Temporary VR and ECMO flow imbalance resulted in dynamically changing VRdP and RAP. In euvolemia, MSFP was increased by increased airway pressure. A moderate increase in positive end-expiratory pressure increased RAP, $MSFP_{RAO}$ and VRdP. Resistance to VR did not change. Changing blood volume led to concordant changes in RAP, $MSFP_{RAO}$, VRdP and flow. Vasoconstriction and volume expansion increased MSFP and maximum achievable ECMO flow with similar effects on oxygen delivery. $MSFP_{insp\_hold}$ overestimated $MSFP_{RAO}$ in euvolemia due to flow restoration predominantly occurring in the inferior vena cava. Methods for MSFP estimation had an accuracy that was dependent on volume status. All methods

tracked changes in the reference method concordantly. However, with the possible exception of $MSFP_a$, the bias was clinically unacceptable.

Conclusion: If pressure effects from volume shifts are accounted for, the concept of VRdP is valid also during dynamic conditions. VR physiology can explain the responses of volume expansion and vasoconstriction on venoarterial ECMO flow. Inspiratory hold maneuvers are unsuitable for the estimation of MSFP due to clinically significant bias.

Keywords: mean systemic filling pressure, venous return, right atrial pressure, positive pressure ventilation, extracorporeal membrane oxygenation

ISBN 978-91-7833-231-1 (PRINT)
ISBN 978-91-7833-232-8 (PDF)

SAMMANFATTNING PÅ SVENSKA

Om kroppens blodflöde plötsligt upphör sker en tryckutjämning mellan artär- och venbäddar och det systemiska medelfyllnadstrycket (MSFP) kan uppmätas. Detta tryck är oberoende av hjärtats aktivitet och bestäms helt av blodvolymen, kärlbäddarnas storlek och deras elasticitet. MSFP är därmed ett uttryck för cirkulationssystemets volym-status. Venöst återflöde (VR) drivs av tryckskillnaden (VRdP) mellan MSFP och höger förmakstryck (RAP). I klinisk forskning kan MSFP uppskattas genom att man i samband med inblåsningsmanövrar hos respiratorbehandlade patienter registrerar de förändringar i RAP och VR som uppstår när trycket i bröstkorgen tillfälligt ändras. Man kan då beräkna MSFP genom att extrapolera det linjära sambandet till flöde noll. En annan metod baseras på matematisk modellering av kretsloppet och beräknar en analog till MSFP utifrån uppmätt RAP, medelartärtryck och blodflöde. Resultaten från kliniska studier är dock inbördes motsägelsefulla och det råder också sedan lång tid oenighet kring helt grundläggande koncept som rör fysiologin för venöst återflöde. Vårt mål har varit att pröva konceptet med drivtryck för venöst återflöde (VRdP) experimentellt och att utvärdera kliniskt användbara metoder för uppskattning av MSFP mot mätningar gjorda med referensmetoder vid nollflöde. Vi har genomfört tre försöksserier på gris, under skiftande blodvolym och under behandling med kärlsammandragande läkemedel och vätskeinfusion, där dessa referensmätningar kunnat göras då cirkulationen tillfälligt stoppats genom ballongocklusion av höger förmak eller genom korta pauser i behandling med hjärtlungmaskin (ECMO).

Vi har kunnat visa att förändringar av höger förmakstryck leder till omedelbara men kortvariga förändringar i motsatt riktning av venöst återflöde. Tillfällig obalans mellan venöst återflöde och ECMO-flöde förflyttar blodvolym mellan områden belägna uppströms och nedströms vilket ger dynamiska förändringar av både drivtrycket för venöst återflöde och höger förmakstryck. Vi kunde också visa att MSFP ökar med ökat luftvägstryck – åtminstone vid normal blodvolym. Ökning av respiratorns slut-expiratoriska tryck (PEEP; används kliniskt för att öka den luftförande delen av lungan) gav en ökning i RAP, MSFP och VRdP. Förändringar i blodvolym ledde till förändringar i RAP, MSFP, VRdP och venöst återflöde i samma riktning, utan ändring av flödesmotståndet för venöst återflöde. Behandling med kärlsammandragande läkemedel och behandling med vätskeinfusion ledde båda till ökat MSFP och möjliggjorde högre maxflöde under ECMO-behandling, med likartad effekt på syrgasleverans till kroppens vävnader. Metoden för att uppskatta MSFP via inblåsningsmanövrar överskattade MSFP mätt genom höger förmaksocklusion

– men bara vid normal blodvolym. Detta förklarades delvis av en kompensatorisk flödesökning i den nedre hålvenen under pågående inblåsningsmanöver. Alla undersökta metoder för uppskattning av MSFP var behäftade med mätfel vars omfattning växlade med volym-status. Förmågan att följa förändringar i referensmetoden växlade mellan de undersökta metoderna. Med möjligt undantag för den matematiska modellanalogen, så var även mätfelet gentemot *förändringar* i referensmetoden för stort för att vara kliniskt acceptabelt.

Vår slutsats blir att konceptet med drivtryck för venöst återflöde är tillämpbart även under dynamiskt skiftande förhållande, så länge man tar hänsyn till de volymskiften som uppstår. Den fysiologiska modellen för venöst återflöde kan förklara behandlingseffekten för kärlsammandragande läkemedel och vätskeinfusion avseende högsta möjliga flöde vid ECMO-behandling. Inblåsningsmanövrar är inte lämpliga för att uppskatta MSFP då de är behäftade med betydande mätfel. Den matematiska modellanalogen förtjänar fortsatt utvärdering inom ramen för klinisk forskning.

LIST OF PAPERS

The thesis is based on the following studies, referred to in the text by their Roman numerals.

I. David Berger, Per Werner Möller, Alberto Weber, Andreas Bloch, Stefan Blöchlinger, Matthias Hänggi, Søren Søndergaard, Stephan Jakob, Sheldon Magder, Jukka Takala. (2016). **Effect of PEEP, blood volume, and inspiratory hold maneuvers on venous return.** *American Journal of Physiology. Heart and Circulatory Physiology, 311*(3), H794-H806.

II. Per Werner Möller, Bernhard Winkler, Samuel Hurni, Paul P. Heinisch, Andreas Bloch, Søren Søndergaard, Stephan Jakob, Jukka Takala, David Berger. (2017). **Right atrial pressure and venous return during cardiopulmonary bypass.** *American Journal of Physiology. Heart and Circulatory Physiology, 313*(2), H408-H420.

III. Per Werner Möller, Anisa Hana, Paul P. Heinisch, Shengchen Liu, Siamak Djafarzadeh, Matthias Hänggi, Andreas Bloch, Jukka Takala, Stephan Jakob, David Berger. (2018). **The effects of vasoconstriction and volume expansion on veno-arterial ECMO Flow.** *SHOCK. E-published ahead of print. Received 3 May; accepted in final form 24 May 2018. DOI: 10.1097/SHK.0000000000001197.*

IV. Per Werner Möller, Søren Søndergaard, Stephan Jakob, Jukka Takala, David Berger. **Effect of volume status on the estimation of mean systemic filling pressure.** *Submitted manuscript*.

CONTENT

ABBREVIATIONS

ABP	arterial blood pressure
B-A	Bland-Altman
bpm	beats per minute
CI	confidence interval
CO	cardiac output
CR	repeatability coefficient
CV	coefficient of variation
CVP	central venous pressure
DO_2	oxygen delivery
ECMO	extracorporeal membrane oxygenation
F_IO_2	fraction of inspired oxygen
HES	hydroxyethyl starch
IVC	inferior vena cava
LA	left atrium
LV	left ventricle
LoA	limits of agreement
MAP	mean arterial pressure
MCFP	mean circulatory filling pressure
MSFP	mean systemic filling pressure
PA	pulmonary artery

P_{AW}	airway pressure
PEEP	positive end-expiratory pressure
$P_{pericard}$	pericardial pressure
Q_{PA}	pulmonary artery blood flow
Q_{IVC}	inferior vena cava blood flow
Q_{SVC}	superior vena cava blood flow
P_{arm}	MSFP estimated by arm-occlusion technique
P_{mcf}	mean circulatory filling pressure (MCFP)
P_{ms}	mean systemic filling pressure (MSFP)
P_{msa}	mean systemic filling pressure analogue
P_{msf}	mean systemic filling pressure (MSFP)
RA	right atrium
RAP	right atrial pressure
RAP_{tm}	right atrial transmural pressure
rpm	revolutions per minute
R_v	resistance in the venous compartment
RV	right ventricle
RVR	resistance to venous return
SV	stroke volume
SVC	superior vena cava
S_VO_2	mixed venous oxygen saturation

VO_2	oxygen consumption
VR	venous return
VRdP	venous return driving pressure

DEFINITIONS IN SHORT

$MSFP_a$	dynamic analogue of static MSFP calculated using mean values of RAP, MAP and CO from 10 beats during tidal ventilation; the original equation for 'P_{msa}' modified for use in pigs
$MSFP_{insp\_hold}$	mean systemic filling pressure estimated as the zero-flow extrapolation of steady state condition data-pairs of pressure and flow in a prolonged inspiratory pause
$MSFP_{inst\_VR}$	mean systemic filling pressure estimated as the zero-flow extrapolation of beat-to-beat instantaneous venous return during tidal ventilation
$MSFP_{RAO}$	MSFP measured at zero-flow caused by right atrial balloon occlusion
Vascular capacitance	The entire volume/pressure relationship
Vascular capacity	The volume in a compartment at a specific distending pressure
Vascular compliance	The inverse slope of the volume/pressure capacitance curve at a specified pressure or volume *or* the change in volume per unit change in pressure [e.g. mL/(Δ)mmHg]
Vascular elastance	The slope of the volume/pressure capacitance curve at a specified pressure or volume *or* the change in pressure per unit change in volume [e.g. mmHg/(Δ)mL]

VRdP	Venous return driving pressure: the pressure difference between the average upstream pressure, represented by MSFP, and downstream pressure, represented by RAP; VRdP = MSFP-RAP
RVR	Resistance to venous return: the resistance encountered by the average vascular element on returning to the right atrium; RVR = VRdP/VR

FUNDING AND GRANTS

The three animal experimental studies that form the base for this thesis were performed at the Experimental Surgery Unit, Department of Clinical Research, and funded by the Department of Intensive Care Medicine, Inselspital, Bern University Hospital - both departments within the University of Bern, Switzerland. The author held a one-year full time position as Visiting Investigator at the Department of Intensive Care Medicine at Inselspital 2015-2016, continuing as a part time affiliation at the time of writing. The PhD studies were partly financed by grants from the Swedish state under the agreement between the government and the county councils (ALF agreement number 75130). The study resulting in Paper II was supported by grant 23/2015 from the Stiftung für Forschung in Anästhesiologie und Intensivmedizin in Bern, to David Berger, Per Werner Möller and Stephan Jakob.

DISCLOSURES

The Department of Intensive Care Medicine of the University Hospital Bern, Inselspital, has, or has had, research contracts with Orion Corporation, Abbott Nutrition International, B. Braun Medical AG, CSEM SA, Edwards Lifesciences Services GmbH, Kenta Biotech Ltd, Maquet Critical Care AB, Omnicare Clinical Research AG and research and development/consulting contracts with Edwards Lifesciences SA, Maquet Critical Care AB, Nestlé and Orion Pharma, where the money was paid into a departmental fund, and none of the study authors gained any personal financial benefit. The Department of Intensive Care Medicine has received unrestricted educational grants from the following organizations for organizing a quarterly postgraduate educational symposium, the Berner Forum for Intensive Care: Fresenius Kabi, GSK, MSD, Lilly, Baxter, Astellas, AstraZeneca, B. Braun, CSL Behring, Maquet, Novartis, Covidien, Nycomed, Orion Pharma and RobaPharma.

ERRATA

In the published version of Paper I, Table 1: the unit for RVR should read "$mmHg \times min \times L^{-1}$"; in Figure 6 (relationship of Q_{PA} *vs.* VRdP): data for r^2 [median (range)] should read "0.977 (0.729-0.9999)".

1 INTRODUCTION

1.1 WHAT IS THE VOLUME STATE?

At the bedside of a hemodynamically unstable patient, clinicians try to characterize the patient's volume state in terms of normovolemia, hypovolemia or hypervolemia. This is not primarily done by measurement or assessment of the actual blood volume, but rather by interpreting the indirect effects of the present *stressed* blood volume on variables like heart rate, blood pressure, filling pressures, vessel collapse, cardiac output and capillary refill time. The total blood volume and the size and stiffness of all vessel beds determine the stressed blood volume, i.e. the fraction of blood volume that distends the vasculature. All three factors are highly regulated by homeostatic mechanisms that in turn can be subject to numerous pathophysiological changes. Stressed volume thereby integrates biological information on the actual blood volume, input and output to the neuro-humoral nervous system (cardiovascular reflexes), as well as collective effects upon these systems caused by sedative, analgesic and anaesthetic (including inhalational, intravenous, neuraxial and regional anaesthesia) and vasoactive medications or vasoplegic disease states such as sepsis. Complex, each in their own right, all these phenomena converge into setting the stressed volume. By this reasoning, the stressed volume is a representation of the volume state. The relation between stressed volume and total blood volume, and the interaction between stressed volume and cardiac function, provides additional information. If the stressed volume could be estimated or measured clinically, it would provide useful information to guide treatment.

1.2 VASCULAR PRESSURE AT ZERO FLOW

If the heart is brought to a sudden standstill, all vascular pressures will equilibrate, as the arterial compartments expel most of their pressurized contents downstream, thereby distending the highly compliant venous system. This shift of volume will cause arterial pressures to fall and venous pressures to rise. When all pressures have equilibrated, flow has ceased as no driving pressure remains. In the functioning organism, the arterial hypotension would lead to a massive sympathetic discharge, aimed at increasing venous return, cardiac function and perfusion pressures. Even if the heart remained unresponsive, this sympathetic activation would lead to vasoconstriction in all vascular beds. Without a functioning heart, local differences in vascular response could still cause small additional volume shifts, i.e. transiently reappearing antegrade and/or retrograde flow, but the main effect would be a further rise in intravascular pressures. However, if the experimental setup includes measures that either abolish the cardiovascular reflexes, and/or a large arteriovenous shunt that could be opened to hasten the process and allowing full pressure equilibration before the onset of reflex mediated vasoconstriction, this equilibrated pressure could be measured anywhere in the circulation.

Imagine again the cardiovascular system at zero flow and pressure equilibration. Imagine also that the *entire* blood volume could be drained into an external reservoir (in reality impossible) causing the vascular walls to collapse. If this process of total exsanguination is reversed, we can now refill the system while monitoring the intravascular pressure. At a certain point, the vasculature will again precisely be filled, but not distended. The transmural pressure remains zero as the 'unstressed blood volume' (V_u) fills the vasculature. At this point, volume will be divided between vascular compartments according to their respective unstressed capacitance. However, the external reservoir still contains about 25-30% of the total blood volume (65). As we pump this remaining volume into the vascular system, pressure starts to build up as blood now distends the vessel walls. The rise in pressure will be proportional to the infused volume and the average vascular elastance. If the walls are stiff (the vascular elastance is high which is equivalent to a low compliance), the pressure will rise quickly. When all blood has been returned, the intravascular pressure is determined by the distending or 'stressed volume' (V_s) and the average compliance of the vascular system (C_{vasc}).

$$P=V_s/C_{vasc} \qquad (1)$$

This (transmural) pressure is a manifestation of the potential energy stored in vessel wall recoil. It is a pressure representation of the stressed volume. The

normal circulatory zero-flow pressure is approximately 7 mmHg in mammals (87). At zero flow, the stressed volume is partitioned between vascular compartments solely according to their relative compliances, and venous vessel beds will therefore contain more blood than arterial beds.

When the heart resumes work, right atrial pressure (RAP) will decrease, forming a pressure gradient in relation to upstream areas, thereby recreating a driving pressure for venous return. Left ventricular stroke work will add volume and increase pressure in the arterial compartment. In transition from a state of zero flow and pressure equilibrium, the working heart will shift volume from the venous to the arterial side. As a consequence of the arterial compartment having a low compliance and high out-flow resistance, the volume-displacing work of the heart results in a considerable rise in pressure. Conversely, as the venous compartment is characterized by high compliance and low resistance to flow, the venous pressure drop will be small. At zero flow, approximately 70% of the blood volume will reside in the venous compartment. This decreases to 60% when blood flow is restored as a consequence of volume shift from the systemic venous compartment, into the pulmonary compartment (60, 64). In a state of flow, the distribution of blood will be determined by the relative in- and outflow resistances *and* the respective compliances of vascular beds. The pulmonary vasculature contains approximately 12-14% of the total blood volume (60). In case of right or left ventricular failure, the proportion of central to peripheral volume may decrease or increase, respectively (66). Acute onset of biventricular failure (as in a ventricular fibrillation model) may leave the proportion unchanged (72).

1.3 HISTORICAL BACKGROUND

The concept of a zero-flow circulatory filling pressure was formulated by Weber in 1851 (101). In 1912, the Danish zoophysiologist August Steenberg Krogh gave an account on how resistances and active and passive recoil of vessel beds modulate flow on both organ and body level. He described the function of the portal system and concluded that it *"acts as a general regulator on the pressure in the central veins and thereby on the output of the heart"* (49). Starling had referenced both Weber and Krogh before he gave his famous Linacre lecture on the Law of the Heart (79). Starling and Patterson wrote *"It thus follows that the neutral point in the vascular system, where the mean systemic pressure is neither raised nor lowered by the inauguration of the circulation, lies considerably on the venous side of the capillaries – at any rate, in most parts of the body"*. Starling and Patterson realized that the portal vein operated at or near this pressure. Starling commented on the neutral point that *"the pressure is neither raised nor lowered and where, therefore, the pressure is independent of the cardiac activity"* (91). The essential consequence of this statement is that the mean filling pressure is unrelated to cardiac function and determined solely by stressed volume and the vascular elastic properties.

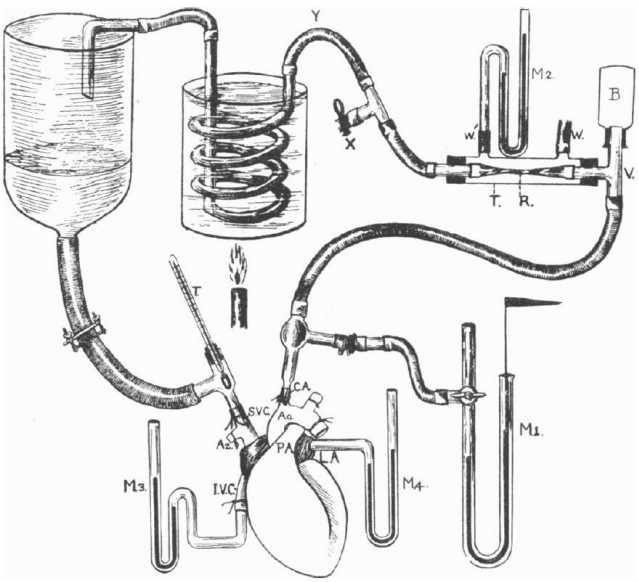

Figure 1 – Heart preparation of Patterson and Starling (79). Venous return was gradually increased by elevating the venous reservoir or unscrewing the clip on the tubing leading into the superior vena cava. Reproduced with permission from John Wiley and Sons.

The Frank-Starling law (also honouring the German physiologist Otto Frank) explains how the heart, based on the mechanism of pre-contraction fibre length setting the contractile force, can servo-control stroke volume (output) to match venous return (input). *"The output of the heart is equal to and determined by the amount of blood flowing into the heart, and may be increased or diminished within very wide limits according to the inflow"* (79). However, it was clear to Starling and co-workers that the demand for flow was dictated by the metabolic needs of the *tissues*. Importantly, they never claimed that the body *controlled* systemic flow by regulating the work of the heart. The experimental setup leading to the formulation of the "Law of the heart" is shown in Figure 1. The inflow to the right atrium was controlled by varying the height of the venous reservoir or simply unscrewing a clip around the venous tubing. As inflow and output gradually increased, there was a slight curved increase in central venous pressure. When the functional capacity of the heart was exceeded, the ventricles became over-distended which resulted in falling output, and rapidly increasing venous pressure (Figure 2). The classical plot of cardiac function, nowadays presented with filling pressure on the x-axis, originally appeared with central venous pressure on the dependent axis, and flow on the independent axis.

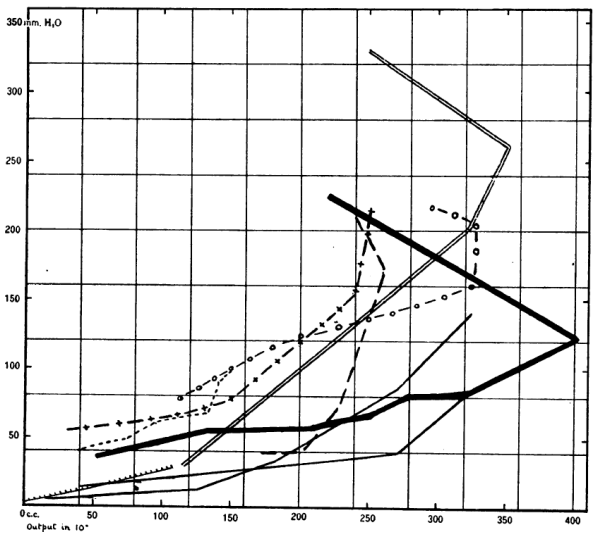

Figure 2 – The original plot of Patterson and Starling showing the effect of gradually increasing inflow on central venous pressure. When the functional limit of the ventricle is exceeded, there is a drop in output with a marked continuous increase in venous pressure, as blood is dammed up in the atrium. A contemporary version of a 'cardiac function curve' or family of 'Starling curves' is presented with the axes flipped: filling pressures (as surrogate for end-diastolic volume) appear on the x-axis, and flow or stroke volume on the y-axis (79). Reproduced with permission from John Wiley and Sons.

1.4 GUYTON'S CARDIOVASCULAR MODEL

1.4.1 THE MEAN CIRCULATORY FILLING PRESSURE

In the 1950s, Arthur Guyton pioneered the studies of the factors determining venous return (VR). In the initial experiments, involving more than 100 dogs, he determined the 'mean circulatory filling pressure' (MCFP) at zero flow caused by ventricular fibrillation, vagal stimulation or ligation of the pulmonary artery (PA), and found it to be ~7 mmHg (40, 42). Rapid arteriovenous equilibration was assisted by the use of a roller pump, and reflex activation was abolished by instituting total spinal anaesthesia and restoring the arterial pressure with infusion of epinephrine. Total spinal anaesthesia without epinephrine gave a MCFP just below 5 mmHg. Attempts to increase MCFP with increasing infusion rates of epinephrine revealed a ceiling effect at about 16 mmHg, above which the effect of further vasoconstriction was counteracted by extensive fluid leakage. [We reproduced this finding in an experiment using modern venoarterial extracorporeal membrane oxygenation (VA-ECMO) – see Paper III (section 4.3)]. Measurement of MCFP after PA ligation, as compared to ventricular fibrillation, resulted in slightly higher values due to volume shift from the cardio-pulmonary compartment into the systemic compartment from continued stroke work (see also section 1.5.1).

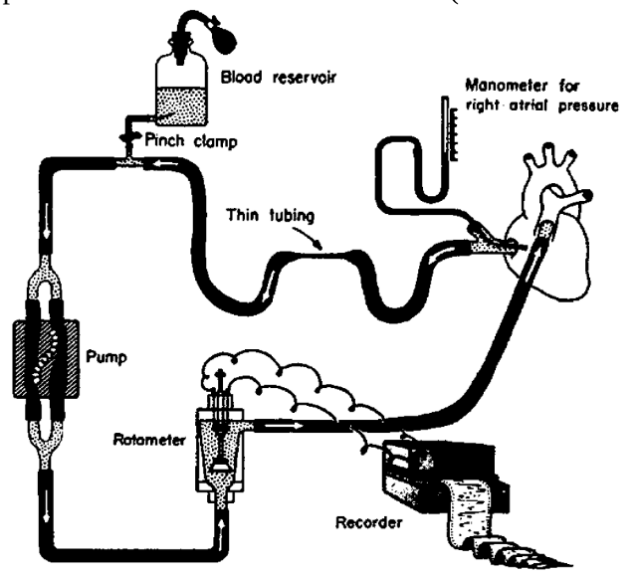

Figure 3 – Right-heart bypass system used by Guyton for controlling right atrial pressure and venous return (40). Reproduced with permission from the American Physiological Society.

1.4.2 THE VENOUS RETURN CURVE

In a landmark series of experiments (39-41), Guyton explored the properties of the vascular circuit and the volume state. In a highly cited and debated paper, Guyton describes the use of a right-heart bypass preparation - the details of which can only be fully understood from later publications (Figure 3) (40). Briefly, venous return was completely drained via a right atrial cannula and led through a horizontal segment of thin, collapsible rubber tubing (a Starling resistor) to a pump and flowmeter, before being returned into the PA. The pressure in the right atrium (RA) was measured with a mercury manometer. The experiment consisted of exposing the circuit to a series of short excursions of increased RAP, while recording the resulting flow. This was achieved by elevating the Starling resistor, increasing the RA hydrostatic pressure and simultaneously adjusting the pump rate to maintain the rubber tubing in a semi-collapsed state. The resultant RAP and flow could be read within 8-10 seconds, before the system was again returned to a negative RAP and maximal pump speed. Pressure-flow data points were presented in what has since been termed 'venous return plots', with RAP on the x-axis and flow on the y-axis (see Figure 4).

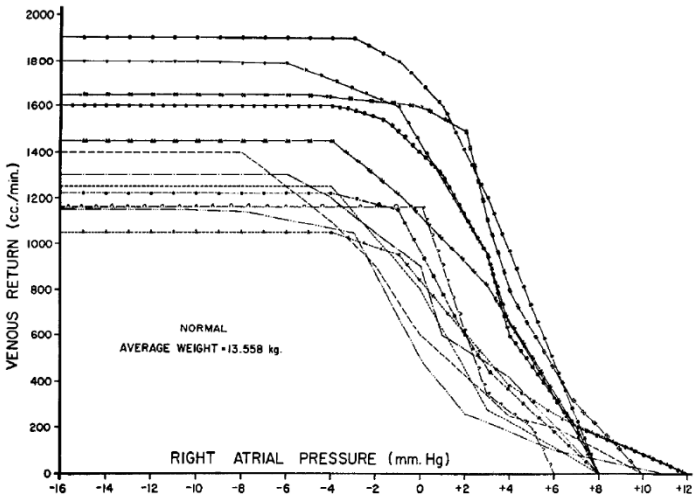

Figure 4 - Venous return curves recorded from 12 normal open-chest dogs. Guyton (40). Reproduced with permission from the American Physiological Society.

Guyton recognized intravascular RAP as the backpressure for VR. Lowering RAP in relation to MCFP allowed an increase in flow proportional to the pressure difference between MCFP and RAP. The maximum flow was found at zero RAP. In the open chest experiments, a decrease of RAP below sub-

atmospheric pressure (i.e. to negative transmural pressures) caused the large venous vessels to collapse, limiting further flow increase. Venous return could also be increased by adjusting the upstream MCFP by blood infusion, or by infusion of epinephrine (Figure 5). In a later experiment, Cowley demonstrated that pacemaker-controlled increase of the heart rate only augmented cardiac output if the experimental conditions permitted an increase in *venous return* (22). Returning to Guyton, he predicted and experimentally verified that RAP could not be elevated above MCFP. An increase in blood volume, apart from elevating MCFP also distended the vessels and lowered the impedance to VR. An induced resistance between the left ventricle and the main vascular reservoirs, although causing a major increase in afterload, only had a minor effect on VR. In contrast, the slightest increase in venous compartment vascular resistance, downstream of the vascular reservoirs, greatly decreased VR.

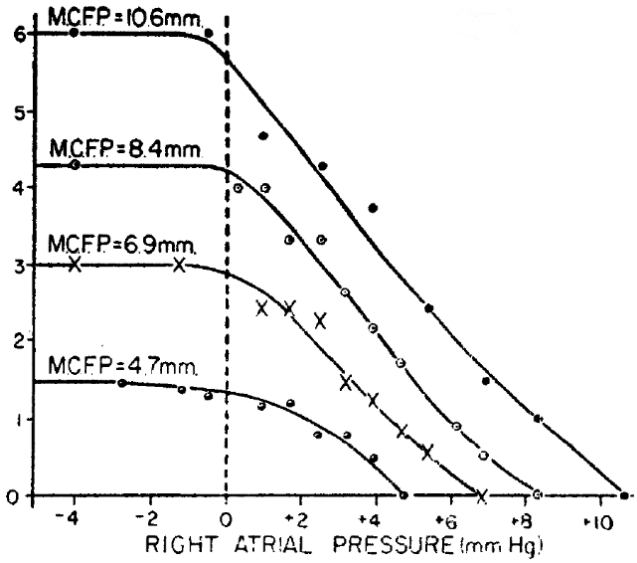

Figure 5 - Venous return curves illustrating the effect of RAP on VR when the MCFP was maintained at different levels. Guyton (39). Reproduced with permission from the American Physiological Society.

1.4.3 EQUATING VENOUS RETURN AND CARDIAC OUTPUT

By superimposing venous return curves with cardiac response curves and acknowledging that at equilibrium, VR is equal to CO, Guyton showed how properties of the vascular circuit and the cardiac function interact to determine flow and RAP.

$$CO = VR = (MCFP-RAP)/RVR = VRdP/RVR \quad (2)$$

RVR = resistance to venous return.

The consequence was that RAP, as a node for cardiac-circuit interaction, was both a determinant of flow, and determined *by* flow. The dual nature of RAP – acting backpressure to oppose VR, *and* being an effect of the volume shifting work of the right heart – is integrated in Guyton's cardiovascular model. This is often overlooked and seemingly hiding in plain sight in the middle of the infected debate on the correct interpretation of Guyton's experiments (see section 1.4.5).

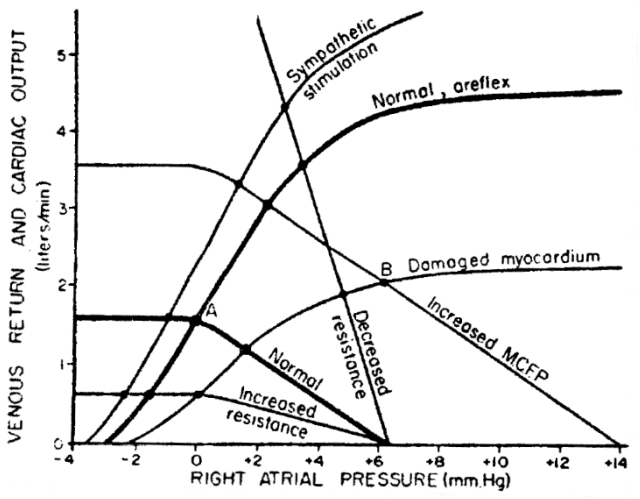

Figure 6 – Equilibration of various venous return curves with different cardiac response curves. Guyton (39). Reproduced with permission from the American Physiological Society.

1.4.4 A GUYTONIAN VIEW OF THE CIRCULATION

To summarize, a ‘Guytonian’ view of the circulation would stress that:

- The role of the heart is to keep RAP low to enhance venous return, and to restore the energy needed for peripheral perfusion by left ventricular stroke work.
- Mean circulatory filling pressure is a representation of the stressed volume and the upstream pressure for venous return.
- Flow is controlled primarily by modulating the properties of the circuit. The exception is cases of heart failure where flow also can be augmented by therapeutic interventions that increase heart function in order to decrease a pathologically elevated RAP.
- Since the venous side of the circulation stores the main part of the blood volume, it is important to understand to what extent therapeutic interventions target the veins.

1.4.5 CRITIQUE OF THE MODEL

In 1979, Levy presented a mathematical analysis and repeated the right-heart bypass experiment of Guyton, but treated flow as the independent experimental variable (52). He omitted the Starling resistor and simply operated the pump rate and recorded the resulting flow and pressures. Although his results were identical to those of Guyton, he came to the opposite conclusion regarding cause and effect. According to Levy's view, pressure gradients found along the circuit were a consequence of flow, not determinants of flow. Regarding RAP, he concluded, *"It probably is not an important determinant of 'venous return' by virtue of any 'back-pressure' effects"*. Since then, there is ongoing and at times infected debate on the validity, interpretation, and application of Guyton's circulatory model (3, 7, 16-18, 59, 62). The interpretations of Levy, adopted by Brengelmann, Beard and Feigl, stress that venous return is caused by the energy provided by the left ventricle. They reject the idea of flow being driven by the pressure gradient between average upstream pressure (MCFP) and downstream pressure (RAP) and point out that energy *stored* as recoil pressure in MCFP must not be seen as *source* of energy. Magder, a proponent of Guyton's model, argue that the pressure drop from MCFP to the right atrium indeed represents the driving force for venous return, but underlines that the energy store is refilled stroke-by-stroke by left ventricular work. Since the pre-capillary resistance is high and actively regulated, venous return cannot be described by the pressure fall in the arterial compartment. Although both sides have certainly made their points, any consensus is out of sight. Critics of the model argue that the basic interpretations are flawed, and that Guyton confused cause and effect. Others state that the model may correctly describe a steady state, but that it should not be applied to explain changes in venous return.

In essence, this means that proponents see the pressure difference between MCFP and RAP as a *de facto* driving pressure for venous return. The opponents, on the other side, state that MCFP may be a valid measure of vascular recoil at zero flow, but that RAP is solely determined by the work of the heart and the pressure difference to upstream areas is caused by flow. Both sides have accused the other of reasoning that would violate the laws of conservation of mass and conservation of energy. Retrospectively, both sides appear guilty of deliberately misinterpreting each other. Tyberg took a more reconciling position and concluded that both views are model based and internally consistent, *"and difficult or perhaps impossible to 'prove' at the expense of the other"* (94). In the debate, the opposing views describe RAP as *either* a consequence of heart work, *or* a determinant for VR. This controversy is not merely academic in nature. If RAP does not act as backpressure for inflow to the right heart, widely used models explaining how positive pressure

ventilation impedes circulation become invalid. Guyton's cardiovascular model is also used as a framework for understanding shock states at the bedside, in particular to delineate pump factors from circuit factors (31, 32). If the model is invalid, it should not be applied for decision making in patients.

1.5 TERMINOLOGY AND DEFINITIONS

1.5.1 MCFP OR MSFP?

The terminology used in the field is inconsistent. In some sources, 'mean circulatory (filling) pressure' and 'mean systemic (filling) pressure' appear interchangeably. This was true also for Guyton who used the term MCFP for the equilibrated pressure measured at zero flow caused by both ventricular fibrillation and by pulmonary artery ligation (42). If the measurement setup with some certainty can claim to achieve vascular equilibrium also including the cardiopulmonary compartment, the term 'mean circulatory filling pressure' is often used (MCFP). If the equilibrium rather refers to the systemic circulation, 'mean systemic filling pressure' (MSFP) is used instead. Regardless of experimental design, it is often impossible to verify the precise degree of vascular equilibrium. Even if arterial and venous pressures approach, this does not preclude locally obstructed vessel beds upstream of the site of measurement. MCFP is sometimes reported as being slightly higher than MSFP – in the range of ≤ 1 mmHg (60, 64). It is however crucial to realise that any method that attempts to estimate the mean filling pressure in the systemic circulation during ongoing circulation, will be affected by potential volume shifts occurring between the cardiopulmonary and systemic compartments. A temporary imbalance between venous return and cardiac output, like the ebb-flood tide of pulmonary blood volume over the respiratory cycle (see section 1.8.2), will at least theoretically be associated with an MSFP changing over time.

1.5.2 THE PIVOTAL PRESSURE OF THE CIRCULATION

There has been some discussion on the possible anatomical location of MCFP. Early investigators such as Bayliss, Starling and Krogh realized that MCFP had many characteristics of a 'venous pressure' (6, 49, 79). In his excellent review, Rothe summarizes that it is *"less than capillary pressure, is closely similar to the portal venous pressure and the venule pressure of most tissues, is at the location of the 'pivot pressure', and is more than the central venous pressure"* (87). If the change in MCFP (or MSFP) after a change in blood volume is used to determine the mean circulatory or systemic compliance, it becomes clear that this value is close to the compliance of the systemic veins (see Figure 19 in section 3.5.2). Stated differently, total body vascular compliance is the sum of all regional compliances, and is highly dominated by systemic vein compliance (61). The pivotal pressure represents the idea of a point along the vasculature with constant pressure, regardless of flow state. With changing flow, volume is shifted around this pivot (see Figure 7) (97). In reality however, as the circulation consists of myriad parallel paths, each will have its own pivot pressure, most of which will be located in the early post-capillary venules. It is important to understand that the locations of these points are constantly changing up and down the flow path along with flow, vasomotor tone, vascular diameter, and changing rheological factors.

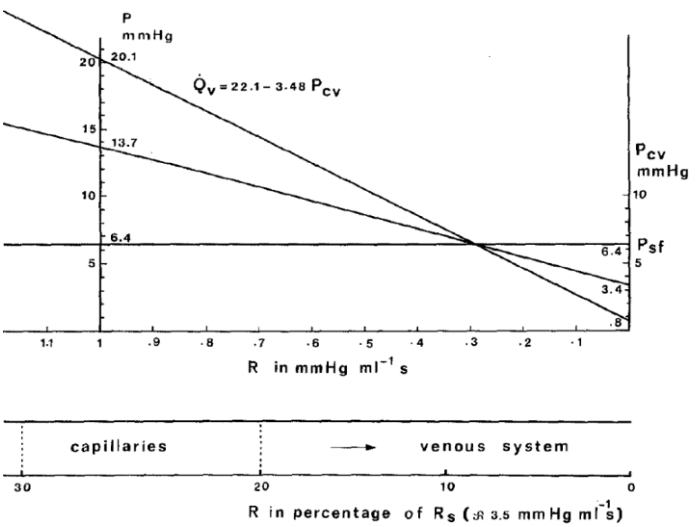

Figure 7 – Physical and graphical model of venous return from Versprille (97). The tube at the bottom represents the capillary and venous parts of the model. The top diagram gives the changes in pressure fall in the tube when central venous pressure (P_{cv}) is increased. The average P_{sf} (MSFP) in the experiment was 6.4 mmHg and is marked by the horizontal line. Reproduced with permission from Springer Nature.

If MSFP is estimated, the pressure will always be numerically close to that of a systemic vein, but conceptually it represents the *average* of all vascular elements in the *entire* systemic compartment – venous as well as arterial. A fluid bolus leading to an increase in stressed volume and MSFP will move the average vascular element downstream (76). In the studies that form the base of this thesis, we have preferred the interpretation of MSFP *as the average pressure in the entire systemic compartment*, rather than using it as a surrogate for venous compartment pressure. Conceptually, when estimating MSFP, we are not interested in the pressures at the pivots, but rather seek a measure of the stressed volume of the system. Therefore, rearranging equation 2 gives:

$$RVR = VRdP/VR \qquad (3)$$

Resistance to venous return (RVR) represents the resistance encountered by the average element on returning to the right atrium. It will be numerically similar to the unmeasured resistance in the venous compartment (R_v). But - however tempting, it is incorrect to imagine that R_v can be calculated by dividing flow by the pressure drop MSFP-RAP:

$$R_v \neq (MSFP\text{-}RAP)/VR$$

Brengelmann, an outspoken critic of the use and interpretation of Guyton's cardiovascular model (including our interpretations), repeatedly fails to recognise this distinction (15), which has led to many unnecessary deviations in the debate. With that said, it is my personal view that attempts to ascribe values of resistance to particular vascular sub-segments located upstream or downstream of the theoretical pivot *by use of a measure of MSFP* are conceptually flawed. Such examples can be seen with Geerts and Maas (34, 53) (Figure 8). MSFP and RVR are best restricted to represent the average characteristics of the entire systemic compartment. Over-interpretation will spur further (and then justified critique) of the entire concept of venous return.

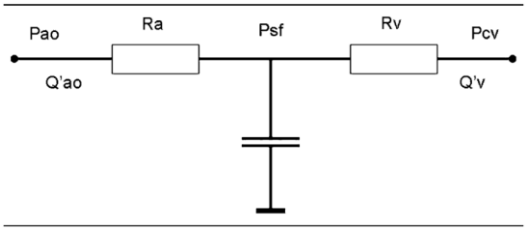

Figure 8 – A conceptually flawed model, with the intended use of computing resistances upstream (R_a) and downstream (R_v) of mean systemic filling pressure (P_{sf}), estimated using inspiratory hold maneuvers. From (34). Reproduced with permission from Springer Nature.

1.6 EXPERIMENTAL METHODS OF ZERO-FLOW PRESSURE DETERMINATION

In animal models, induced ventricular fibrillation and subsequent defibrillation of the heart can been used to achieve repeated episodes of circulatory arrest. As both ventricles stop pumping simultaneously, there is no active transfer of blood between the cardiopulmonary and systemic compartments. Arterial and central venous pressures change asymptotically towards a common plateau. An injection of potassium chloride can be used as an effective but irreversible way of inducing fibrillation. Acetylcholine can be used to stop the heart by asystole that usually lasts for 5 s or more. Full recovery requires about 10 min and repeated doses may cause respiratory failure. MCFP and MSFP are expected to be equal with all three methods. Intermittent mechanical obstruction to flow with intact circulation can be achieved by external occlusion of the PA, or by inflating an endovascular balloon in the RA, blocking flow into the right ventricle (RV). These methods allow the beating ventricle/-s to shift some blood from the cardiopulmonary to the systemic compartment, from the time of vascular obstruction until pressure equilibrium. As the average vascular compliance of the systemic compartment is high (~3 $mL \times kg^{-1} \times mmHg^{-1}$), the pressure effect of this volume shift will be small (72). In a porcine model with right atrial balloon occlusion and pump-assisted arteriovenous (AV) volume equilibration, MCFP at baseline was (mean ± SD) 12.3 ± 1.3 mmHg, compared to 12.0 ± 1.9 mmHg at circulatory arrest from injection of potassium chloride (72). The equilibrated pressure measured in a central vein after a RA or PA occlusion is therefore representative of both MSFP and MCFP, with the caveat that pressures may increase as a consequence of central to systemic volume shift.

1.6.1 INCOMPLETE ARTERIOVENOUS PRESSURE EQUILIBRATION

If volume transfer is not assisted at circulatory arrest, a certain arteriovenous pressure difference will persist at the time of best equilibrium. In the experiment cited above, MCFP from right atrial balloon occlusion without volume transfer was 11.0 ± 1.1 mmHg, and underestimated the value obtained by volume transfer by 1.3 mmHg. Attempts have been made to estimate the additional rise in central venous pressure, which would have occurred provided complete AV equilibration. A correction factor can be calculated using the ratio of arterial pressure decay to central venous pressure increase, assuming that venous compliance is the major component of total vascular compliance. In experiments using RA balloon occlusion with and without volume transfer, applying the correction factor still led to an underestimation of true MCFP (72). However, an elegant study on dogs using a right-heart bypass technique compared the MSFP (measured at the venous pressure plateau) obtained with and without pump-assisted AV volume transfer. MSFP of both methods were found to be identical, irrespective of different remaining AV pressure gradient at the time of venous pressure plateau (35). This is probably explained by the fact that the remaining volume of blood associated with a zero-flow arterial pressure of ~20-30 mmHg is quite low, and the compliance of the venous compartment high enough to make the final contribution to equilibrated pressure almost insignificant. It is also worth noting that some volume might be trapped on the arterial side due to vascular waterfalls (physiological Starling resistor mechanism). Volume contained by such a mechanism would be excluded from pressure equilibration regardless of how long time is allowed (63, 90). It should be noted that the relation between estimates taken at incomplete equilibration *vs*. pressures measured after full equilibration might depend on the underlying volume state. This has not been experimentally verified.

1.7 INVASIVE METHODS IN HUMAN RESEARCH

In two studies, MCFP has been determined in human patients undergoing testing of implantable cardioverter/defibrillator devices (ICDs). As part of the clinical procedure, fibrillation-defibrillation sequences (FDSs) are induced to confirm the operability of the device. At the onset of ventricular fibrillation, the asymptotic merging of arterial and venous pressures can be documented. Arrhythmias were always successfully terminated before full pressure equilibrium, or any signs of reflex mediated vasoconstriction occurred. The study by Jellinek (46) primarily investigated the influence of an immediate change in airway pressure (P_{AW}) on MCFP and VRdP. The P_{AW} was set 5 s prior to FDS by either disconnecting the ventilator, or performing an inspiratory hold maneuver. MCFP (n=13), taken as the central venous pressure (CVP) 7.5 s into the FDS, was found to be 10.2 ± 3.5 mmHg and 12.7 ± 3.2 mmHg at P_{AW} of 0 and 15 cm H_2O, respectively. The remaining AV pressure difference was 20 ± 7 and 18 ± 4 mmHg. If a correction factor based on estimated AV compliance ratio was used, the estimated MCFP increased by 1.2 mmHg to 11.4 ± 3.6 and 13.9 ± 3.4 mmHg, respectively, at the two levels of P_{AW}. Venous return driving pressure was ~ 4 mmHg, and did not change with P_{AW}. Schipke studied patients undergoing in total 323 FDSs (90). In all patients, 13 s into ventricular fibrillation, a pressure difference of 13 ± 6.2 mmHg remained. The MCFP reported for 36 patients undergoing in total 141 FDSs, was 11.0 ± 5.4 mmHg. The estimated value of MCFP at full equilibrium was ~ 12 mmHg. CVP prior to FDS was 7.5 ± 5.2 mmHg, and VRdP would have been ~ 4.5 mmHg. Regrettably, values of airway pressure or ventilator regime was not reported. The study focus was on the estimated time constants for the approximately exponential change in vascular pressures. The initial rapid pressure change, occurring during the first 10 s, could be characterized by a mono-exponential function. At 20 s, the time constant for arterial pressure decay became significantly longer, which supports the idea of a waterfall mechanism: as more vessels begin to close at the lower arterial pressures, the

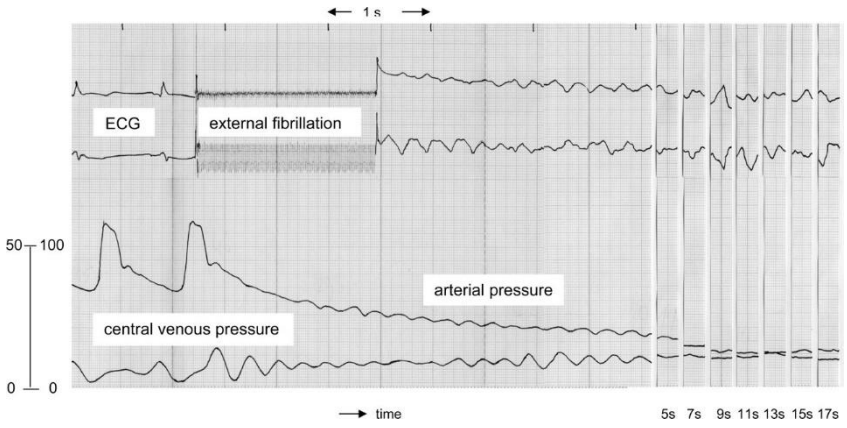

Figure 9 - An example of a Fibrillation-Defibrillation Sequence (FDS) from Schipke (90). After the induction of ventricular fibrillation, the arterial pressure decreased and the venous pressure increased. At the end of fibrillation, both pressures had not reached an equilibrium pressure (note the different scales). With permission from the author.

overall resistance for emptying increase. The two studies are very interesting for the following reasons: First, they represent measurements actually performed *at zero flow* in contrast to methods that estimate zero-flow pressures during ongoing circulation. Second, the subjects studied were patients (and not healthy animals) with elevated central venous pressures reflecting a combination of heart failure and pathological and perioperative volume loading. In this setting, both studies report MCFP in the range of 10-13 mmHg with venous return driving pressure (although not reported) in the range of 4-4.5 mmHg.

1.8 ESTIMATION OF ZERO-FLOW PRESSURE FROM AIRWAY PRESSURE MANEUVERS

In the following subchapter, the development leading to the currently used clinical concept for estimation of MSFP is described ('MSFP estimated by inspiratory hold' or $MSFP_{insp\_hold}$)

1.8.1 INSTANTANEOUS VENOUS RETURN CURVE

In a landmark study presented in two separate papers 1984, Pinsky advanced the understanding of circuit-heart-lung interactions by a comprehensive characterization of right ventricular (RV) working conditions and provided an estimate of MSFP available without circulatory standstill (81, 82). Using what he called "instantaneous venous return curves", he demonstrated that RV stroke volume (SV_{RV}) was inversely proportional to the cyclically changing RAP caused by tidal ventilation. Dogs were mechanically ventilated with intermittent positive pressure breathing (IPPB) and tidal volumes between 5-10 mL/kg. An arteriovenous fistula could be opened to assist pressure equilibration at circulatory arrest from ventricular fibrillation, for the determination of a reference MSFP ('stop flow P_{ms}'). Data-pairs consisting of beat-to-beat, right ventricular stroke volume (SV_{RV}; measured with an electromagnetic flowprobe around the PA) and RAP from the preceding beat (measured at the onset of QRS complex) were used to describe the venous return function. Zero-flow extrapolation of the linear regression for this relation (answering the question: "at what level of RAP would venous return cease?") provided 'instantaneous P_{ms}'. The relationship was highly linear and 'instantaneous P_{ms}' agreed well with 'stop flow P_{ms}': (mean ± SE) 8.4 ± 0.7 and 8.1 ± 0.8 mmHg, respectively. Correlation between the two methods was high, with a slope not different from one, and the x-intercept not different from the origin. Volume loading of the animals shifted the instantaneous VR curves to the right and appeared to increase instantaneous and stop flow P_{ms} by the same degree.

Pinsky stressed some important conditions that needed to be fulfilled for the assumptions to be valid. For changes in SV_{RV} and RAP during tidal ventilation to accurately reflect venous return, RAP must be the effective downstream pressure, and SV_{RV} must proportionally reflect changes in venous return. Vascular collapse during the respiratory cycle would introduce a waterfall mechanism and dissociate the pressure-flow relationship. In that case, the measured RAP would not represent the effective downstream pressure. The assumption that SV_{RV} reflects venous blood flow requires heart rate to remain constant, and that the relation between preload and SV is independent of the

respiratory phase. Pinsky had shown that the only determinant of RV output, in the context of small tidal volume positive pressure ventilation, was the RV filling pressure. Although venous return was shown to vary during respiration, Pinsky concluded that the upstream pressure was essentially constant during IPPB: First, the absolute value of SV_{RV} variation was small (<10 mL) in relation to the entire high-compliance systemic vascular volume. Second, since the time constant for vascular smooth muscle contraction was longer than the respiratory cycle, there could be no dynamic response of autonomic or reflex mediated control of vascular tone to these changes (89).

This comment may be a convenient way of disputing possible reflex interaction without access to kinetic data for the reflex arch - but it also draw focus away from another issue: Do volume shifts between the cardiopulmonary and the systemic compartment affect upstream and/or downstream pressures in a way that changes venous return driving pressure? The answer should later turn out to be 'yes', as we showed in Paper II (see sections 4.2 and 5.2). However, this does not make Pinsky's contribution less valuable, but an analysis, already in this stage, of the possible impact of positive pressure ventilation on the dynamic components of VRdP, might have made the investigators (with whom Pinsky collaborated during the following years) less prone to neglect the influence of volume state on estimates of MSFP. More problematic was the claim that *"Volume loading causes a parallel shift of the instantaneous venous return curve to the right without significantly changing its slope"*. This important conclusion was not supported by any quantitative data. The method section is devoid of statistics that could test the possible agreement between instantaneous P_{ms} and stop flow P_{ms} over changing volume state.

1.8.2 THE HEMODYNAMICS OF AIRWAY PRESSURE MANEUVERS

Versprille and Jansen examined the hemodynamic response during inspiratory hold procedures described as a cycle length of 12 s with an inspiratory pause of 7.2 s (97). The experimental model used piglets with flow measured by electromagnetic (EM) flowprobes mounted around the PA and ascending aorta (Q_{PA} and Q_{AO} respectively). End-expiratory Q_{PA} was constant during tidal ventilation. Central venous pressure (CVP) was increased to varying levels by lung inflation to tidal volumes between 25-300 mL applied in random order. The PEEP level was kept at 2 cmH_2O. During the last 5 s of the inspiratory pause, CVP and venous return (measured as Q_{PA}) were found to be stable and mean values were fitted to a linear equation. As P_{AW} was increased, CVP increased concomitantly and Q_{PA} fell, *"recovering slightly to a plateau during the inspiratory hold"* (97). With an average delay of 3 beats, aortic flow and pressure followed the decrease in RV output. No signs of reflex activation was observed during the maneuvers. An average of 7 inspiratory hold procedures were applied per animal, and the pressure-flow relation was linear. The zero-flow extrapolations for the normovolemic animals were (mean ± SD) 10.5 ± 2.3 mmHg, and were interpreted as representing MSFP. As CVP was 0.8 ± 1.0 mmHg, VRdP (although not presented in the paper) would have been ~9.7 mmHg, which is a high value compared with measurement at zero flow. The authors comment on the phenomenon of venous loading: *"During insufflation venous capacitance will be loaded due to the increasing central venous pressure, which causes an extra fall in venous return and RV output"*. To avoid errors in the estimation of MSFP, they recommend measuring pressure and flow at *"short periods of steady state circumstances"*, i.e. at the end of the inspiratory pause. The authors argue against Levy by stressing the order of events in hemodynamic changes following a step change in airway pressure. As the rise in CVP was *immediately* coupled to a decrease in VR, and the decrease in LV output followed after a delay, they showed that, in this moment, VR was driven by the pressure difference between MSFP and downstream pressure, and not by arterial perfusion pressure.

Versprille and Jansen continued with two comprehensive studies (96, 98) that quantified the effect of increased intrathoracic pressure on VR, CO and pulmonary blood flow. Using the same model as above, but also evaluating aortic pulse contour cardiac output as a surrogate for invasive flowprobes on the left side, they could measure inflow and outflow to the pulmonary compartment. Changes in pulmonary blood volume as well as shifts between systemic and pulmonary compartments were quantified. A maximal shift of blood, amounting to ~1 mL/kg, out from the lungs and into the systemic

circulation, was estimated to occur at tidal volumes of 20 mL/kg. An important finding was that both Q_{PA} and Q_{AO} quickly reached steady states during the end-expiratory phase of tidal ventilation as well as a few seconds into an inspiratory paus. Since one aim of the study was to develop a method of MSFP estimation, this finding was reassuring. It is notable that only the first study included data sampling over changing blood volumes - and then only during tidal breathing. The impact of changing blood volume *on the flow recovery* during inspiratory pauses was not studied. The authors did however note that during tidal ventilation, the inspiratory shift of pulmonary blood volume into the systemic circulation was significantly *lower* in hypervolemia than in normo- and hypovolemia. There was no definitive explanation for this pattern. The finding of a pulmonary blood volume shift affected by the volume state should have been a warning sign: the observation that pulmonary and aortic flows reach new steady states in the end-inspiratory paus suddenly becomes less reassuring for someone with the goal of estimating steady state venous return. As we later show (Paper I), the degree of flow recovery turns out to be dependent on the underlying volume state.

In the same period, Pinsky and Vincent published a related study describing the effect of positive pressure and PEEP on RV function (83, 85). Apart from being valuable descriptions of heart-lung-interactions in a general sense, these studies were necessary for the development of airway pressure maneuvers for the estimation of MSFP that was to follow. One of many results from these studies was a synthesis on how positive pressure insufflation causes a cyclic ebb-flood tide of blood volume shifting out from the pulmonary compartment and into the systemic compartment during inspiration, and that an overlapping similar modulation with higher frequency occur as a consequence of cardiac contractions. This is of special relevance for this thesis - in particular papers I, II and IV.

1.8.3 LOADING OF VENOUS CAPACITANCE

The previously described method for the construction of a VR curve requires a time consuming series of inspiratory pause procedures (IPPs) to several levels of P_{AW}. As a possible alternative, den Hartog together with Versprille and Jansen, evaluated the performance of a slow inflation procedure (SIP) (25). If the instantaneous VR curve of Pinsky used cyclic changes during tidal ventilation, the idea with a SIP was to perform a beat-to-beat analysis of Q_{PA} matched with mean CVP from the previous beat, for all consecutive beats falling under a slow increase in P_{AW}. As an increasing backpressure is associated with volume loading in upstream vessels, the concept acknowledges that each data pair in a SIP will slightly underestimate steady state VR at that level of CVP. In a variant of the pig model described above (EM flowprobe around the PA, PEEP 2 cmH_2O), slow inflation procedures of 2.4, 4.8, 7.2, 9.6, and 12 s were performed to tidal volumes of 15 and 30 mL/kg. As a reference, MSFP was calculated as the zero-flow extrapolation from linear regression of IPPs (inflation time 2.4 s, inspiratory pause 12 s, and expiration during 3.6 s with data collected as mean values of the last 5 s; '$P_{sf,\ IPP}$') to tidal volumes between 0-30 mL/kg. Determination of $P_{sf,\ IPP}$ was performed at baseline and repeated after the SIPs. $P_{sf,\ IPP}$ = 12.9 ± 1.9 mmHg, and the 95% repeatability coefficient was 0.75 mmHg [the least true change detectable with a 95% probability (73)]. The result confirmed that use of SIP underestimated MSFP as determined with IPP, but this was less pronounced at the longer inflation times. At an inflation time of 12 s, mean values from SIP was ~1 mmHg lower than the reference method. After fitting an exponential function to the data, the theoretical inflation time needed to reduce the difference between $P_{sf,\ SIP}$ and $P_{sf,\ IPP}$ to ≤0.75 mmHg, was estimated to 18 s. A long inflation time holds the additional benefit of including more data points. However, even if the SIP was less time consuming than a standard inspiratory hold procedure, an inflation time of 18 s could risk reflex activation. If a reliable measure of SV_{RV} would become available at the bedside, automated data extraction during slow inflation in sedated patients was suggested as a future possibility.

In my opinion, the merit of the study lies in exploring the mechanisms and quantifying the impact of upstream volume loading on the estimation of MSFP. It is a pity that the authors already seemed to perceive $MSFP_{insp\_hold}$ as an established reference method. If the authors would have included a zero-flow reference method and extended the protocol to include changing blood volume, the results could have changed the following 15 years of research.

1.8.4 TOWARDS CLINICAL APPLICATION

The final step in validation of the inspiratory hold model for clinical estimation of MSFP was to compare the performance of right- and left-sided measures of flow during the steady state phase of inspiratory pause. A second objective was to determine the effects of reducing the number of airway pressure levels included in the estimate. These questions were addressed in an animal experiment by Maas (54). In 10 piglets, ventilated at PEEP 2 cmH_2O, flow was measured with EM probes on the PA and ascending aorta (CO_r and CO_l, respectively). In addition, flow was estimated by pulse contour cardiac output (CO_{pc}) from the arterial pressure waveform measured in the aorta (Modelflow technique modified for pigs, FMS, Amsterdam, the Netherlands). The relation between CVP and flow during inspiratory maneuvers was evaluated twice in normovolemia, separated by 50 min. Inspiratory hold maneuvers lasting 12 s were applied with tidal volumes between 0-300 mL. Mean values for pressure-flow data were extracted during the last 5 s of inspiratory pause. An example is presented in Figure 10. A total of 133 paired measurements were examined. When pooled data taken during tidal ventilation was compared, no difference was seen between CO_r and CO_l, but small significant differences were found between CO_r and CO_{pc}, and CO_l and CO_{pc} respectively. Interestingly, the bias between CO_r and CO_{pc} was 0.32 $mL \times s^{-1}$, with limits of agreement (LoA) -1.24 to 1.88 $mL \times s^{-1}$, compared to a mean of methods of 11.06 $mL \times s^{-1}$. Although not reported, this amounts to a percentage error of 28%. All pressure-flow relations were highly linear. The zero-flow extrapolations resulted in a P_{msf} (CO_l) = 10.8 ± 1.0 mmHg and P_{msf} (CO_{pc}) = 10.4 ± 1.1 mmHg. Bias was 0.40 ± 0.48 mmHg with LoA -0.56 to 1.35 mmHg. The repeatability coefficients were 0.67 and 0.63 mmHg respectively. With a CVP of 3.7 ± 0.5 mmHg, VRdP was ~6.7-7.1 mmHg.

From a methodological point, comparison between P_{msf} (CO_{pc}) and P_{msf} (CO_r) would have been more appropriate, as the hypothesis was that a left-sided flow measurement could be used to assess the right-sided process of venous return. To put the method agreement into physiological perspective (my note), a LoA of 1.91 mmHg amounts to ~28% of normovolemic VRdP, which is a lot. Reducing the number of inspiratory holds performed from 7 to 2 did not appear to change the method agreement between P_{msf} (CO_l) and P_{msf} (CO_{pc}), but data supporting this claim was not presented. The authors conclude that MSFP can be estimated using changes in CVP and pulse contour cardiac output from inspiratory hold maneuvers to 3-4 levels of airway pressure. Left without comment is the obvious difference in early phase inspiratory hold flow restoration between the PA and aorta that can be seen in Figure 10. A dynamic decrease and restoration can be observed in the PA (see also Figure 18), with

considerable less action visible on the left side. This phenomenon was described in section 1.8.2 and is associated with volume shift from the cardiopulmonary compartment to the systemic compartment, with the potential to affect the estimation of MSFP.

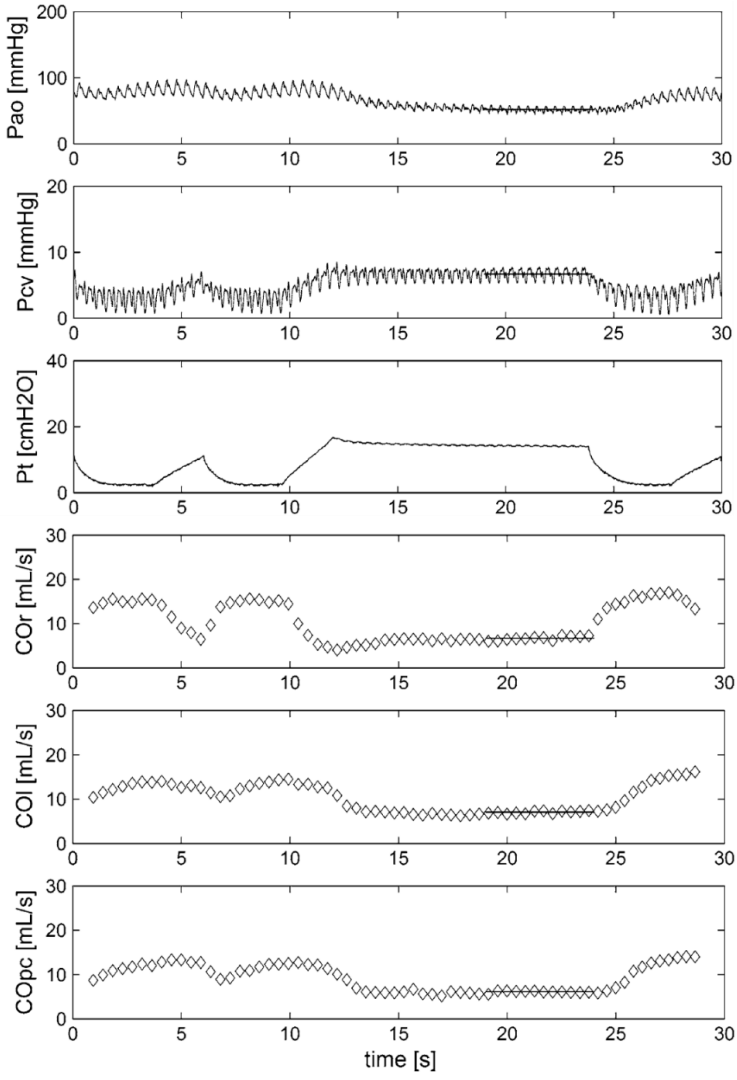

Figure 10 – Effects of an inspiratory hold on aortic pressure (P_{ao}), central venous pressure (P_{cv}), airway pressure (P_t) and beat-to-beat cardiac output (CO) with a probe around the pulmonary artery (CO_r), around the aorta (CO_l) and by pulse contour analysis (CO_{pc}). Preceding the hold, the effects of a normal respiratory cycle are plotted. From Maas (54). Note the difference in beat-to-beat changes in flow as measured by CO_r and CO_l or CO_{pc} – especially during the first 2 s of increasing P_t. Reproduced with permission from Springer Nature.

1.8.5 INSPIRATORY HOLD MANEUVERS IN THE ICU

The first patient study on the technique was published 2009 by Maas and co-workers (55). The study included 12 sedated and mechanically ventilated patients after cardiac surgery. Flow was measured as pulse contour cardiac output (Modelflow, FMS, Amsterdam, the Netherlands), and CVP was measured with a central venous catheter. The method assumes that changes in VR is transmitted to the left side, and that a new steady state can be measured during the last 3 s of a 12 s inspiratory hold (Figure 11). Central venous pressure was increased by inspiratory hold maneuvers to airway plateau pressures of 5, 15, 25 and 35 cmH_2O, separated by 1 min intervals (PEEP levels were not reported). A linear equation was fitted to mean values of CVP and CO from the four levels, and MSFP was estimated by extrapolation to zero flow. The inspiratory hold maneuvers were performed under three volume

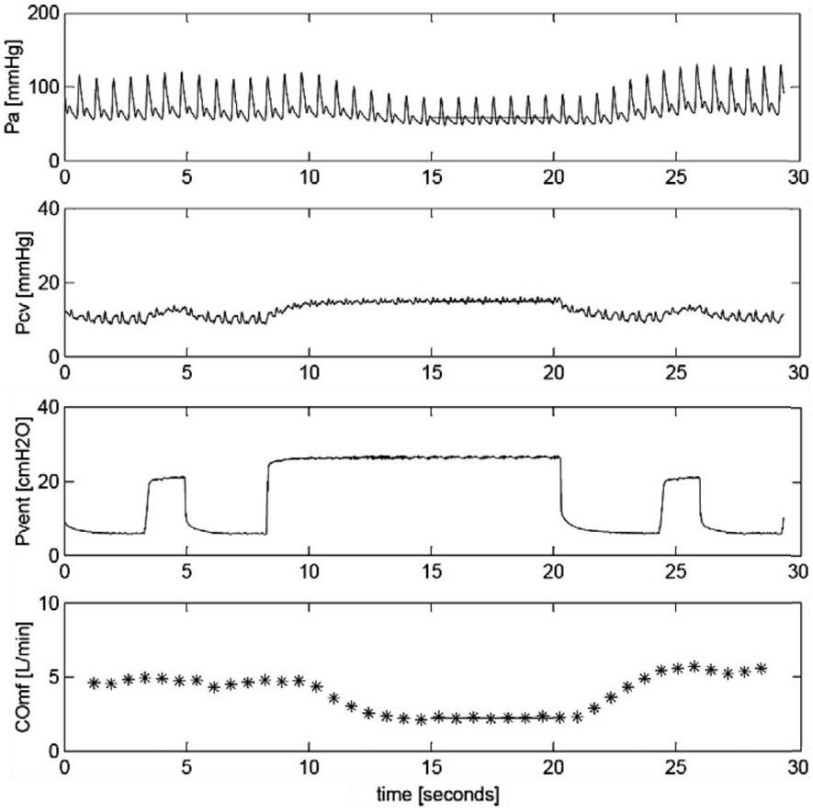

Figure 11 - Effects of an inspiratory hold maneuver on arterial pressure (P_a), central venous pressure (P_{cv}), airway pressure (P_{vent}), and beat-to-beat cardiac output (CO_{mf}). Preceding the hold maneuver, the effects of tidal ventilation can be seen. From Maas (55). Reproduced with permission from Wolters Kluwer.

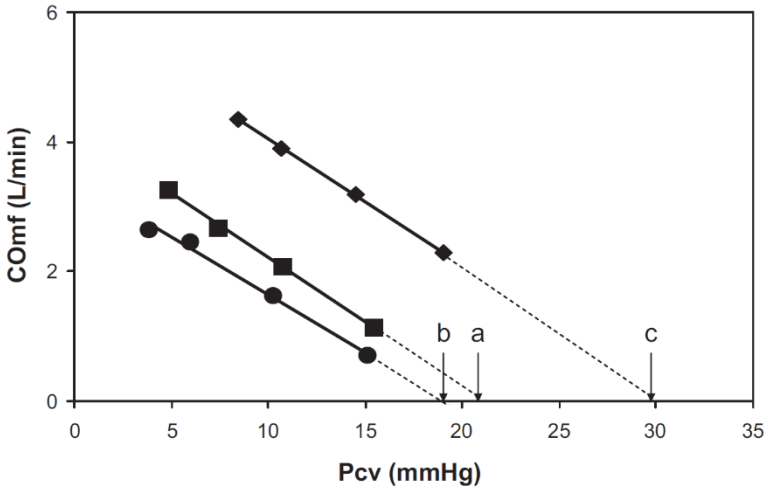

Figure 12 – Relationship between venous return (CO_{mf}) and central venous pressure (P_{cv}) for an individual patient. Venous return curves are plotted for three conditions: baseline (a), hypovolemia (b), and hypervolemia (c). From Maas (55). Reproduced with permission from Wolters Kluwer.

states: baseline, in relative hypovolemia induced by anti-Trendelenburg tilt, and after volume expansion with 500 mL of hydroxyethyl starch (hypervolemia). The effects of an inspiratory hold maneuver and examples of VR curves for one individual can be seen in Figures 11-12. P_{msf} was 18.8 ± 4.5, 14.5 ± 3.0, and 29.1 ± 5.2 mmHg at baseline, hypovolemia and hypervolemia, respectively. CVP at baseline was 6.7 ± 2.3 mmHg, and the resulting VRdP (with changing CVP and MSFP over volume states) was 12.0 ± 3.7, 10.5 ± 2.3, and 19.4 ± 6.9 mmHg, at baseline, hypovolemia and hypervolemia, respectively. This is surprisingly high compared to VRdP of ~ 7 mmHg, obtained with the same technique in the porcine model described above, but is left without comment in the paper. When compared to the estimated values of VRdP ~ 4-4.5 mmHg from the ICD studies of Jellinek and Schipke, the VRdP estimated with the inspiratory hold method is remarkably high. The authors still conclude this to reflect the true volume status in postoperative patients.

1.9 THE IMPACT OF AIRWAY PRESSURE ON ZERO-FLOW PRESSURES

1.9.1 THE EFFECT OF PEEP

The use of positive end-expiratory pressure (PEEP) as an adjunct to ventilator therapy is associated with a decrease in CO. The main effect was first thought to be a decrease in venous return driving pressure caused by the elevated RAP. Fessler showed that PEEP did increased RAP, with an associated decrease in flow and arterial pressure (30). However, within a minute, VRdP had been restored by a compensatory increase in MSFP. The fact that VR still was decreased compared to the situation with zero PEEP, was explained by an increase in the resistance to venous return (RVR). The alternative explanation was that the increase in PEEP level was associated with development of vascular waterfalls that decoupled RAP from VR, so that the effective backpressure was exerted further upstream from the RA. This would mean that true VRdP was decreased.

Fessler's study included three groups of six anesthetized dogs each, all ventilated with tidal volumes of 15 mL/kg. All animals were examined at PEEP levels of 0 and 15 cmH_2O. Cardiac output was measured by thermodilution and MSFP was determined at zero flow induced by ventricular fibrillation (unassisted AV equilibration and no correction factor used). The effect of increased and decreased abdominal pressure was studied by binding the abdomen, or exposing the exteriorized intestines to atmospheric pressure, respectively. In the first group, cardiovascular reflexes were left intact. In the second, group the reflex arch was cut by carotid sinus and vagal denervation (CSV), and in the third group total spinal anaesthesia was induced and arterial pressure restored by infusion of epinephrine (SAE). With intact reflexes, altering the abdominal pressure had no effect on the rise in MSFP during PEEP. CSV attenuated the rise in MSFP by 17% and SAE did so by 49%. The conclusion was that the PEEP-associated increase of MSFP was caused by both reflex mediated changes in vascular capacity, and mechanical effects of central to peripheral translocation of blood. Stated differently, the initial fall in arterial pressure caused by the added PEEP led to activation of the sympathetic nervous system. The resulting vasoconstriction decreased vascular capacitance, recruited stressed volume (V_s) and thereby increased MSFP. Importantly, more than 50% of the increase in MSFP was unrelated to reflex activation: simply pressurizing the thorax led to a shift of blood volume to the periphery. A shift of volume from regions of high compliance to low compliance will increase stressed volume and MSFP, even if the capacitance is unchanged.

Fessler verified the results of increased RVR on PEEP in a bypass experiment where VR was uncoupled from cardiac function at PEEP levels of 0 and 10 cmH_2O (29). PEEP increased the backpressure for VR in both SVC and IVC circulations, and in SVC, it also decreased venous conductance.

Nanas and Magder studied the effect of increasing PEEP from 0-10 and 10-20 cmH_2O in 13 splenectomised dogs, with tidal volumes (TV) 12-15 mL/kg. MCFP was determined at zero flow induced by right atrial balloon occlusion (unassisted AV equilibration and no correction factor used). The ventilator was turned off while the RA balloon was inflated, but it was not specified if this was done in a defined phase of the respiratory cycle. The impact of airway pressure on the measured MSFP is therefore unclear. Blood volume (BV) was estimated with Evans blue dye dilution technique. Vascular compliance (C_{vasc}) was determined in 3-point pressure-volume plots (P-V plots or elastance curves) where MCFP was determined immediately after blood volume expansion in two steps (adding 4 and 8 mL/kg blood from donor dogs). Increasing levels of PEEP increased CVP and decreased CO, with VRdP preserved (at ~ 8 mmHg) by concomitant increases in MCFP. At PEEP levels 10 and 20 cmH_2O, the elastance curve was shifted to the left (slope unchanged). Since the blood volume was stable, this implied recruitment of V_s.

1.9.2 THE EFFECT OF POSITIVE PRESSURE *VS.* SPONTANEOUS BREATHING

Chihara studied the effect of spontaneous *vs.* intermittent positive pressure ventilation (IPPV) on MSFP and VRdP in rats (21). MSFP was determined by RA balloon occlusion with a correction factor of AV compliance ratio used to adjust for incomplete pressure equilibration. CO was determined by trans-pulmonary thermodilution and BV was determined by dilution of ^{51}Cr-labeled erythrocytes. Three groups of tracheotomised animals under anaesthesia were studied in the transition from spontaneous to controlled ventilation at zero PEEP and TV 15 mL/kg. CVP increased (0.7 ± 1.3 *vs.* 3.2 ± 1.2 mmHg), and CO decreased when IPPV was started. MSFP increased from 7.1 ± 1.2 to 8.6 ± 1.1 mmHg and VRdP decreased from 6.4 ± 1.1 to 5.4 ± 0.9 mmHg (all data as mean ± SD). Total peripheral resistance (TPR) increased but RVR was *unchanged*. IPPV caused a parallel shift of the VR curve to the right. Maintained arterial pressure in spite of decreased CO (i.e. increased TPR) indicated vasoconstriction by activation of the sympathetic nervous system. C_{vasc} and BV were unchanged between ventilation modes and therefore V_s had been recruited. Vasoconstriction and central-to-peripheral volume shift were thought to have increased MSFP. As the increased intra-thoracic pressure associated with positive pressure ventilation is also transmitted to the abdominal compartment (14, 30), the blood would be shifted preferentially to extra-abdominal regions of the systemic compartment, where vascular compliance is low (21).

To summarize so far, Versprille quantified the dynamic central-to-peripheral volume shifts during tidal ventilation and found them to have negligible effects on upstream pressure (96, 97). The findings of Fessler, Nanas and Chihara (21, 30, 71) all showed that a *sustained* increase in P_{AW} was associated with increases in both downstream pressure (RAP) and upstream pressure – i.e. stressed volume and MSFP. Part of that increase was mechanical in nature, related to volume shifts from the central compartment to the periphery. Importantly, the increase from volume displacement was unrelated to reflex activation and most likely effective immediately. This is supported by the finding of Jellinek, where an inspiratory hold started 5 s prior to the FDS resulted in an increase of MCFP by 1.2 mmHg. This has implications for the estimation of MSFP by airway pressure maneuvers.

1.9.3 THE EFFECT OF IMMEDIATE CHANGES IN AIRWAY PRESSURE

In 2017 (just after Paper II of this thesis was submitted), Repessé published a study on the impact of positive pressure ventilation on MCFP. Right atrial and mean arterial pressures were measured in 112 critically ill patients, within one minute after death, while still on mechanical ventilation (Figure 13). Data representing end-expiration and inspiration, on and off PEEP (8.2 ± 2.6 *vs*. 0 cmH_2O) was recorded and extracted off-line. Off ventilator, the RAP (representing MCFP), was ~ 10 mmHg. Tidal ventilation (6.6 ± 1.6 mL/kg) increased RAP by 2.4 mmHg, and the (acute) application of PEEP increased RAP by 1.2 mmHg. Since no time was allowed for the possibly intact reflexes to act, only mechanical effects on stressed volume could explain the documented changes in vascular pressures. Therefore, what the authors actually investigated was the impact on zero-flow pressure of *four levels of acutely changing* P_{AW}, rather than two levels of PEEP levels with superimposed tidal inflations, in the sense understood by Fessler or Nanas. Although the absolute value of MCFP has to be interpreted in context of a mixed population of critically ill patients just after death, the effect of changing P_{AW} on MCFP was reproduced.

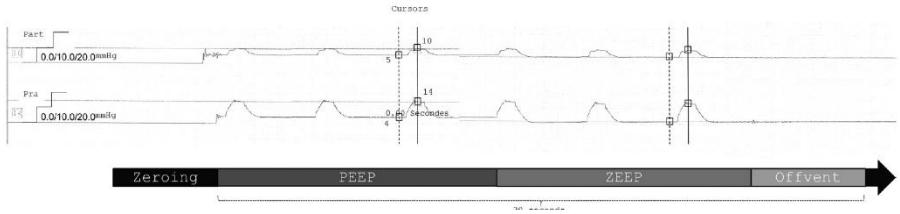

Figure 13 – Illustration of the design of the study with the different experimental conditions along a time scale. Tidal ventilation and PEEP induced increases in arterial (P_{art}) and central venous (P_{ra}) pressures. The continuous vertical line represents the cursor for measurement during inspiration and the dotted vertical line the cursor for measurement during end-expiration. From Repessé (86). Reproduced with permission from the American Physiological Society.

1.10 DYNAMIC ANALOGUE OF STATIC FILLING PRESSURE

Parkin and Leaning developed a dynamic analogue of MSFP for the intended use within a clinical decision support system (76-78). It is based on a two-compartment model of the systemic circulation. It is not related to any intervention on the patient and therefore does not interfere with the system under examination. The underlying static (or zero-flow) systemic filling pressure is calculated from the prevailing (dynamic) steady state values of RAP, MAP and CO, in the running circulation. Assuming that normal *venoarterial compliance* ratio is 24:1, the dynamic analogue of systemic filling pressure (P_{msa}) is calculated as:

$$P_{msa} = 0.96 \times RAP + 0.04 \times MAP + c \times CO \qquad (4)$$

where 'c' is $0.96 \times R_v$, and R_v=resistance in the venous compartment. The factor 'c' has the dimensions of resistance and scales the flow component of P_{msa} to fit the subject. By assuming that the normal *arteriovenous resistance* ratio is 25:1, R_v is estimated as SVR / (25+1), using normal values for age-dependent MAP and age- and size-dependent CO. As a consequence, 'c' varies between ~0.3 in a large young patient to ~1.2 in a small, elderly patient. A normal P_{msa} for a young healthy person with a c=0.5 $mmHg \times min \times L^{-1}$, a RAP of 0 mmHg, a MAP of 100 mmHg and a CO of 6 $L \times min^{-1}$ would be:

$$P_{msa} = 0.96 \times 0 + 0.04 \times 100 + 0.5 \times 6 = 0 + 4 + 3 = 7 \text{ mmHg} \qquad (5)$$

In clinical use, 'c' is calculated once for each patient and the continuously updated P_{msa}, incorporating the changing values of RAP, MAP and CO, relies on the assumption that true R_v remains constant. P_{msa} therefore is a composite variable, where the true and unknown values of MSFP and R_v are combined and presented as an 'effective upstream filling pressure'. It reflects clinical reality where, based on the available central hemodynamics, it is impossible to distinguish a falling VR caused by *increased* R_v and preserved MSFP, from a falling VR caused by unchanged R_v and *decreased* MSFP (e.g. "is the surgeon compressing the vena cava, or is the patient hypovolemic?").

A derived variable of global heart efficiency can be calculated from P_{msa} as:

$$E_h = (P_{msa} - RAP)/P_{msa} \qquad (6)$$

E_h is a dimensionless number between 1 and 0, that quantifies the heart's ability to keep RAP low in respect to the upstream pressure. In the clinical decision

support system, anthropometric data is entered together with the desired goals for MAP and CO. At any time point, the patient's current position in relation to the set target is presented on a screen and provides a graphic guide to the interpretation of the inotropic, resistive and volumetric state of the circulation.

The model was tested in a closed-loop control of fluid replacement to ten patients receiving continuous haemodiafiltration (75). P_{msa} was continuously calculated using cardiovascular variables acquired from the bedside monitors, and compared to a target value. A computer-controlled clamp, where the input signal was the difference between current and target values of P_{msa}, guided gravitational fluid replacement to the dialysis circuit. Closed-loop fluid replacement was associated with hemodynamic stability and considered safe.

Gupta assessed the response to fluid boluses in 61 cardiac postsurgical patients, mechanically ventilated (PEEP 5 cmH_2O and TV 6-8 mL/kg) and CO measured by thermodilution in triplicate (38). For both responders (defined as an increase in CO ≥10%) and non-responders, baseline RAP was 11 ± 4 mmHg and P_{msa} was 17 ± 3.7 and 17 ± 3.6 mmHg respectively. VRdP was 5.7 ± 0.8 and 6.6 ± 1.1 mmHg and CO 4.4 ± 0.9 and 5.6 ± 1.6 $L \times min^{-1}$ respectively. Although not commented on in the paper, the values for RAP are clearly pathological, but for this group of patients together with an acceptable CO, it represents a common postoperative finding. The combination of surgical trauma, perioperative volume treatment, mechanical ventilation with PEEP and an unspecified amount of temporarily decreased heart function commonly presents with an increased RAP. In the calculation, RAP will always affect P_{msa} by a factor 0.96. Importantly, VRdP is in the range of what can be expected from human data reported by Jellinek and Schipke (4-4.5 mmHg), and invasive animal data from Fessler (~4 mmHg) and Nanas (~8 mmHg) (30, 46, 71, 90).

1.11 TRANSIENT STOP-FLOW – THE ARM-OCCLUSION TECHNIQUE

If the circulation in the arm could be immediately isolated from the remaining body by means of a rapidly inflating tourniquet, the vascular pressures within the arm would equilibrate to MSFP. The vascular compartments of the arm must behave like an integral part of the total systemic compartment, and since pumps do not separate them, their equilibrated pressures must be equal. Per definition, if the zero-flow pressures would not be the same, the arm and the remaining systemic circulation would not have been in equilibrium prior to the inflation, but rather in the midst of volume shift, expanding or decreasing the total volume of the arm. The technique, as described by Anderson and Pang (2, 74), requires the use of a narrow blood pressure cuff, in order to avoid displacement of blood volume distally into the arm. The pressures measured in the radial artery and a peripheral vein can be seen to equilibrate within 30 s (P_{arm}) (Figure 14). Persistent flow via incompletely occluded vessels will affect the measurement.

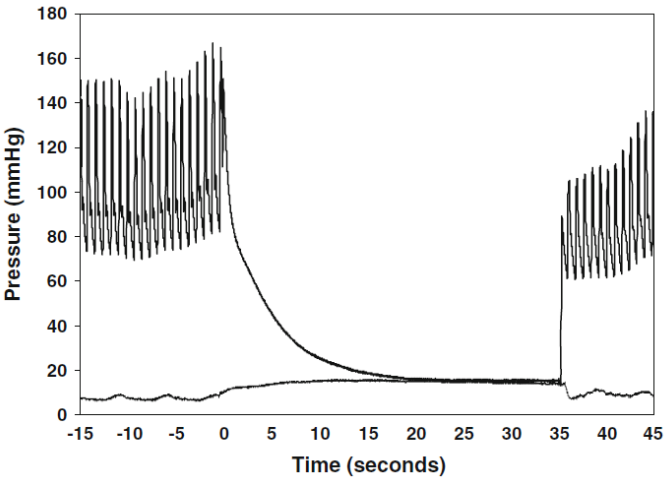

Figure 14 - Radial artery pressure and peripheral venous pressure during the course of occlusion of the upper arm of a patient. The effect of mechanical ventilation on both pressures can be seen before and after occlusion. From Maas (58). Reproduced under the terms of Creative Commons Attribution License.

The method has been tested by Maas and Geerts (33, 56, 58), and its precision was evaluated by Aya (5). The later study included 23 patients following cardiac surgery (mechanically ventilated with TV 7 ± 2 mL/kg at PEEP 5 ± 1

cm H_2O). Mean CVP was 11.1 ± 2.9 mmHg. Mean P_{arm} was 22.4 ± 7.7 mmHg. Although not reported, the group mean VRdP would have been ~11 mmHg. The least significant change (LSC, equivalent to 95% repeatability coefficient) was reported as 14% or 6.2 mmHg. If four measurements were averaged, the LSC was still 3 mmHg, corresponding to 27% of the reported VRdP. With such low precision the method becomes practically useless.

In the study by Geerts, 24 postoperative cardiac surgery patients under mechanical ventilation (PEEP 5 cm H_2O, TV 8-10 mL/kg) received a fluid bolus of 500 mL of hydroxyethyl starch. If CO (as measured by Modelflow, FMS, Amsterdam, the Netherlands) increased >10%, the patient was classified as a responder. Responders (n=17) had baseline values of RAP 8.6 ± 2.6 mmHg, CO 5.1 ± 1.3 $L \times min^{-1}$, and P_{arm} 16.2 ± 6.3 mmHg. Although not reported, the group average VRdP would have been 7.5 mmHg. Only seven patients were non-responders with baseline values of RAP 9.9 ± 2.5 mmHg, P_{arm} 24.3± 8.2 mmHg, and CO 5.5 ± 1.3 $L \times min^{-1}$. The group average VRdP would be ~14 mmHg. After fluid infusion, non-responders had a mean P_{arm} ~30 mmHg.

The combination of un-physiologically high values of VRdP and a low precision raise serious concerns regarding the method. Judging from the results presented here, the method in its current form does not qualify for clinical use.

1.12 METHOD COMPARISON IN CLINICAL POPULATION

In a very illustrative study, Maas compared the estimation of MSFP in postoperative cardiac surgery patients with three methods (58). Eleven mechanically ventilated patients (the same settings as in Geerts above) were examined at baseline, at 30º head up tilt (HUT), and after volume loading with 500 mL of colloid (VOL). Estimation of MSFP was done with inspiratory hold to four levels (P_{msf}), by arm occlusion (P_{arm}), and with the dynamic analogue of Parkin (P_{msa}). The study design focused on assessment of method agreement and did not report VRdP. Hemodynamic variables, MSFP and VRdP are compiled in Table 1. VRdP has been calculated from group means of MSFP and CVP.

	Baseline		**HUT**		**VOL**	
		VRdP (mmHg)		VRdP (mmHg)		VRdP (mmHg)
P_{cv} (mmHg)	7.1 ± 2.0		4.4 ± 1.8		10.4 ± 1.3	
CO (L×min^{-1})	5.8 ± 1.6		4.8 ± 1.2		7.0 ± 1.7	
P_{msf} (mmHg)	19.7 ± 3.9	~12.6	16.2 ± 3.0	~11.8	28.3 ± 4.0	~17.9
P_{arm} (mmHg)	18.4 ± 3.7	~11.3	15.4 ± 3.1	~11.0	27.1 ± 4.0	~16.7
P_{msa} (mmHg)	14.7 ± 2.7	~7.6	10.9 ± 2.0	~6.5	19.2 ± 1.1	~8.8

Table 1 – Hemodynamic variables, MSFP and venous return driving pressure for three volume states. Table compiled with data from Maas (58). Venous return driving pressures (VRdP) was not reported in the original study, but calculated from mean values of MSFP and CVP.

The authors conclude that P_{msf} and P_{arm} are interchangeable and that changes in volume status are similarly tracked by all three methods. They also conclude that the absolute difference between P_{msf} and P_{arm} of – 1.0 ± 3.1 mmHg was not clinically relevant, even though the LoA was -7.3 to 5.2 mmHg. The authors do not comment on the fact that P_{msf} and P_{arm} produce values of MSFP far above what was found by Jellinek and Schipke in patients at zero flow. The related driving pressures for venous return either suggest a state of hyperdynamic circulation, or a remarkably high resistance to flow. In contrast,

the Parkin dynamic analogue reports reasonable estimations of both MSFP and VRdP, when compared to animal and invasive human data. What is lacking is a discussion regarding the intended use of the measured MSFP. Without this, the result from the method comparison cannot be interpreted. What is clinically relevant? In our Paper IV we chose to define a desirable method agreement as ≤10% of euvolemic VRdP. This corresponds to a 10% change in flow which is a commonly used threshold for evaluation of hemodynamic response from volume expansion.

In a systematic review of 17 prospective cohort studies, published in 2018 (before study III of this thesis was submitted), Wijnberge (103) characterized the three clinically used methods for estimation of MCFP: P_{mcf} hold, P_{mcf} arm ($=P_{arm}$), and P_{mcf} analogue ($=P_{msa}$). P_{mcf} hold ranged from 14-33 mmHg. The authors conclude P_{mcf} *"to accurately follow intravascular fluid administration and vascular compliance following drug-induced hemodynamic changes"*. Since none of the three methods were compared to a zero-flow reference, accuracy was actually not assessed at all. All estimates however increased and decreased as could be expected from the hemodynamic interventions. The authors called for studies to determine cut-off values to allow MCFP to trigger therapeutic interventions, as well as to determine its clinical value.

1.13 SUMMARY – FROM GUYTON TO THE ICU

- Mean systemic filling pressure (MSFP) is a function of blood volume and the size and stiffness of the vasculature.
- MSFP can be measured at zero flow.
- In Guyton's cardiovascular model, venous return is driven by the pressure difference between MSFP and right atrial pressure (RAP).
- Fundamental critique of the concept remains, and the controversy has not been resolved in ongoing theoretical debate. The main objection concerns whether RAP exerts active backpressure for venous return, or if it should only be seen as a consequence of the volume redistributive work of the heart. A second matter of conflict is whether Guyton's model should be confined to a descriptive role for steady states, or if it can be applied to changing conditions.
- At zero-flow measurement, a remaining arteriovenous pressure difference reflects an incomplete equilibration. Assisted volume transfer confers only a marginal further increase in venous pressure, which is explained by the relative compliances of the arterial and venous compartments.
- An extensive series of experimental work has led to the development of a method for estimation of MSFP by zero-flow extrapolation from inspiratory hold maneuvers ($MSFP_{insp\_hold}$). This method has been used in several clinical studies on postcardiac surgery patients and general ICU patients, including those with septic shock.
- MSFP can be estimated in patients using an arm-occlusion technique (P_{arm}).
- A dynamic pressure analogue of MSFP (P_{msa}) can be calculated from mean values of RAP, MAP and CO measured with running circulation.
- Application of PEEP leads to an increase in MSFP, involving activation of cardiovascular reflexes, and a shift of central blood volume into the systemic compartment. Conflicting results exist whether the PEEP-associated decrease in venous return is primarily caused by a decreased driving pressure for venous return (VRdP), or an increase in resistance to VR.
- Since acute changes in airway pressure are transmitted to vascular pressures and cause volume shifts, they affect MSFP.

- The range of values from $MSFP_{insp\_hold}$ maneuvers and P_{arm} occlusion techniques *considerably exceeds* that which can be expected based on animal data and zero-flow measurements in patients undergoing ICD testing.
- Values of MSFP estimated using the dynamic analogue P_{msa} are in the same range as data from patients undergoing ICD testing, but also include higher values in volume loaded postoperative patients.

2 AIM

The venous return physiology of Guyton has been introduced into clinical research, with interesting albeit sometimes unexpected results. At the same time, the underlying physiology with possible interaction between airway pressure maneuvers and stressed volume, is partly unexplored. Fundamental controversies regarding the determinants of venous return are still unresolved.

Many of the remaining questions can only be addressed with direct access to zero-flow measurements of MSFP, which requires experimental animal models. Since the concept of MSFP was brought from Guyton's physiology laboratory into the ICU, the overall aim of the studies included in this thesis, was to bring it back to the lab again.

2.1 MSFP – FROM GUYTON TO THE ICU, AND BACK AGAIN

Paper I addresses the following questions:

- Do changes in PEEP, volume status, and tidal breaths alter MSFP and the slope of the venous return curve?
- Does MSFP estimated by inspiratory hold maneuvers correspond to MSFP measured at zero-flow caused by right atrial occlusion?
- Do inspiratory hold maneuvers *per se* modify the hemodynamic variables of the venous return function? If they do, are these responses dependent on PEEP level and/or volume status?

Paper II addresses the following questions:

- If all technical and design issues of Guyton's original experiments, highlighted in the ongoing debate, are addressed - can RAP be experimentally proven to act as backpressure for venous return?
- Guyton's cardiovascular model was formulated for steady state. Temporary imbalance between venous return and cardiac output is associated with volume shifts. Which qualitative and/or quantitative modifications are necessary for the model to be applicable during dynamic transition from one steady state to the next?

Paper III addresses the following questions:

- In severe cardiorespiratory failure, venoarterial extracorporeal membrane oxygenation (VA-ECMO) can be lifesaving. Volume expansion is the most common means to increase a clinically inadequate flow, but positive fluid balance is associated with worsening prognosis. As an alternative to volume expansion, can stressed volume be increased by vasoconstriction, to augment driving pressure for venous return and thereby increase maximum ECMO flow?

Paper IV addresses the following questions:

- MSFP estimated by inspiratory hold maneuvers overestimated MSFP measured during right atrial balloon occlusion in euvolemic conditions, but not in hypervolemia or after bleeding. This was explained by different degrees of flow restoration during the static increase in airway pressure. Could the method agreement be improved if the inspiratory hold technique is modified to minimise the impact of flow restoration, using instantaneous VR curves and zero-flow extrapolation from nadir flow data-pairs?
- The dynamic model analogue of static filling pressure P_{msa} is non-interventional. We adapted the model for use in pigs. What is the method agreement *vs*. MSFP estimated with right atrial balloon occlusion over changing volume state?

3 METHODS

Condensed detailed descriptions of the experimental methods can be found in the Method sections of Papers I-IV, respectively. The purpose of the following section is to give a general orientation of the methods used, and provide comparisons of experimental techniques between sub-studies.

3.1 ETHICAL CONSIDERATIONS

The four papers included in this thesis are based on three series of animal experiments, all performed in the Experimental Surgery Unit, Department of Clinical Research, University of Bern (Bern, Switzerland). The studies complied with the Guide for the Care and Use of Laboratory Animals (USA, 1996) and were approved by the Commission of Animal Experimentation of Canton Bern (Bern, Switzerland) (BE7114, BE8315, and BE1617). Results are reported according to the ARRIVE Guidelines (1). We used a total of 38 domestic pigs from a trusted local farmer. The first two-three animals in each series were used in pilot studies to establish the instrumentation and confirm feasibility of the procedures. The animals (females and castrated males) weighed ~40 kg, at twelve weeks of age. They were brought to the Animal Hospital of the University of Bern for a three-day quarantine under veterinary observation. After fasting 12 h with free access to water, one animal per day of experiment was delivered to the Experimental Surgery Unit ('ESI') into the care of a veterinary assisted by properly trained study personnel.

The animals were premedicated with intramuscular ketamine and xylazine, followed by establishment of vascular access via a peripheral vein in the ear. Anaesthesia was induced intravenously using midazolam and atropine, and maintained with infusions of propofol and fentanyl. Adequate depth of anaesthesia was checked at regular intervals, by examining the response to a standardized nose pinch. As an additional means of monitoring (Paper III), we targeted a bispectral index <60 (BIS Quatro, Covidien, Mansfield, MA, USA). If necessary, additional injections of fentanyl and/or midazolam were given before muscle relaxation was induced with rocuronium. At the end of study measurements, the animals were killed in deep anaesthesia by injecting potassium-chloride (experimental series reported in Paper I and IV) or by withdrawal of the ECMO support (Papers II-III).

In order to test the hypotheses in question, the experimental model had to be based on repeated episodes of circulatory arrest. To study the dynamic response to airway pressure maneuvers, venous and arterial flows were

measured invasively with high fidelity perivascular probes. In experimental series II and III, venoarterial ECMO was established and the native circulation was interrupted by ligation of the pulmonary artery, or by inducing ventricular fibrillation, respectively. For obvious reasons, human testing was not an option. Computer modelling, although highly valuable within the research field, could likely not simulate the complex and desired reflex modulation associated with changing PEEP levels and blood volume. Rodent models were not considered feasible due to the small size and incompatibility to available extracorporeal devices. A porcine model was a suitable compromise for several reasons, including existing experience within the research group. Translating the findings into human context was not expected to be problematic. Finally, power calculations were performed to estimate a reasonable sample size (see further in section 3.11). The resulting data sets have proved to be of high quality and will likely allow further hypotheses to be tested in separate papers. Overall, the principles of replacement, refinement or reduction (the 3Rs) have been honoured.

3.2 MEASUREMENTS AND DATA ACQUISITION

Flow was measured using appropriately sized ultrasonic transit time flowprobes, mounted around individual vessels and on the ECMO reperfusion tubing (PAU and ME9 PXL Tubing sensors, respectively; Transonic, Ithaca, NY, USA). Flowprobes around the superior and inferior vena cava (SVC and IVC) were positioned as close to the right atrium as possible, downstream of the vena azygos when this vessel could be identified. For the size of animals used (~40 kg), the IVC required a probe size of 16-20 mm, the SVC 14-16 mm, the pulmonary artery (PA) 16 mm, and the descending (intrathoracic) aorta 14-16 mm. An ascending aortic flowprobe position was not possible due to interference with the arterial reperfusion cannula. A 12×20 mm balloon catheter (Tyshak II, Numed, Canada) was fixed in the pericardium at the level of the right atrium. An oesophageal balloon catheter (Sidam, Mirandola, Italy) was orally inserted. A cystostomy was established to drain the urinary bladder. Intravascular, oesophageal, pericardial and airway pressures were measured using transducers (xtrans, Codan Medical, Lensahn, Germany) and a modular multiparameter monitor (S/5 Critical Care Monitor, Datex-Ohmeda, GE Healthcare, Helsinki, Finland), also displaying ECG, peripheral oxygen saturation and end-tidal carbon CO_2. Correct positions of the pericardial and oesophageal balloons were confirmed by chest compression during an expiratory hold (84). Transmural caval pressures were calculated as [P_{caval_vein}–$P_{oesophagus}$], and transmural right atrial pressure as [RAP–$P_{pericard}$]. Since the reliability for the *absolute* values of oesophageal and pericardial pressures are notorious, we use instead the *change* in transmural pressures between conditions (10, 36, 37). Mixed venous blood gases were sampled via the venous drainage tubing in the ECMO experiments (series II-III). Arterial pressure and blood gases were measured via a catheter in the right carotid artery, with the tip advanced to the aortic arch. Blood gases were analysed on a standard bedside monitor (ABL90 Flex, Radiometer Medical, Brønshøj, Denmark) while haematocrit was analysed separately in an assay suitable for pig blood (Clinical laboratory of the Animal Hospital, University of Bern).

The output from pressure transducers and flowmeters were recorded at 100 Hz using a data-acquisition system (LabVIEW, National Instruments, Austin, TX, USA). Offline processing was done using a customized analysis software (Soleasy, Alea Solutions, Zürich, Switzerland). The correct position of the tip of the catheter used for measuring RAP was verified either by lateral-lateral fluoroscopy, or manually by the surgeon during open chest procedures. The level of the RA was marked on the external aspect of the chest. Pressure

transducers and the level of the venous inlet port of the ECMO (series II-III) were vertically aligned to the RA using a spirit level.

Pressure transducers were zeroed and two-point calibrated against atmospheric pressure and a U-manometer. Flowmeters were zeroed and calibrated electronically before the study measurements. Baseline drift for both pressures and flows was checked at the end of the experiment. During experimental series II-III (ECMO setup, Papers II-III), duplicate transducers connected to the same catheter lumen were used to measure RAP. If relevant baseline drift was noted in the offline analysis, the channel with least signal drift was chosen. The recorded data sets were corrected for offset and scale factors prior to analysis.

3.3 ZERO-FLOW MEASUREMENTS

3.3.1 RIGHT ATRIAL BALLOON OCCLUSION

In the first experimental series (Paper I), we used the technique of right atrial balloon occlusion (RAO) as a means to induce reversible circulatory arrest, as described by Ogilvie [section 1.6 and reference (72)]. Via an introducer sheath in the right femoral vein, a catheter with a 50×34 mm inflatable high compliance balloon was advanced to a position distal to the IVC flowprobe (Amplatzer sizing balloon, St. Jude Medical, St. Paul, MN, USA). At the time of zero-flow measurement, the catheter was advanced further, under fluoroscopic control, to lie within the right atrium (RA). To measure $MSFP_{RAO}$, the balloon was filled with a mixture of radiocontrast and saline with the ventilator in expiratory hold. Circulatory arrest was confirmed as PA flow dropped to zero. Rapid pressure equilibration followed and central venous pressures reached a clear plateau (Figure 15). To avoid possible interference between the catheter for RAP measurement and the balloon, $MSFP_{RAO}$ was taken as the mean value of SVC and IVC pressures during 3 s of venous plateau pressure. The effects of sympathetic activation was seen as a secondary sharp increase in all vascular pressures. The venous pressure plateau was reached around 9 s after balloon occlusion and always prior to reflex activation. Since both ventricles continued to beat, volume was shifted *between* the

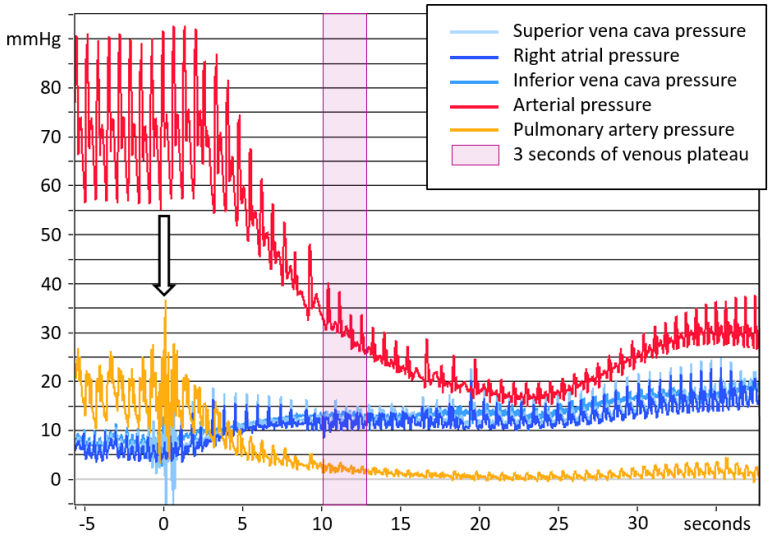

Figure 15 – Right atrial balloon occlusion. The arrow marks balloon inflation. MSFP was taken as the mean value of pressures in superior and inferior vena cava during 3 s of venous pressure plateau. The effects of sympathetic activation can be seen as a secondary increase in pressures ~10 s later. From Paper I.

cardiopulmonary and systemic vascular compartments, as well as *within* the systemic compartment (as arteries emptied into venous vessel beds). After deflation of the balloon, hemodynamics quickly normalised. At least 3 min were given for heart rate and arterial blood pressure to return to baseline levels. The remaining arteriovenous pressure difference at the time of MSFP measurement was (n=43, all volume states, mean ± SD) 10.8 ± 5.4 mmHg, ranging from 0 to 22 mmHg. This represents an almost full equilibrium as the remaining AV pressure differences in the experiments of Ogilvie (72) and Jellinek (46) were 22 and 18-20 mmHg respectively. Based on his and supported by the study of Green (35), we did not apply any correction factor.

3.3.2 VENOARTERIAL BYPASS AND LIGATED PULMONARY ARTERY

In the second experimental series, we wished to examine the determinants of venous return excluding any interference from cardiac factors. The experimental setup was that of a closed-chest venoarterial, total heart-bypass model, with ligated pulmonary artery. The ventilator was not used for gas exchange, but as a means of controlling the intrathoracic pressure. The heart was still beating, but the circulation was fully dependent on extracorporeal membrane oxygenation (ECMO). We used a conventional venoarterial ECMO circuit (Cardiohelp, HLS Set Advanced 5.0, Maquet, Rastatt, Germany) with an added arteriovenous shunt between the arterial and venous tubing (see Figure 16). The shunt was kept closed with a clamp. Venous return was drained through a right-angle metal tip 28 Fr venous cannula, and the arterialised blood was reperfused thru a wire-reinforced 18 Fr arterial cannula (Medtronic, Minneapolis, MN, USA). The ECMO unit generated non-pulsatile flow by use of a centrifugal pump. Venous pulsations were still visible since the contracting right ventricle affected RAP - in many animals also with signs of tricuspid regurgitation. Flow mas measured in the SVC, IVC, in the arterial reperfusion tubing, and in the descending thoracic aorta as described in section 3.2. Intermittent heparin boluses were used to keep an activated clotting time >180 s.

In the stop flow maneuvers, the arterial and venous tubing was clamped simultaneously. If the shunt was kept closed (CS), pressure equilibration occurred in antegrade direction only, as the arterial compartment emptied into venous vessel beds. If the shunt was opened (OS), pressure equilibration occurred in both antegrade and retrograde directions (including directly from the aorta into central veins). The protocol also included stop flow maneuvers performed with the ventilator either in expiratory hold or inspiratory hold, as well as with ongoing tidal ventilation. Flow was resumed after 30 s, or earlier if reflex-mediated increase in arterial blood pressure (ABP) was seen on the bedside monitor (see Figure 17).

MSFP was taken as the mean value of RAP during three beats of equilibrium, defined from the ABP nadir. With open shunt (OS) in expiration, the remaining pressure difference at time of best equilibrium was (n=29, all volume states, mean ± SD) 0.1 ± 1.4 mmHg – i.e. not different from zero. With closed shunt (CS) in expiration, the corresponding value was (n=29) 2.9 ± 2.3 mmHg.

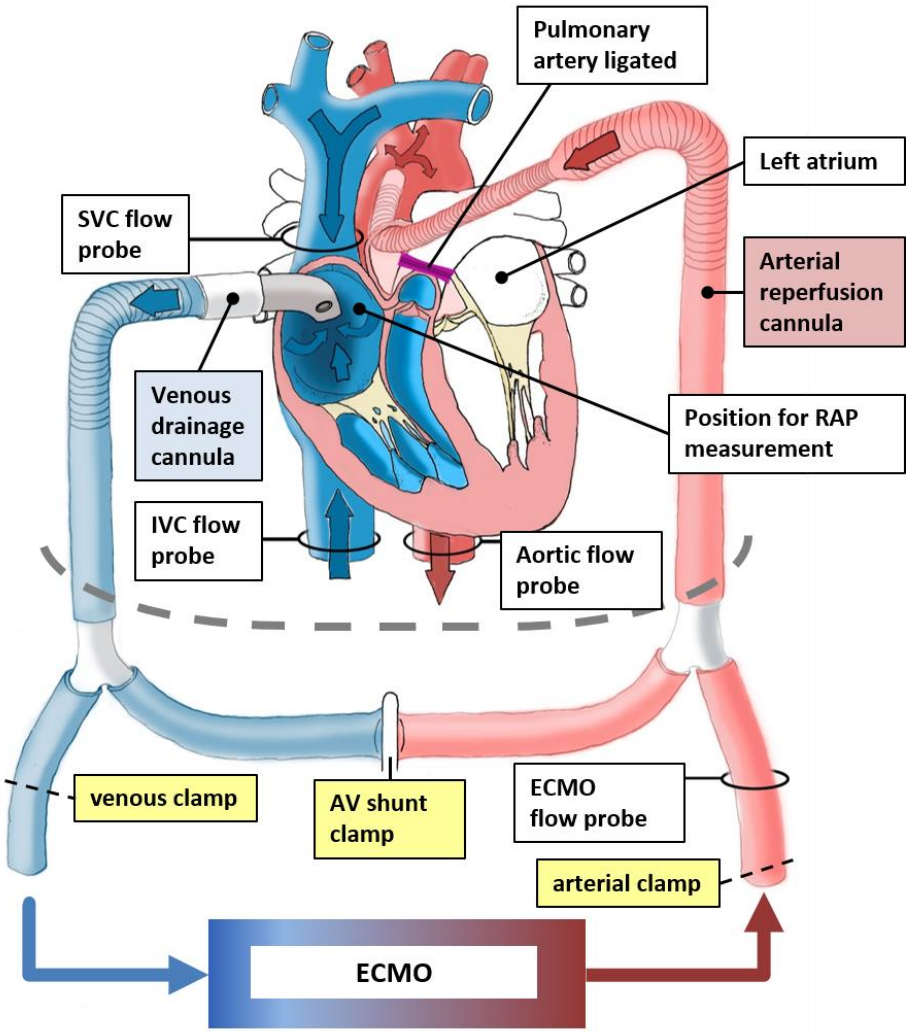

Figure 16 – Extracorporeal membrane oxygenation (ECMO) circuit used in Paper II, including cannulas, arteriovenous (AV) shunt, and sites for flowprobes and RAP measurement. Items below the grey dashed line were located outside the chest. In Paper III, the pulmonary artery was left intact and ventricular fibrillation was induced. To evacuate blood accumulating upstream from the failing left ventricle, a left atrial vent was added. This cannula was connected to the main venous tubing, upstream of the venous clamp.

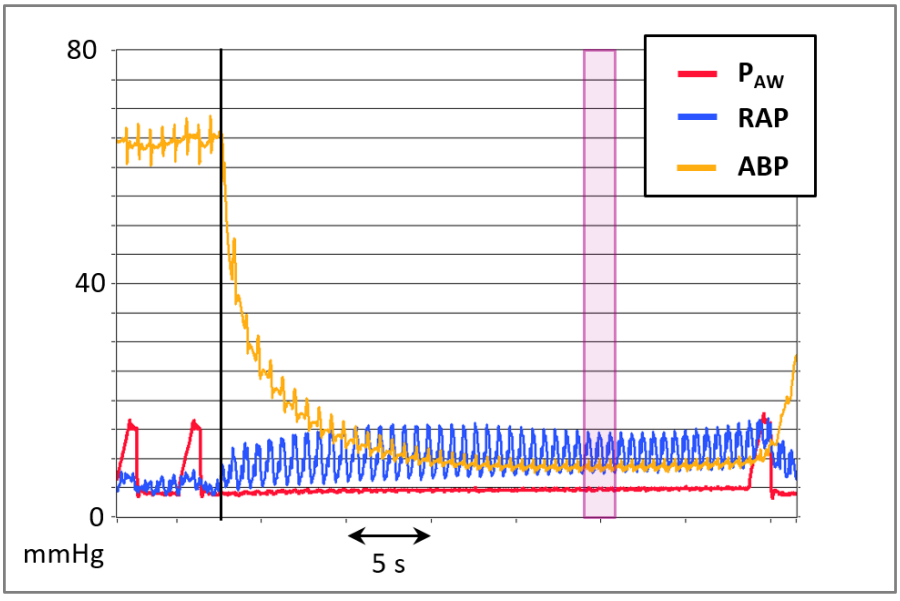

Figure 17 – A stop flow maneuver. The black line marks the beginning of the maneuver where ECMO tubing was clamped and the shunt opened in expiratory hold. Arterial and right atrial pressures can be seen to approach asymptotically. MSFP was taken as mean RAP during three beats of equilibrium defined from ABP nadir (purple bar). The rationale was to ensure full equilibrium as well as avoiding influence from reflex activation. From Paper II.

3.3.3 VENOARTERIAL BYPASS AND VENTRICULAR FIBRILLATION

In the third experimental series (Paper III), we examined the determinants of venous return and VA-ECMO flow, in a porcine model of ventricular fibrillation. We compared the effects of volume expansion with Ringer's lactate and vasoconstriction with norepinephrine on ECMO blood flow and delivery of oxygen (DO_2). Ventricular fibrillation was induced with high rate pacing (1000 bpm, ventricular electrical output 18 mV via epicardial electrodes, Pace 203, Osypka, Berlin, Germany). The ECMO setup was similar to what was described in section 3.3.2, but the pulmonary artery was left intact (see Figure 16). Venous return was drained via a 3-stage venous cannula (29 Fr MC2X) and blood was returned in the ascending aorta (18 Fr elongated one-piece arterial cannula). In addition, a left atrial vent was added to drain blood accumulating upstream of the severely failing left ventricle (16 Fr DLP; all cannulas by Medtronic, Minneapolis, MN, USA). The vent was connected to the main venous tubing. Flowprobes were mounted around the PA (to confirm total loss of right-to-left pump function) and on the arterial ECMO tubing.

In the stop flow maneuvers, all performed in expiratory hold, the arterial and venous tubing were clamped simultaneously and the AV-shunt opened, which also ceased drainage via the left atrial vent. MSFP was taken as the mean value of RAP during 2 s of equilibrium defined from ABP nadir. From offline analysis, the duration from clamping to the end of the 2 s of MSFP measurement was determined to be (n=122, all volume states, mean ± SD) 13 ± 4 s, ranging from 7 to 30 s. Pressure equilibrium was excellent and the remaining pressure difference at time of equilibrium was (n=123, all volume states, mean ± SD) 0.0 ± 1.2 mmHg, range -4.1 to 3.3.

Interestingly, in the pilot studies the preparation was highly unstable. The animals lost plasma volume to such an extent that ECMO pump speed had to be successively lowered to avoid right atrial and venous vessel walls being pushed into the cannula. The resulting flow was inadequate to support a stable preparation. *Post mortem* examination revealed massive pulmonary oedema. When we added the left atrial vent, we regained the excellent stability seen in the first experimental series, using VA-ECMO and ligated PA (Paper II).

3.4 ESTIMATION OF ZERO-FLOW PRESSURE

3.4.1 INSPIRATORY HOLD MANEUVERS

In the first experimental series (Paper I) we estimated MSFP by airway pressure maneuvers to stepwise increasing levels of plateau airway pressure. The animals were ventilated in a volume-controlled mode with tidal volumes of 300 mL (7.7 ± 0.3 mL/kg, F_IO_2 0.3, inspiration-to-expiration ratio 1:2) (Servo-I, Maquet Critical Care, Solna, Sweden) at PEEP 5 or 10 cmH_2O according to the protocol. Before each series of airway pressure maneuvers, the approximate tidal volumes needed to reach plateau pressures of 15, 20, 25, and 30 cmH_2O, were titrated. After 1 min of undisturbed tidal ventilation, the ventilator was set to *expiratory* hold for 30 s, followed again by 1 min of tidal ventilation. The maneuver was repeated with *inspiratory* holds to the target plateau pressures using the previously defined tidal volumes, all separated by 1 min of tidal ventilation (see Figure 18).

The mean values for pulmonary artery flow (Q_{PA}) and RAP of the first three beats occurring 9 s into the maneuver were extracted. The time point of 9 s was chosen to match the settings used by Maas et al (55). Not all animals tolerated the inspiratory hold to 30 cmH_2O. In order to maximise the number of complete data sets, only holds up to 25 cmH_2O were included in the analysis. $MSFP_{insp\_hold}$ was defined as the zero-flow extrapolation of pressure-flow data-pairs (using linear regression) for each animal and condition. A proportion of variance (Pearson correlation coefficient squared; r^2) > 0.7 was required for inclusion in analysis.

The inspiratory maneuvers led to an immediate increase in RAP, with a reciprocal decrease in caval vein flows. In beat-to-beat analysis, the respective beats with nadir values of mean flow for caval veins and PA were identified. Caval vein nadir flow was always seen in the beat with maximally increased RAP, approaching or at peak airway pressure. Nadir PA flow beat followed immediately after caval nadir beat, or in some instances with a delay of one beat. During the following few beats, there was a marked restoration of caval vein and PA flows, as described by Versprille (97). To quantify the *decrease* of flow, we compared flow ratios at nadir to the mean values of all beats during one respiratory cycle preceding the inspiratory hold steps (baseline). In the same manner, *restoration* of flow was quantified as the ratio of [three beats 9 s into the hold] to [baseline].

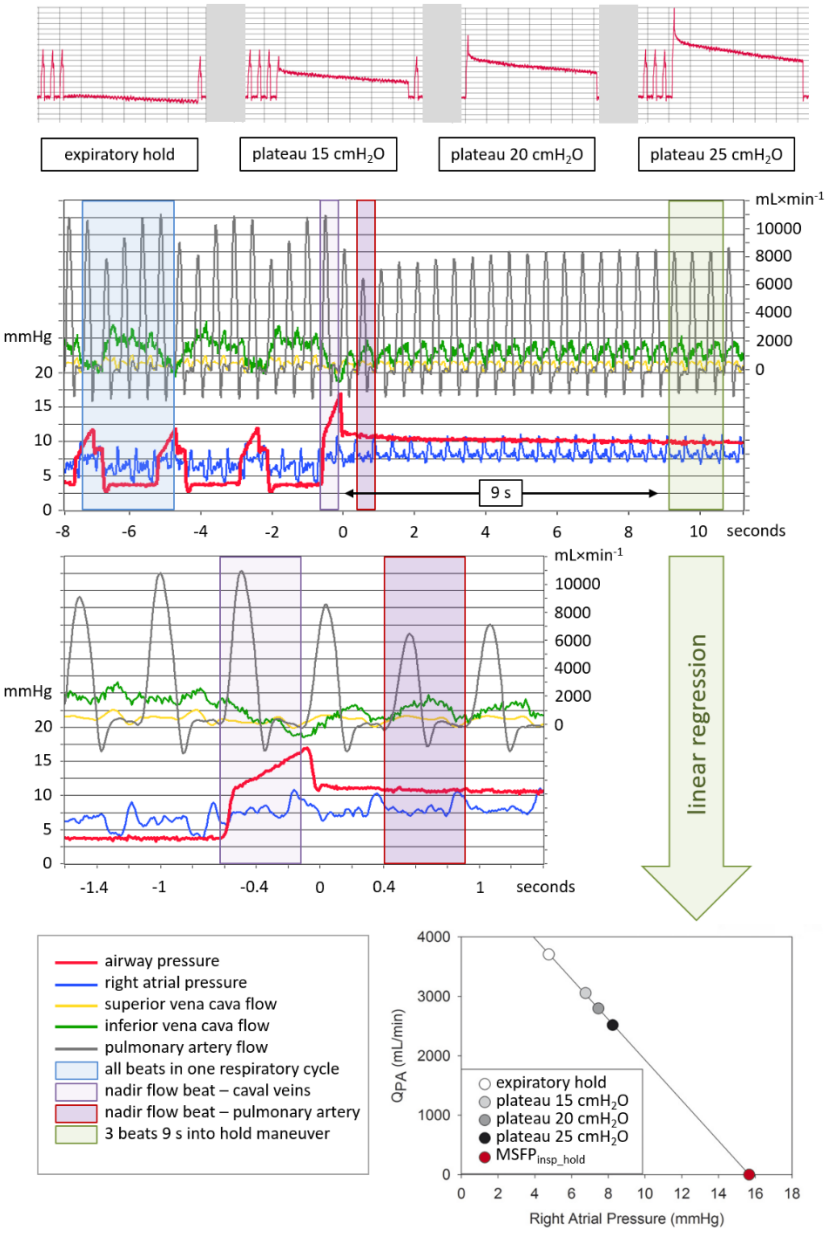

Figure 18 – A series of airway pressure maneuvers. $MSFP_{insp\_hold}$ was estimated as the zero-flow extrapolation of data-pairs consisting of mean values for pulmonary artery flow (Q_{PA}) and right atrial pressure (RAP) of the first three beats occurring 9 s into the maneuver. To quantify the decrease and restoration of flow during the maneuver, mean values for all beats during one respiratory cycle preceding the maneuver (baseline - blue) were compared to nadir flow in caval veins and pulmonary artery (purple) and the three beats 9 s into the maneuver (green). See main text for details.

3.4.2 NADIR HOLD EXTRAPOLATIONS

As can be seen in Figure 18, an inspiratory hold maneuver to a static plateau pressure is associated with dynamic decrease and restoration of venous return. Versprille, Jansen and Maas came to the conclusion that the later part of the hold maneuver represented a new steady state VR. We found in our first experimental series (Paper I), that the degree of flow restoration was related to the underlying volume state. In Paper IV we introduced a new method for zero-flow estimation based on pressure-flow data-pairs at nadir Q_{PA}. The beat displaying nadir mean Q_{PA} was matched to mean RAP of the preceding beat. Linear regression and zero-flow extrapolation of data-pairs from expiratory hold up to plateau pressures of 30 [*sic*] cmH_2O yielded an MSFP estimation conceptually unaffected by differential flow restoration ($MSFP_{nadir\_hold}$).

3.4.3 INSTANTANEOUS VENOUS RETURN

The concept of venous return being inversely proportional to the changing RAP over the respiratory cycle was introduced by Pinsky (82), as described in section 1.8.1. By beat-to-beat analysis, pressure-flow data-pairs are extracted from the data set. Depending on where the flow is measured, it is matched to RAP from the same (in case of caval veins) or the preceding beat (pulmonary artery). We have used this approach in Paper II and IV.

In Paper II (VA-ECMO with ligated PA) we analysed three consecutive respiratory cycles of tidal ventilation (tidal volume 7 mL/kg, PEEP 5 cmH_2O) at baseline pump speed. Data-pairs of mean values of RAP and venous return flow (Q_{VR}; the sum of caval vein flows) were extracted. One breath, including at least two beats in inspiration and two beats in expiration, was integrated into a common venous return curve. The rationale was to test the hypothesis that, within the same volume state, pressure-flow data-pairs from different interventions ("airway pressure maneuvers" and "pump speed maneuvers" – see section 3.7) operated on a common VR curve.

In Paper IV, we expanded the data analysis from experiment I. A zero-flow estimate of MSFP ($MSFP_{inst\_VR}$) was calculated from the linear regression of beat-to-beat data-pairs consisting of mean values from single beat Q_{PA} matched with mean RAP from the preceding beat over three respiratory cycles of undisturbed tidal ventilation preceding RA balloon inflation.

In both papers (II and IV), we used the same arbitrary criterion as for the $MSFP_{insp\_hold}$ maneuvers: an $r^2 > 0.7$ was required for inclusion in analysis.

3.4.4 DYNAMIC ANALOGUE OF STATIC FILLING PRESSURE

The dynamic model analogue of static filling pressure, P_{msa}, formulated by Parkin, has previously been adapted for animal use. Lee and Pinsky examined the performance of P_{msa} compared to instantaneous VR curves in a model of endotoxemic dogs (51). To fit the numeric value of "dog P_{msa}" to the expected normal value for a healthy human (7 mmHg), the authors adjusted the equation for the factor 'c' by setting the animal age to 15 and the length to 250 cm. Between the six animals studied, factor 'c' therefore only varied slightly according to actual weight.

With the ambition to represent better the original model characteristics, we chose a different approach (in Paper IV, using data from experimental series I). In the original equation, factor 'c' = $0.96 \times R_v$, where 0.96 is a function of the chosen estimate of VA *compliance* ratio [0.96 = 24/(24+1)] and R_v is the resistance in the venous compartment. If an AV *resistance* ratio of 25 is chosen, R_v can be estimated as normal SVR/(25+1). Our pigs were *abnormal* in the sense that the cardiovascular system was affected by anaesthetic medications and positive pressure ventilation. We have discussed in section 1.9 how increased IPPV and PEEP lead to an increase in both RAP and MSFP. True porcine MSFP in this setting is therefore likely >7 mmHg. However, our experimental protocol was designed to create normovolemia at the start of measurements. Judging from the hemodynamics and blood volumes, this goal was probably reached. Therefore, we assumed that the animals all had a *normal* SVR at PEEP 5 cmH_2O and euvolemic conditions. We calculated $MSFP_a$ ('a' for analogue) as:

$$MSFP_a = 0.96 \times RAP + 0.04 \times MAP + 0.96 \times [(\text{normal SVR})/(25+1)] \times Q_{PA} \qquad (7)$$

Normal SVR was calculated for once each individual animal from the respective mean values of MAP, RAP, and Q_{PA} from 10 beats of tidal ventilation at PEEP 5 cmH_2O, under steady state conditions. In each experimental condition, $MSFP_a$ was then calculated using data from steady state conditions where Q_{PA} is equal to CO.

3.5 BLOOD VOLUME DETERMINATION

3.5.1 TOTAL BLOOD VOLUME

Plasma volume was measured using the indocyanine green (ICG) dye dilution technique (45) (whole blood method). Before each measurement, blood was taken for a two-point calibration *in vitro* against two artificially determined ICG concentrations. Starting two min after a bolus injection of dye (0.25 mg/kg), ten blood samples were then taken at 20 s intervals using a standardized three-person procedure with stopwatch timing. Plasma dye concentration was determined via spectrophotometry. The theoretical plasma volume at t_0 was calculated from the dye disappearance rate, assuming a mono-exponential elimination kinetic during the first 5 min. Finally, blood volume was calculated using the mean value of arterial and venous haematocrit obtained prior to the dye bolus.

3.5.2 STRESSED AND UNSTRESSED VOLUMES

MSFP can be plotted as a function of blood volume in a pressure-volume vascular capacitance plot (71, 87). Using linear regression, the pressure-volume relationship can be solved. Extrapolation to zero pressure gives the unstressed volume (V_u) at the specific volume state. The slope of the line has the units of vascular elastance (mmHg/ΔmL). Vascular elastance assumes an independent role of volume and a dependent role of pressure. The inverse slope of the line has the units of vascular compliance (mL/ΔmmHg). Vascular compliance (C_{vasc}) assumes an independent role of pressure and a dependent role of volume. When the experimentally controlled variable is a change in total blood volume [with secondary reflex adjustments of vascular capacitance and stressed volume (V_s)], it makes sense to describe the relationship in terms of pressure-volume or vascular elastance. The same applies if the focus is redistribution of volume (volume shifts). However, in the research field it is customary to report distensibility in terms of systemic vascular compliance.

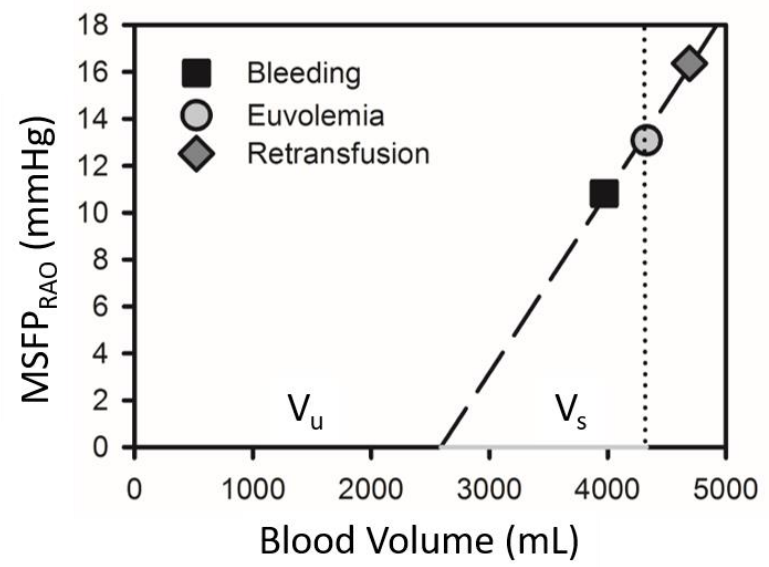

Figure 19 – A pressure-volume plot from an individual animal (Study I). $MSFP_{RAO}$ is plotted as a function of changing blood volume measured with ICG. The slope of the line equals vascular elastance. The equation for the line for this individual was MSFP = -19.94 + 0.0077× blood volume. r^2 = 0.988. Vascular compliance [=1/(elastance)] was 130 mL×mmHg^{-1} or 3.2 mL×mmHg^{-1}×kg^{-1}.

3.5.3 TWO-POINT VASCULAR ELASTANCE – RAPID BLEEDING MANEUVERS

In the third experimental series (VA-ECMO and ventricular fibrillation, Paper III), we constructed two-point vascular elastance plots using the difference between MSFP measured before and immediately after a rapid bleeding sequence. Vascular elastance was assumed to be linear in the pressure-volume range studied (4, 12, 26, 69, 71), and was calculated as $E_{vasc} = \Delta MSFP/\Delta blood$ volume. Blood volume had been determined with the ICG dye dilution technique and MSFP as described in section 3.5.1. Rapid bleeding was started by directing all ECMO output into a bleeding bag resting on an electronic scale, while the reperfusion tubing was clamped to prevent arterial backflow. Venous return was continuously drained into the ECMO circuit until approximately 9 mL/kg of blood had entered the bag. At that point, the venous tubing was clamped and the AV-shunt opened to immediately determine MSFP in a stop flow maneuver. The actual weight of the shed blood was noted, and the exact volume (363 ± 26 mL) could be calculated using the blood density obtained at the end of the experiment. As soon as the stop flow maneuver was complete, flow was resumed and the blood was returned to the circulation. The entire sequence from start of bleeding to measurement of MSFP took 21 ± 4 s, ranging from 14 to 31 s (n=18, mean ± SD, time determined in offline analysis). Reflex activation did not visibly interfere with the measurement of pressure equilibrium.

3.6 TITRATING MAXIMUM ECMO FLOW

As ECMO pump speed is progressively increased, at some point the vascular walls will collapse around the venous cannula. This occurs because the pressure on the outside of the vessel is greater than on the inside, and the vessel walls are being *pushed* into the cannula orifice. The transmural pressure has become negative, and a Starling resistor or vascular waterfall has been established (80). Some or all of the cannula inlet orifices will be occluded, and the resistance to flow increases dramatically. As drainage suddenly drops, volume will again accumulate around the cannula and flow is temporarily re-established. This oscillating process is referred to as 'staccato flow' (102). It illustrates that the *transmural* pressure is one of the determinants of maximum flow. At all times however, venous return down to the point of the vascular collapse will be determined by the pressure difference between upstream and downstream *intravascular* pressures. When the pump operates at a level of vascular collapse, depending on the relative locations of the site of pressure measurement and vessel collapse, RAP may or may not represent the actual backpressure to VR.

At the bedside, vascular collapse can sometimes be realised as fluttering of the venous ECMO tubing. Increased intrathoracic pressure will decrease the transmural pressure in the RA and susceptible parts of the caval veins. In the second experimental series (Paper II) we defined maximum pump speed as the highest possible speed that allowed an inspiratory hold without signs of RA collapse. This was a pragmatic approach of finding the *approximate* upper inflection point of the VR curve. Focus lay on the descending, clearly linear part of the VR curve. In the third experimental series (Paper III) we actively pursued the upper limit of maximum achievable ECMO flow, as this was the main experimental outcome. This was done by titrating short excursions of increased pump speed during expiratory hold, while observing the measured ECMO flow online for signs of flutter. However, if one operates too long at a high pump speed, there may be risk of damage to the caval and/or right atrial walls, as well as risk of haemolysis. Furthermore, the resulting high flow and arterial pressure may affect the output from the baroreceptors, potentially leading to vasodilation with decreased stressed volume and lower venous return driving pressure. It may therefore be impossible to sustain the high flow over time.

3.7 VENOUS RETURN CURVES FROM PUMP SPEED MANEUVERS

In the experimental series II-III (Papers II-III), we constructed VR curves by stepwise changing the ECMO pump speed and recording the resulting pressure-flow data-pairs. First, maintenance (or 'baseline') pump speed was adjusted to achieve an ECMO flow resulting in a mixed venous saturation (S_VO_2) of 50% [the lower normal range for pigs (43)]. The pump speed maneuvers consisted of 30 s excursions to higher and lower levels, starting from and returning to maintenance pump speed. The maneuvers had to be brief in order to prevent baroreceptor activation from the changing arterial pressure. Any sustained decrease or increase in pump speed and arterial pressure would lead to reflex adjustment of the vascular tone to increase or decrease stressed volume and MSFP.

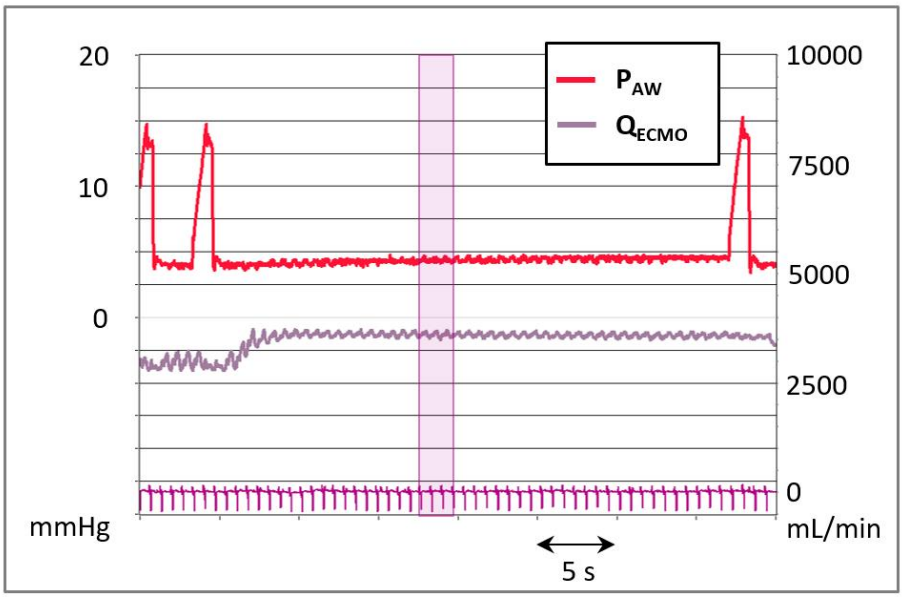

Figure 20 – An example of a pump speed maneuver from Paper II. Starting in expiratory hold, the pump speed was rapidly adjusted to a predefined level. The ECG trace (at the bottom, in pink) was used to select the three first beats to follow 9 s after ECMO flow (Q_{ECMO}) had reached its new level.

Data was extracted as mean values for three beats (or two seconds in the ventricular fibrillation model) 9 s after ECMO flow had reached its new level. In series II, the pump speed maneuvers were performed during both expiratory and inspiratory hold, in randomized order. In series III, the maneuvers were

only performed in expiratory hold. Depending on the relationship of interest, data-pairs from pump speed maneuvers and stop flow maneuvers were used to construct plots of RAP *vs*. pump speed, flow *vs*. pump speed, and venous return curves of flow *vs*. RAP. The different plots were used to illustrate the volume shifting work of the pump, pump performance characteristics, or the circuit characteristics of the systemic vascular compartment, respectively.

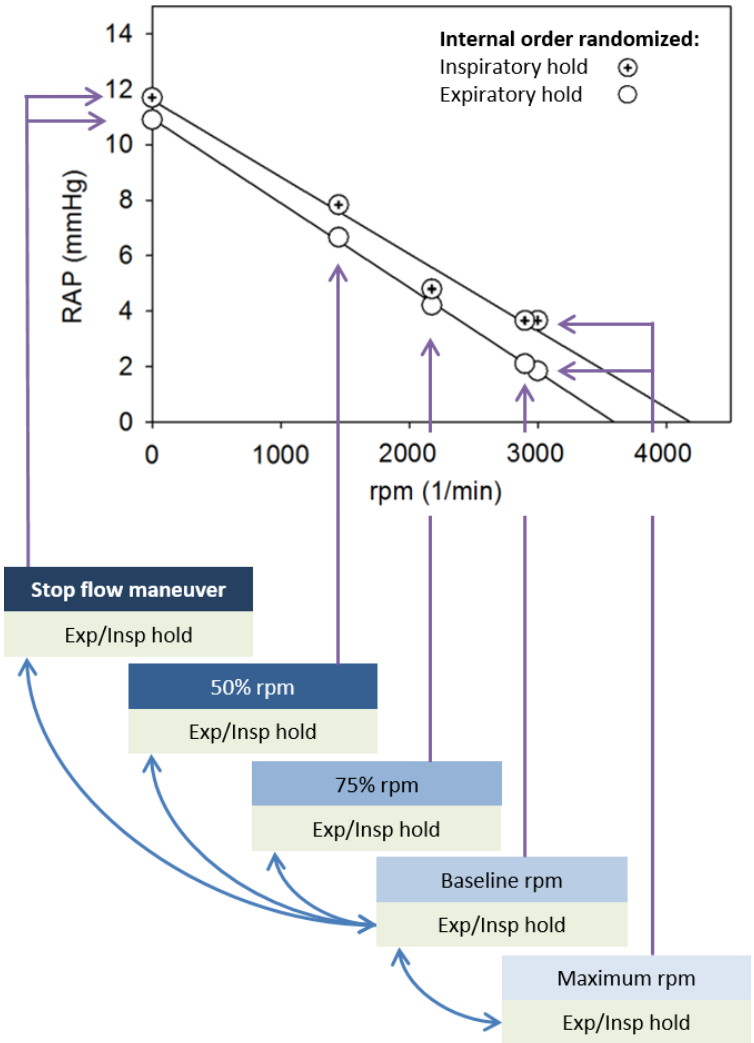

Figure 21 – Pump speed maneuvers from Paper II. Brief excursions to higher and lower levels of pump speed (revolutions per minute, rpm) were made in expiration and inspiration (the order randomized). Here the resulting right atrial pressure (RAP) is plotted as a function of pump speed. For the experimental series III (Paper III), Maintenance, Maximum and 80%, 60%, and 50% thereof were applied.

3.8 TESTING THE BACKPRESSURE HYPOTHESIS

The protocol for the second experimental series (Paper II, VA-ECMO with ligated PA) included maneuvers where we changed airway pressure with the ventilator, while keeping pump speed constant ("airway pressure maneuvers). Venous return flow (Q_{VR}) was calculated as the sum of caval vein flows (measured by individual flowprobes on SVC and IVC – see Figure 16). To ensure that dynamically changing venous flow would not be limited by vessel collapse, pump speed was set to 75% of maximum (for definitions – see section 3.6 and 3.7). For the *inspiratory hold maneuver*, after 10 s of expiratory hold at PEEP 5 cmH_2O, the ventilator was set to inspiratory hold for 10 s. After this, tidal ventilation was resumed for 1 min. For the *zero PEEP maneuver*, after 10 s of inspiratory hold, the ventilator circuit was disconnected (zero PEEP). Pressure-flow data (mean values) was extracted for the last three beats preceding the hold ("pre"), for the beat displaying maximum caval flow change ("ΔQ_{VC}max"), for the three following beats ("early"), and for the last three beats before tidal ventilation and baseline pump speed were resumed ("late") (Figure 22).

With constant ECMO pump function, acute changes in airway pressure, transmitted to the RAP would lead to a transient imbalance between inflow and outflow from the right atrium (97), associated with volume shifts between the right atrium and the systemic compartment. To estimate these volume shifts, we integrated the difference between inflow and outflow to the right atrium during the four beats of "ΔQ_{VC}max" and "early", assuming that ECMO flow was constant.

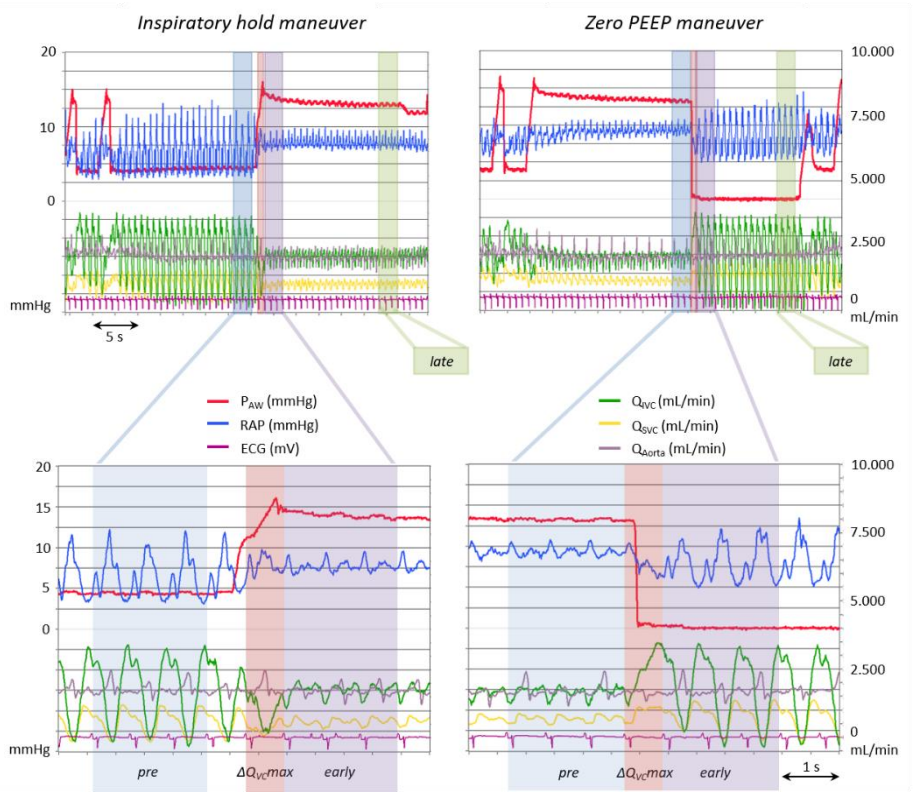

Figure 22 - Airway pressure maneuvers from Paper II. ECMO speed was kept at 75% of maximum throughout both maneuvers. For the inspiratory hold maneuver (left), after 10 s of expiratory hold at PEEP 5 cmH_2O, the ventilator was set to inspiratory hold. Mean values were selected for the three last beats preceding the hold ("pre", blue shade), for the beat in which maximum change in caval flow was seen ("$\Delta Q_{VC}max$", red), for the three following beats ("early", purple), and for the last three beats of the hold ("late", green), after which pump speed was reset and tidal ventilation resumed.

3.9 CROSS CORRELATION

Cross correlation is defined as the correlation between two variables as a function of time shift. It allows analysis of the dynamic behaviour and time delay between two signals, recorded simultaneously with the same sample frequency. The correlation between the two signals is calculated repeatedly by introducing a successive time shift between the two. In this process, one data set is "dragged thru" the other and the resulting correlation is plotted as a function of time shift. A data set composed of 500 samples will therefore result in 999 sets of progressively increasing and decreasing overlap.

In Paper II, we analysed the behaviour of acutely changing Q_{VR} (the sum of caval flows) and RAP elicited by changing airway pressure. Data from the beginning of "pre" to the end of "early" (3+1+3 beats) was used. In order to focus on the time shift, the amplitudes of Q_{VR} and RAP was individually normalised from -1 to +1. All data sets included the same number of beats, but a varying number of samples. The cross correlation was first performed individually for each animal in all three volume states using a customised analysis software (Soleasy, Alea Solutions, Zürich). To allow averaging of all animals, the time axis was then normalised to 1000 samples for the construction of summary plots.

Prior to the cross correlation analysis, the raw data set had to be corrected for any signal propagation delay inherent to the measurement and data acquisition systems (pressure transducer and flowprobe/monitors, and different connections to the recording computer, respectively). This technical propagation delay of pressure *vs*. flow in the measurement setup was quantified experimentally using a roller pump and low-compliance closed tube circuit, with data recorded at 1000 Hz sample rate. Clamping the tube caused simultaneous changes in flow and pressure. The reference point for flow change was visually estimated as a step change in the slope from baseline. The pressure change was estimated as an increase of >2 SDs from baseline. The signal propagation delay of pressure *vs*. flow in the measurement setup was quantified to (n=5) 41 ± 7.5 ms. The data set from the main experiment (recorded at 100 Hz) was therefore corrected by shifting the RAP signal four samples ahead of Q_{VR} before the cross correlation analysis.

3.10 STUDY PROTOCOLS

3.10.1 STUDY PROTOCOL - PAPER I

We used an intact circulation, porcine model with mechanically ventilated animals under propofol and fentanyl anaesthesia to address the following questions: 1) Do changes in PEEP, volume status, and tidal breaths alter MSFP and the slope of the venous return curve? 2) Does a measurement of MSFP obtained with inspiratory hold maneuvers correspond to MSFP measured at zero flow induced by right atrial balloon occlusion? 3) Do inspiratory hold maneuvers *per se* modify the hemodynamic variables of the venous return function, and do PEEP and volume status modify these responses? The animals were ventilated in a volume-controlled mode at PEEP 5 cmH_2O, F_IO_2 of 0.3 and tidal volumes of 300 mL (7.7 ± 0.3 mL/kg) with respiratory rate adjusted to maintain an end-expiratory PCO_2 of 40 mmHg. Surgery was followed by 90 min of stabilisation. A bolus of 100 mL HES was administered to replace potential perioperative volume deficit. If Q_{PA} increased >10%, one further bolus was given. At this point, the animals were considered euvolemic and baseline determination of plasma volume was performed. The study protocol is represented graphically in Figure 23 (and in detail in Paper I). Measurements and interventions have been described in the previous sections.

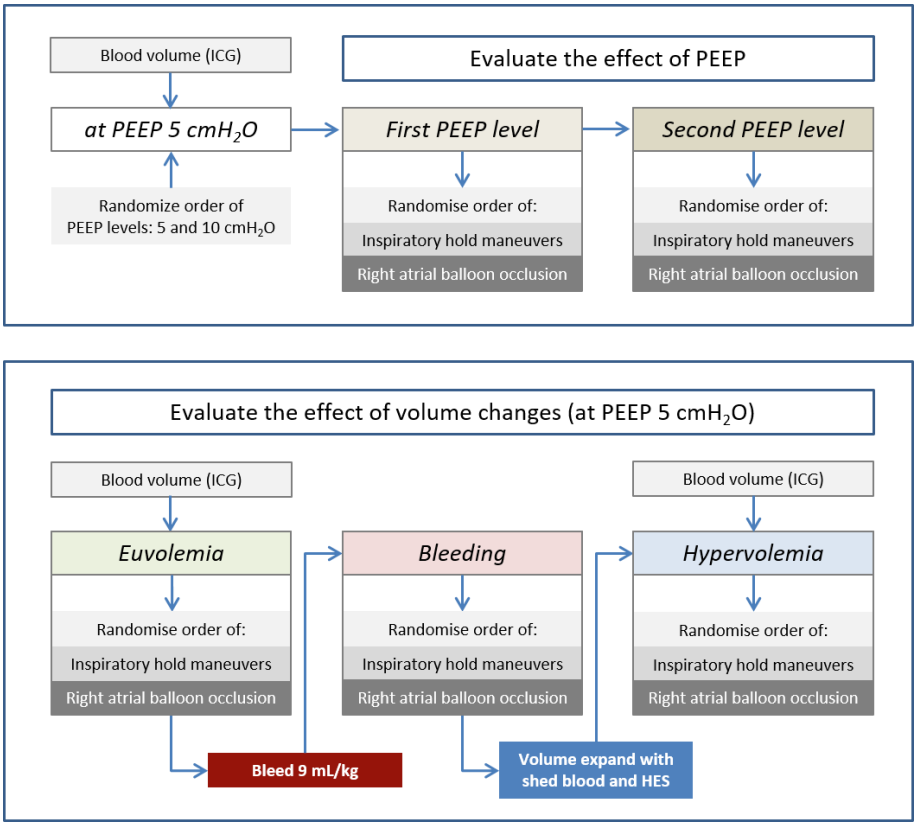

Figure 23 – Protocol summary for experimental series I (Paper I). The first part examined the effects of changes in PEEP on the venous return function. The second part assessed the effects of volume changes.

3.10.2 STUDY PROTOCOL - PAPER II

This closed chest, heart-bypass model used VA-ECMO and a ligated pulmonary artery. We hypothesised that RAP acts as backpressure for venous return. This was tested by examining the response of RAP, VR, and MSFP to acute changes in airway pressure (*airway pressure maneuvers*, see section 3.8), and the effect of acute changes in ECMO flow on RAP and VR (*pump speed maneuvers*). We could thereby evaluate separately the effects of RAP and pump function on VR, and whether Guyton's model of VR would be valid during dynamic changes, if the effects of transient volume shifts on MSFP and RAP were accounted for (section 3.3.2 for details on the preparation). Volume-controlled ventilation at PEEP 5 cmH_2O and tidal volumes of 7 mL/kg was continued also on bypass. Perioperative blood loss was replaced by HES. After closing the chest, Q_{ECMO} was adjusted during tidal ventilation to achieve a S_VO_2 of 50%. If necessary, HES boluses were given to allow an inspiratory hold without RA collapse (sections 3.6 and 3.7). This pump speed (*baseline rpm*) resulted in a baseline Q_{ECMO} in *Euvolemia*. After volume expansion with 9.75 mL/kg HES, the pump speed was again adjusted to a new baseline, under tidal ventilation, to reach the S_VO_2 target (at *Volume Expansion*). After bleeding up to 19.5 mL/kg or until MAP decreased to 35 mmHg (*Hypovolemia*), pump speed was reduced under tidal ventilation to allow an inspiratory hold without RA collapse, abandoning if necessary the S_VO_2 target. In each volume state, a further attempt was made to increase the ECMO pump speed from baseline until just below RA collapse during inspiratory hold. This was considered as the maximum (*maximum rpm*) for each volume state and was used for reference in the pump speed maneuvers (see Figure 21). Pump speed and Stop flow maneuvers were performed both during expiratory and inspiratory holds, with the internal order randomised. Airway pressure maneuvers were performed at constant pump speed. Cross correlation analysis was performed on data from the airway pressure maneuvers (see section 3.9). Measurements and interventions have been described in the previous sections.

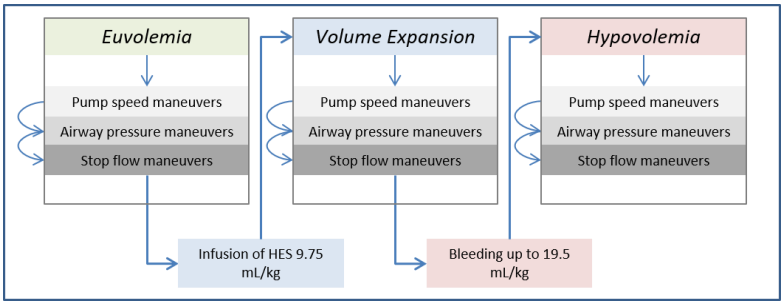

Figure 24 – Abbreviated experimental protocol (Paper II).

3.10.3 STUDY PROTOCOL - PAPER III

This model of ventricular fibrillation and VA-ECMO compared the effects of volume expansion with Ringer's lactate and vasoconstriction using norepinephrine on maximum ECMO flow (*Maximum* Q_{ECMO}) and oxygen delivery (DO_2). The same ventilator settings were used, as previously described for Paper II. For details on the preparation – see section 3.3.3. Perioperative blood loss was supplemented by HES. Rapid pacing induced ventricular fibrillation. The ECMO pump speed was adjusted to reach an S_VO_2 of 50% during tidal ventilation. If necessary, HES was added in boluses of 50 mL. After this state, defined as *Euvolemia* (where also blood volume was determined with ICG dye dilution), no further HES was given. The protocol consisted of eight conditions. *Euvolemia* was followed by three conditions of stepwise increasing rates of norepinephrine infusion [0.05, 0.125, and 0.2 $\mu g \times kg^{-1} \times min^{-1}$, each beginning with a bolus of 5 μkg^{-1} (*Vasoconstriction 1-3*)]. After this, norepinephrine was discontinued and the animal entered a state of *Post Vasoconstriction*. This was followed by three levels of stepwise *Volume Expansion* (VE 1-3) where 10 $mL \times kg^{-1}$ of Ringer's lactate was infused over three min at each step. The study measurements were started after 5 min at each step. Pump speed and stop flow maneuvers were performed in expiratory hold only, but in all eight conditions. In *Vasoconstriction 3* and *Volume Expansion 3*, blood volume determination was repeated and vascular elastance was determined by rapid bleeding and retransfusion (see section 3.5.3). The stability of MSFP over time was determined by repeating the stop flow maneuver three times over 40 min. Changes in plasma volume were estimated based on haematocrit and haemoglobin concentrations using Beaumont's method (44) at time points in the protocol when no ICG measurements were available.

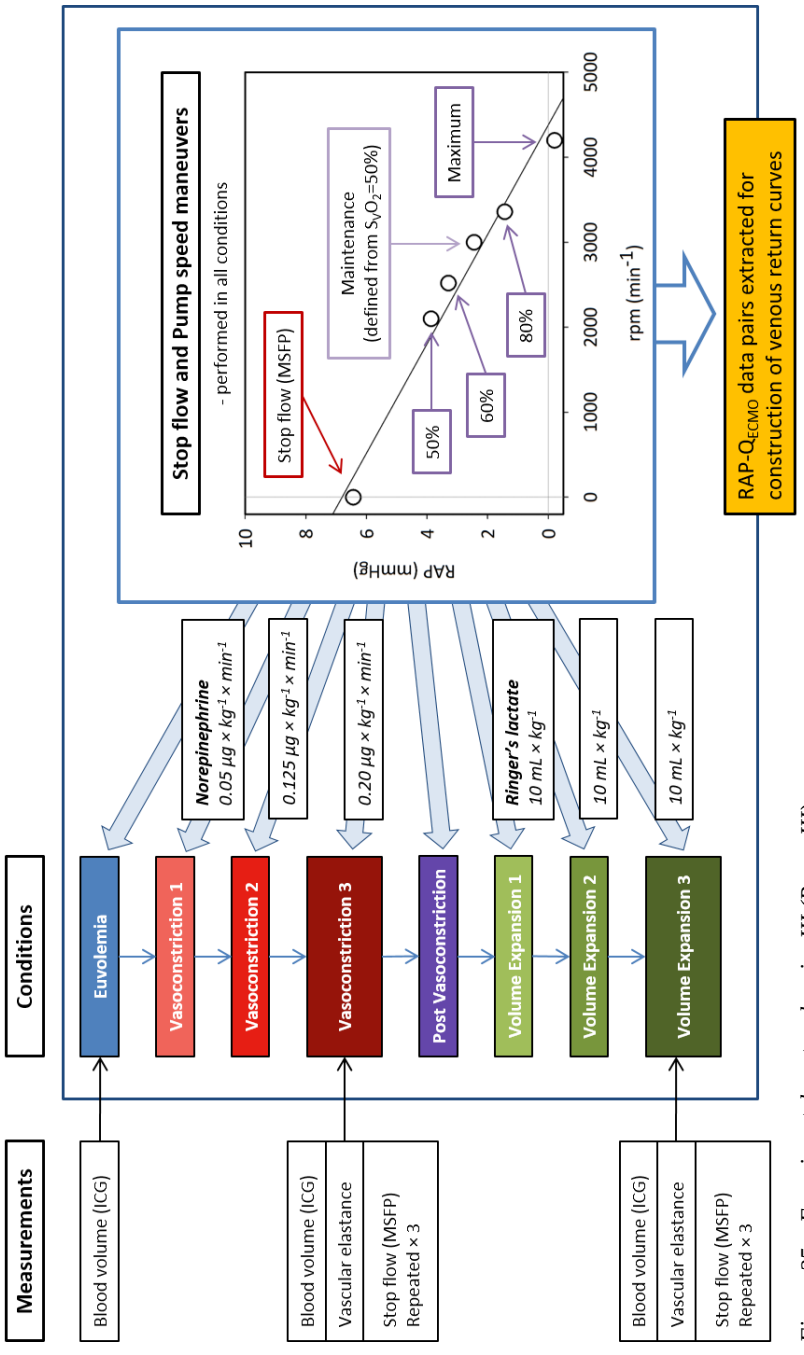

Figure 25 – Experimental protocol series III (Paper III).

3.10.4 STUDY PROTOCOL - PAPER IV

In this study of method agreement, data of the zero-flow reference $MSFP_{RAO}$ from the volume states *Euvolemia*, *Bleeding*, and *Hypervolemia* from the first experimental series were reused, and compared to three estimates of MSFP obtained with a running circulation. Instantaneous VR ($MSFP_{inst\_VR}$) was calculated from three respiratory cycles of undisturbed tidal ventilation preceding the right atrial occlusion maneuver (see section 3.4.3). Nadir-flow extrapolation ($MSFP_{nadir\_hold}$) was calculated from the nadir Q_{PA} early in the inspiratory hold maneuvers to plateau pressures of 15, 20, 25, and 30 cmH_2O (see section 3.4.2). The dynamic model analogue adapted to pigs ($MSFP_a$) used data of RAP, MAP and Q_{PA} from 10 beats of undisturbed tidal ventilation preceding right atrial occlusion (see section 3.4.4). In order to assess the impact of changing resistance in the venous compartment (R_v), and/or changing arteriovenous resistance ratio on the calculation of $MSFP_a$ we compared the value of 'c' calculated at *Euvolemia* to a 'c' calculated anew from the current SVR in each experimental condition. Method agreement for absolute values between each of the estimates and the reference $MSFP_{RAO}$, as well as *change* in test methods *vs*. *change* in the reference method were analysed using repeated measurements ANOVA and Bland-Altman for repeated measurements. An *a priori* desired agreement between change in test method *vs*. change in reference method was set to ≤10% of venous return driving pressure in *Euvolemia* (23).

3.11 STATISTICAL CONSIDERATIONS

A type I error is the probability of falsely rejecting the null-hypothesis. If statistical significance is accepted for $p<0.05$, this probability is 5%. A type II error is the probability of *failing* to reject a false null-hypothesis. The statistical power equals one minus the probability for a type II error. Stated differently, the statistical power is the probability, given a specified significance level, to correctly identify a true difference, if such a difference exists.

The sample size will always be a compromise between on one hand the wish to minimise (for ethical and economic reasons) the number of animals used, and, on the other hand, to maximise the statistical power. In the preparations for the first study, we considered the data of Ogilvie (72): $MSFP_{RAO}$ for pigs was reported to be (mean ± SD) 12.3 ± 0.5 mmHg. We estimated the SD for change to ~1 mmHg, and wished to detect a physiologically relevant change in VRdP of 1 mmHg. With a significance level of 0.05 and a power of 0.80, the sample size was calculated to 8 animals. We added two animals as a safety margin to account for unanticipated problems such as technical errors in the measurement setup, or loss of animals. The calculated power relates to the primary outcome of change in VRdP. We did not attempt to *a priori* calculate the related power of detecting multi-level associations of interaction between methods of MSFP estimation and experimental conditions.

The robustness of any statistical test is dependent on the sample size. As in most animal experiments, our sample sizes were small ($n<10$). The two main tests used in the studies were paired t-tests and repeated measurements analysis of variance (ANOVA) – both comparing means. The tests assume equal variances (i.e. homoscedasticity) and normal distribution of data. Formal tests for equal variance between groups rely on normal distribution, are not robust when this assumption is violated, and do not perform well in small sample sizes (70). Formal tests for normal distribution of data, such as Kolmogorov-Smirnov and Shapiro-Wilks, are also reported to be appropriate only in larger sample sizes (95).

We relied on a combination of graphical assessment of data and formal testing. Assumptions of equal variances and normal distribution were assessed as Studentized residuals $< \pm 3$, visually by Q-Q plots and histograms, and by use of Kolmogorov-Smirnov and Shapiro-Wilks testing. In the repeated measurements ANOVA, the assumption of sphericity (i.e. equal variance between all combinations of levels of within-subjects factor) was tested *ad modum* Mauchly. If this assumption was violated, the degrees of freedom was adjusted by using the Greenhose-Geisser correction. In case outliers were

identified, sensitivity analysis was performed by repeating the tests with the outlier excluded. If this did not change the significance levels, the outlier was kept in the main analysis. When the assumption of normality was violated, non-parametric tests were used as appropriate (e.g., Wilcoxon signed ranks test and Friedman's test replacing paired t-test and one-way repeated measurements ANOVA, respectively).

Guyton did not use statistical modelling at all. Traditionally, the venous return function has been characterised by VR plots of data-pairs, described by least squares linear regression. Data sets composed of multiple zero-flow extrapolations can be compared as groups. In Papers II-III we used Generalized Estimating Equations (GEE), to describe the venous return function, the pump function and the time-dependent decay of MSFP from groups of animals, where each animal was represented by multiple data-points. GEE is a marginal model where the estimate is based on the population average. It is related to Generalized Linear Mixed Models (GLMM). When a linear model is chosen in the GEE, the results from GEE and GLMM analyses will often be similar. The GEE model is versatile, easy to use and can handle repeated measurements of two continuous variables with possible interaction of a categorical covariate. The data structure was approximated to a first order auto-regressive correlation matrix (AR1). In Paper III, all analyses eventually presented as GEE were also performed in the form of GLMM. The choice of model did not affect conclusions, and slopes and intercepts varied only marginally.

In Paper IV, we assessed agreement *vs*. the reference method $MSFP_{RAO}$ for estimates of MSFP using the Bland-Altman method. The analysis included repeated measurements from each animal. If this data structure is not taken into account, the variance of the differences is underestimated which leads to progressively serious underestimations of the limits of agreement (LoA), of the variance of the bias, of the variance of the LoA, and finally resulting in too narrow confidence intervals (CIs) (73).

Data is presented as mean ± SD [or mean (SD) depending on journal style] or median (range), as appropriate. The results of statistical tests are reported including both the effect size (different group means) and the actual *p*-value (rather than a binary statement of significant/not significant).

Physiological studies typically generate a multiplicity of data. Multiple tests increase the overall risk of type I errors. To control for the experiment-wise error rate (ERR), we restricted the statistical testing to hypothesis driven analyses. Instead of using multiple separate paired comparisons, we used global tests like ANOVA (9). *Post hoc* paired comparisons were done with the

Bonferroni correction for multiple testing (either by multiplying the obtained *p*-value or by reducing the significance level by division). Although the Bonferroni method is often seen as overly conservative, we think its use in this context is appropriate in light of the very small sample sizes. Additional *post hoc* exploratory analyses, not part of the pre-analysis plan, was motivated by a clear physiological rationale.

4 RESULTS

In this chapter, the main results from Papers I-IV are presented.

4.1 RESULTS – PAPER I

Of the 10 animals studied, one died from a combined RA/SVC rupture caused by the balloon occlusion, and a second animal developed intractable ventricular fibrillation before measurements at *Euvolemia* were completed. Nine animals weighing 39 ± 1.5 kg were included in the analysis. Of the 50 planned $MSFP_{RAO}$ measurements, 43 were performed. As a consequence of the study design, with PEEP levels randomized and volume states performed in fixed order, 42 $MSFP_{RAO}$ measurements were included in the analysis. In the general description of the method found in section 3.3.1, further details are given.

	PEEP 5 (n=9)	**PEEP 10** (n=9)	*p*	**Euvolemia** (n=8)	**Bleeding** (n=8)	**Hypervolemia** (n=8)	*p*
Heart rate: min^{-1}	100 ± 29	96 ± 23	0.658	102 ± 21	129 ± 31	106 ± 20	<0.0005
MAP: mmHg	63 ± 7	61 ± 12	0.609	60 ± 10	50 ± 11	63 ± 12	0.003
PAP: mmHg	18 ± 3	20 ± 3	0.018	19 ± 3	17 ± 3	23 ± 3	<0.0005
RAP: mmHg	5.9 ± 1.6	7.5 ± 1.4	<0.0005	5.9 ± 1.6	5.1 ± 1.7	8.2 ± 1.9	<0.0005
$\Delta RAP_{tm}exp$: mmHg	0.26 ± 1.02		0.496		0.29 ± 0.62	0.98 ± 1.26	0.033
Q_{PA}: $L \times min^{-1}$	2.75 ± 0.43	2.56 ± 0.45	0.094	2.80 ± 0.46	2.20 ± 0.42	3.27 ± 0.42	<0.0005
$MSFP_{RAO}$: mmHg	12.9 ± 2.5	14.0 ± 2.6	0.002	13.0 ± 2.8	10.8 ± 2.2	16.4 ± 3.0	<0.0005
VRdP: mmHg	7.0 ± 2.2	6.5 ± 2.3	0.033	7.0 ± 2.4	5.7 ± 1.7	8.2 ± 2.2	<0.0005
RVR: $mmHg \times min \times L^{-1}$	2.53 ± 0.52	2.53 ± 0.63	0.945	2.49 ± 0.59	2.60 ± 0.58	2.50 ± 0.52	0.489
	Before PEEP changes			*Before bleeding*	*After bleeding*	*In hypervolemia*	
Blood volume: $mL \times kg^{-1}$	97 ± 14			98 ± 16	89 ± 15	113 ± 21	0.001

Table 2 - Data is mean ± SD. Variables were calculated as a mean of 10 cardiac cycles before right atrial balloon occlusion during volume controlled ventilation; tidal volume 300 mL (7.7 ± 0.3 $mL \times kg^{-1}$) at PEEP 5 unless stated otherwise. MAP: mean arterial pressure; PAP: pulmonary arter pressure; RAP: right atrial pressure; $\Delta RAP_{tm}exp$: change in mean value of RA transmural pressure from 5 end-expiratory beats (preceding right atrial balloon occlusion) between the experimental conditions (n=8: one animal excluded due to local hematoma around pericardial catheter); Q_{PA}: pulmonary artery blood flow; $MSFP_{RAO}$: mean systemic filling pressure at zero flow caused by right atrial balloon occlusion in end-expiration; VRdP: venous return driving pressure (VRdP= $MSFP_{RAO}$-RAP); RVR: resistance to venous return (RVR=VRdP/Q_{PA}). Blood volume after bleeding calculated as volume measured before bleeding – volume of shed blood. Paired t-tests for PEEP levels; repeated measurements ANOVA, within-subjects effect volume state.

At the end of the stabilization period, the coefficients of variation for heart rate, MAP, PAP, RAP, and Q_{PA} for end-expiratory beats over 10 consecutive respiratory cycles, were ≤ 6%. Increasing PEEP from 5-10 cmH_2O led to an increase in both RAP and MSP_{RAO}. As RAP increased more than MSP_{RAO}, VRdP decreased. RVR remained unchanged. Q_{PA} decreased slightly, but the change was not statistically significant. There was no significant change in end-expiratory RAP_{tm} between PEEP levels.

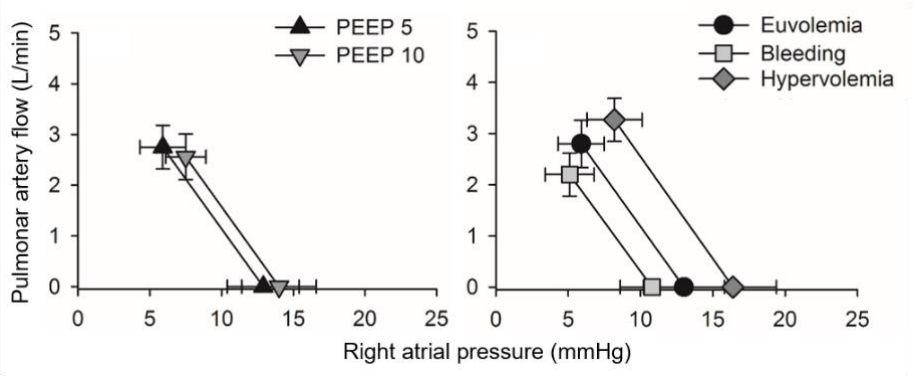

Figure 26 – The effect of PEEP and changing blood volume on the venous return function. Mean values of RAP and Q_{PA} measured for 10 beats during tidal ventilation preceding right atrial balloon occlusion are connected with solid lines to mean values of $MSFP_{RAO}$ measured as the mean of caval vein pressures during 3 s of venous plateau at zero flow in expiratory hold. Error bars indicate 1 SD.

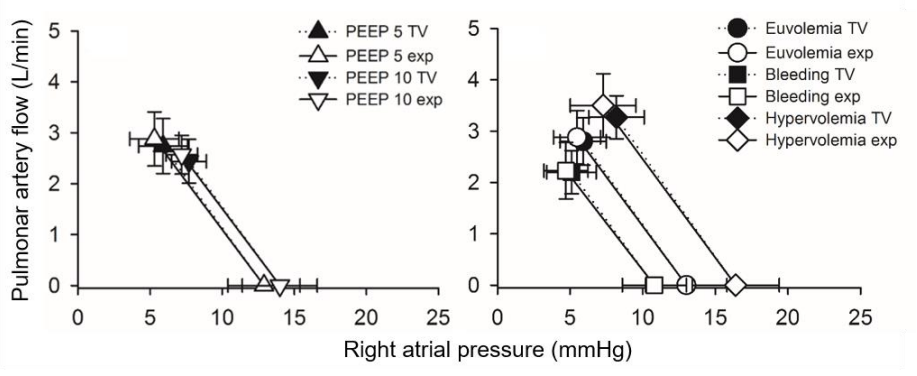

Figure 27 – Effect of tidal ventilation on the venous return function. RAP and Q_{PA} were measured for 10 beats during tidal ventilation and during an expiratory hold. Mean pressure-flow values are plotted with the $MSFP_{RAO}$ (measured at expiratory hold). Solid lines for end-expiration, dotted lines for tidal ventilation. Panel A: effect of tidal ventilation at PEEP 5 and 10 cmH_2O: RAP, $p<0.001$; Q_{PA}, $p<0.001$. Panel B: effect of tidal ventilation at changing blood volumes: RAP $p<0.001$; Q_{PA}, $p<0.001$. Values are shown as means, error bars indicate 1 SD.

RAP, $MSFP_{RAO}$, and VRdP changed in parallel with acute changes in blood volume. RVR did not change. The relationship of Q_{PA} *vs.* VRdP was linear [n=8, median (range) r^2=0.977 (0.729-0.9999)]. The volume state had a significant effect on the change in RAP_{tm}.

RAP increased and Q_{PA} decreased slightly but significantly in tidal breathing as compared to expiratory hold, for all experimental conditions. When data was plotted against the reference VR curve and connected to $MSFP_{RAO}$, the VR curve of tidal ventilation was shifted slightly to the right. Under the assumption that true MSFP did not change with the transition to tidal ventilation, RVR was consequently lower under tidal ventilation than during static expiratory hold.

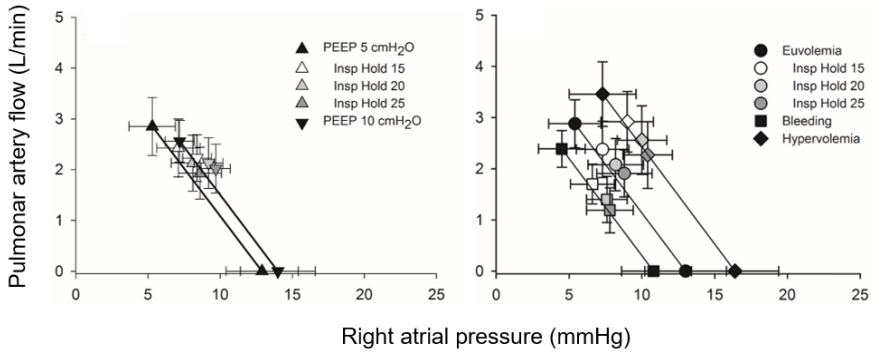

Figure 28 – Venous return at end-expiratory and inspiratory holds. Mean values of RAP and Q_{PA} were taken for 3 beats 9 s into hold. Their zero-flow extrapolations represent $MSFP_{insp\_hold}$ (not included in the plot). End-expiratory values and the respective $MSFP_{RAO}$ were used as the reference VR function (solid lines). Values shown as mean, error bars indicate 1 SD. Inspiratory hold data-pairs are shifted to the right of the reference VR curve at PEEP 5 and Euvolemia.

Systemic vascular compliance, C_{vasc}, was 3.2 ± 0.7 $mL \times mmHg^{-1} \times kg^{-1}$. The stressed volume in *Euvolemia* was 42 ± 9 $mL \times kg^{-1}$, or 43 ± 10 % of the total blood volume, respectively.

Paired comparisons between $MSFP_{insp\_hold}$ and $MSFP_{RAO}$ were available for n=37 over all conditions. $MSFP_{insp\_hold}$ overestimated $MSFP_{RAO}$: 16.5 ± 5.8 *vs.* 13.6 ± 3.2 mmHg respectively (p=0.001). The difference between methods was significant for both PEEP levels, but not significant for the three volume states (Table 3).

Method	n	PEEP 5	PEEP 10	*p*
$MSFP_{RAO}$	9	12.9 ± 2.5	14.0 ± 2.6	0.002
$MSFP_{insp\_hold}$	7	16.1 ± 2.7	18.7 ± 4.0	0.247

Method	n	Euvolemia	Bleeding	Hypervolemia	*p*
$MSFP_{RAO}$	8	13.0 ± 2.8	10.8 ± 2.2[a, b]	16.4 ± 3.0[c]	<0.0005
$MSFP_{insp\_hold}$	6	15.2 ± 4.1	11.9 ± 2.0[b]	21.1 ± 11.2	0.012*

Table 3 – Effect of PEEP level and volume state on the two methods of MSFP measurement. Data is mean ± SD (mmHg). Paired t-tests for PEEP levels. Repeated measurements ANOVA (or Friedman's test if appropriate) for volume state (within-subjects factor volume state). Pairwise comparisons with Bonferroni adjustment. Significant difference marked as: [a] Bleeding vs. Euvolemia, [b] Bleeding vs. Hypervolemia, [c] Hypervolemia vs. Euvolemia.*

When the methods were compared in each volume state, the difference was significant only in *Euvolemia*. When the VR curves from inspiratory hold maneuvers were plotted together with the reference VR curve from $MSFP_{RAO}$, the inspiratory hold VR curves were shifted to the right in euvolemic conditions only (=both PEEP levels and *Euvolemia*), but not in *Bleeding* or *Hypervolemia*.

Method	n	PEEP 5	PEEP 10	Method	PEEP level	Inter-action
$MSFP_{RAO}$	7	12.9 ± 2.8	14.1 ± 3.0	0.024	0.128	0.494
$MSFP_{insp\_hold}$		16.1 ± 2.7	18.7 ± 4.0			

Method	n	Euvolemia	Bleeding	Hypervolemia	Method	Volume state	Inter-action
$MSFP_{RAO}$	6	13.0 ± 3.3	10.9 ± 2.6	16.8 ± 3.4	0.245	0.009	0.494
$MSFP_{insp\_hold}$		15.2 ± 4.1	11.9 ± 2.0	21.1 ± 11.2			

Table 4 – Effect of method, PEEP level and volume state on MSFP. Data is mean ± SD (mmHg). Two-way repeated measurements ANOVA, within-subject factors method and PEEP level, and method and volume state respectively. Sensitivity analysis excluding the outlier ($MSFP_{insp\_hold}$ for animal 8 in Hypervolemia) gave the same result (albeit at n=5) - effect of volume state $p<0.0005$.

Inspiratory hold was associated with a rapid initial decrease in Q_{PA}, which partially recovered during the static hold. The maximum decrease in flow was different between SVC and IVC, and was modified by PEEP level and inspiratory plateau pressure. Q_{IVC} decreased more than Q_{SVC}, and was lowest after bleeding. The difference between vessels was most prominent at PEEP 5 cmH_2O and in *Euvolemia*. Q_{IVC} recovered more at lower plateau pressures, and

more than Q_{SVC} – regardless of volume state. The decrease and recovery were similar between both vessels in *Bleeding* and *Hypervolemia*.

The variable of $MSFP_{insp\_hold}$ contained one outlier in *Hypervolemia*: $MSFP_{insp\_hold}$ for animal 8 was 43.7 mmHg. As a sensitivity analysis, all comparisons between the two methods were performed with and without the outlier included. The difference between methods was consistent.

The inspiratory hold maneuvers led to progressively negative transmural pressures in SVC and IVC, with increasing plateau pressures. The relationship between change in transmural pressure and caval vein flow was linear with a negative slope.

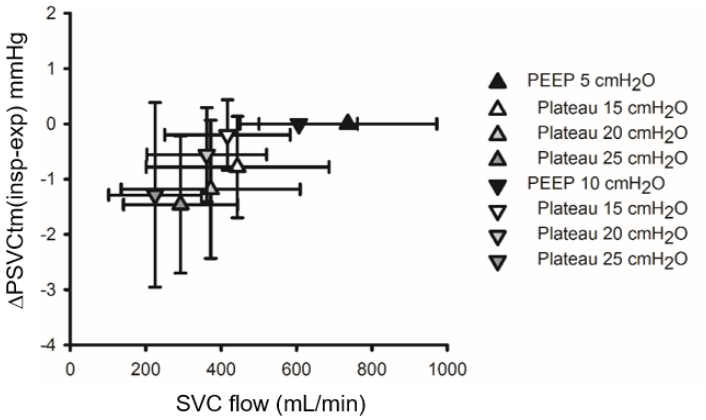

Figure 29 – Mean values of respiratory changes in SVC transmural pressure plotted against the SVC flow at PEEP 5 and 10 cmH_2O. Transmural pressures became progressively more negative at increasing airway plateau pressures.

4.2 RESULTS – PAPER II

One animal died at start of bypass, and *post mortem* examination revealed complex heart malformations. Ten animals were included in the study, weighing 42 ± 2.1 kg. In spite of the preceding volume expansion, in all animals, the bleeding had to be discontinued due to hypotension. The actual bled volume was [mean (range)] 12 (9-17) mL/kg.

	n	Euvolemia	Volume Expansion	Hypovolemia	*p*
rpm: min^{-1}	10	3095 (175)	3224 (247) [b]	2550 (153) [d]	<0.0005
Q_{ECMO}; $mL \times min^{-1}$	10	3497 (76)	3782 (160) [b]	2605 (84) [d]	<0.0005
Q_{VR}: $mL \times min^{-1}$	10	3126 (412)	3329 (654) [b]	2307 (297) [d]	<0.0005
S_vO_2: %	9	52 (4)	55 (6) [b]	38 (6) [d]	<0.0005
RAP†: mmHg	10	4.5 (1.8-6.0)	5.7 (3.6-8.0) [b]	2.4 (-1.6-4.6)	<0.0005†
Lactate: $mmol \times L^{-1}$	8	2.6 (0.8)	3.5 (1.2)	3.9 (2.1)	0.042
MAP†: mmHg	10	60 (51-74)	60 (53-73) [b]	45 (36-57) [d]	<0.0005†
Heart rate: $beats \times min^{-1}$	10	93 (15)	96 (19)	107 (36)	n.s.
MSFP: mmHg	9	10.3 (0.5) [a]	12.3 (1.2) [b]	8.7 (1.0) [d]	<0.0005
VRdP†: mmHg	9	5.2 (4.9-9.1)	6.6 (4.8-9.5)	5.9 (4.7-10.7)	n.s.†
RVR†: $mmHg \times min \times L^{-1}$	9	1.9 (1.3-2.9)	1.9 (1.3-2.8) [c]	2.5 (2.0-5.6)	0.013†

Table 5 - Data is averaged over three heart beats in expiratory hold at PEEP 5 cmH_2O and Baseline pump speed, S_vO_2 and lactate was sampled at Baseline pump speed in the beginning of each volume state. Data is mean (SD), or median (range) if not normally distributed (†). p-values: repeated measurements ANOVA for effect of volume state or Friedman's test (†) was performed as appropriate. Post hoc analysis with Bonferroni correction is indicated as: [a] Euvolemia vs. Volume Expansion (p = 0.002); [b] Volume Expansion vs. Hypovolemia (p ≤ 0.001; [c] for RVR p = 0.029); [d] Hypovolemia vs. Euvolemia (p ≤ 0.012). rpm= revolutions per min; RAP= right atrial pressure; Q_{ECMO}= ECMO flow; Q_{VR}= venous return flow (sum of caval vein flows); MAP= mean arterial pressure; MSFP= mean systemic filling pressure; VRdP= venous return driving pressure (VRdP=MSFP-RAP); RVR=resistance to venous return (RVR=VRdP/Q_{VR}).

Zero-flow pressure equilibration was always more complete with open shunt. In *Euvolemia*, inspiratory hold increased MSFP, but not in *Volume Expansion* or *Hypovolemia* (Table 6). Systemic vascular compliance, C_{vasc}, was 4.3 ± 1.8 $mL \times mmHg^{-1} \times kg^{-1}$.

		MSFP (mmHg)		p		
	Resp. cycle	**Open shunt**	**Closed shunt**	Resp. cycle	Shunt state	Interaction
Euvolemia (n=10)	Expiration	10.0 (1.1)	9.0 (1.0)	0.005	0.002	n.s.
	Inspiration	10.4 (1.0)	9.4 (0.9)			
Volume Expansion (n=10)	Expiration	11.9 (1.6)	10.8 (1.7)	n.s.	<0.0005	n.s.
	Inspiration	12.2 (1.7)	10.8 (1.7)			
Hypovolemia (n=9)	Expiration	8.7 (1.0)	7.9 (0.9)	n.s.	0.004	n.s.
	Inspiration	8.8 (1.2)	8.4 (0.9)			

Table 6 - MSFP was taken as the mean value of RAP during three beats of equilibrium defined from ABP nadir. p-values: repeated measurements ANOVA, within-subject factors; respiratory cycle and shunt state. Hypovolemia: n=9 as one animal lack valid MSFP Expiration Open Shunt.

The RAP-pump speed relation was highly linear, independent of volume state and respiratory cycle (expiration/inspiration). However, despite efforts of setting the maximum ECMO speed as the highest without RA collapse, negative values of RAP were detected during offline analysis in two animals. This may be associated with vessel collapse upstream of the venous cannula, thereby dissociating the pressure-flow relation.

Instantaneous VR curves incorporating beat-to-beat data pairs from one respiratory cycle and the open shunt expiratory MSFP were highly linear.

Nine animals had complete sets of airway pressure maneuvers for all volume states (Figure 30). A change in airway pressure resulted in a change in RAP in the same direction. During the hold maneuvers, RAP returned towards its "pre" levels earlier than did airway pressure. When RAP was changed by means of changing airway pressure, there was an immediate, transient change in VR in the opposite direction. During the inspiratory hold maneuvers, VR partially recovered already during the three first beats ("early") after the maximum decrease in VR, while RAP still remained elevated. During the zero PEEP maneuvers, this pattern was reversed.

The transient imbalance between inflow to the RA (=VR) and outflow from the ECMO (=cardiac output), caused by the airway pressure maneuvers, was associated with volume shifts out from, or into the RA. VR decreased during inspiratory hold, and increased during zero PEEP maneuvers. The aortic flow was unchanged or even slightly increased (during inspiratory hold in *Euvolemia*). During the first four beats ("ΔQ_{VC}max", and "early"), the median volume shifted upstream was 9 (-2 to 35) mL in inspiratory hold, and the

median volume shifted downstream in expiratory hold at zero PEEP, was 12 (4-68) mL.

When Q_{VR}-RAP data-pairs from pump speed maneuvers (in expiration and inspiration), tidal ventilation (all beats in one breath), the immediate effects of the airway pressure maneuvers (inspiratory hold and zero PEEP maneuvers; "pre" and "ΔQ_{VC}max"), and the stop flow maneuvers (MSFP; open shunt in expiration and inspiration) were combined, the overall relationship was linear.

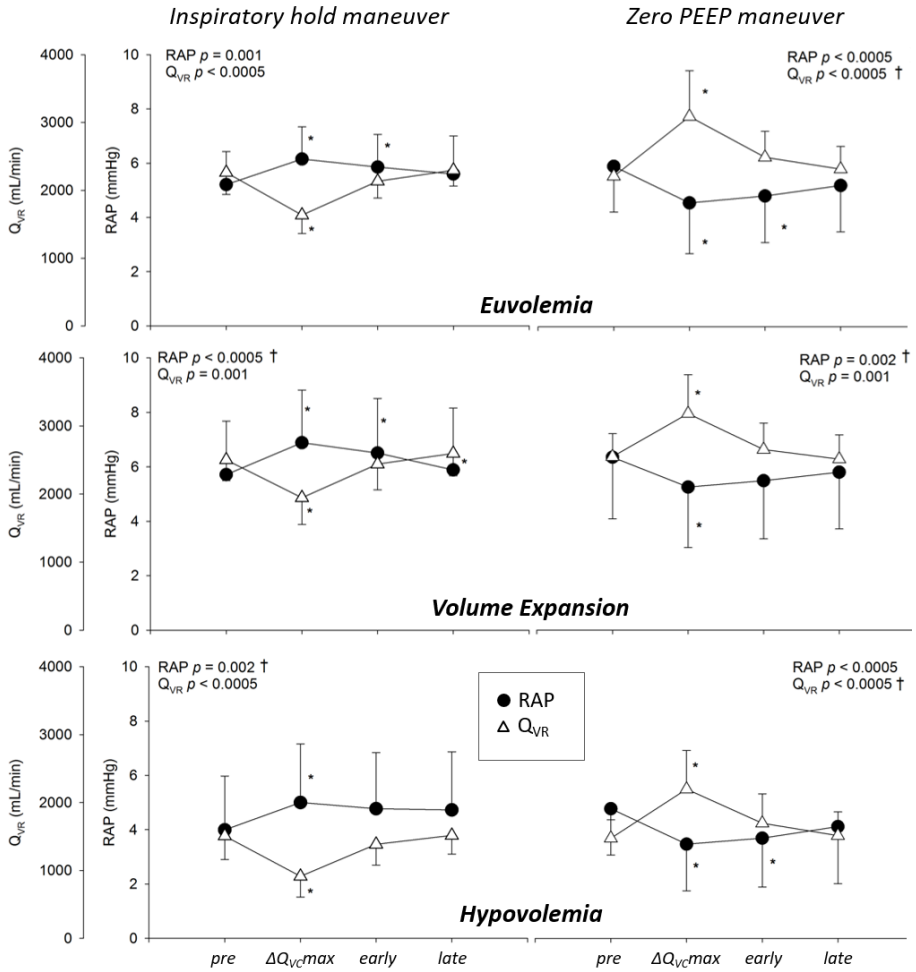

*Figure 30 – Behavior of RAP and venous return (Q_{VR}) during inspiratory hold (left) and zero PEEP maneuvers (right). Repeated measurements ANOVA († or Friedman's test as appropriate), within-subjects effect time. * $p<0.05$ for post hoc pairwise comparison vs. "pre" level, with Bonferroni correction.*

The effect of experimentally controlled variable (pump speed *vs*. airway pressure) on the VR-RAP relation was analysed using GEE. Two animals showing signs of caval collapse were excluded from this analysis (animal 10 in *Volume Expansion* and *Hypovolemia*, and animal 11 in inspiration in *Euvolemia* and *Hypovolemia*). The control variable had no effect on the pressure-flow relationship (Figure 31).

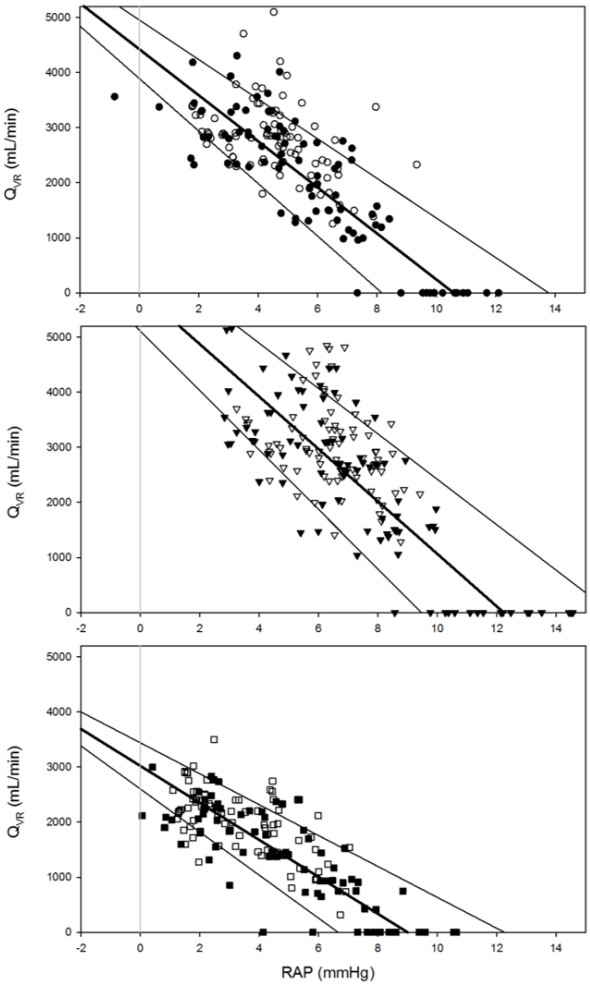

Figure 31 – Venous return plots. Q_{VR}-RAP data-pairs from pump speed and stop flow maneuvers, representing changing pump effect (filled symbols), and the corresponding data-pairs obtained during tidal ventilation and the immediate effect of airway pressure maneuvers representing changing RAP (open symbols). Using GEE, interaction of the controlled variable (change in pump speed vs. change in RAP) on the Q_{VR}-RAP relationship was studied over volume states. GEE model parameters including 95% CIs are drawn as thick and thin lines. Due to markedly negative RAPs and possible caval collapse, animal 10 was excluded from analysis in Volume Expansion and Hypovolemia; animal 11 was excluded in Euvolemia and Hypovolemia.

The cross correlation analysis revealed a peak negative correlation between RAP and Q_{VR} close to zero time lag. Changes in RAP preceded changes in Q_{VR} with at least 1.2 samples (=12 ms) for increasing and decreasing airway pressure in all volume states.

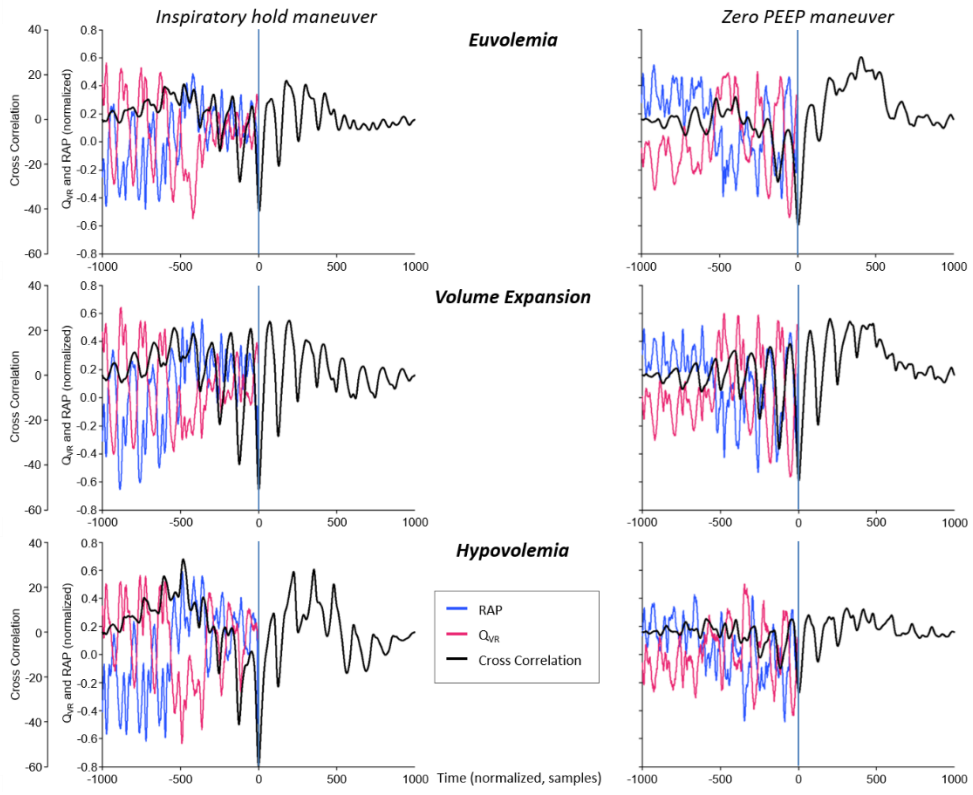

Figure 32 – Cross correlation analysis between RAP and Q_{VR} during seven beats of acutely changing VR caused by airway pressure maneuvers. RAP and Q_{VR} were normalized in amplitude (-1 to +1). For the (summary) plots above, time was normalized to 1000 samples to allow averaging of all animals. Changes in RAP preceded changes in Q_{VR}: mean ± SD (samples) Euvolemia: 3.2 ± 2.7; Volume Expansion: 1.7 ± 3.4; Hypovolemia: 2.4 ± 3.2.

4.3 RESULTS – PAPER III

Ventricular fibrillation resulted in complete cessation of pulmonary artery blood flow for all animals (n=9, weight 40 ± 2.1 kg). The pump function (expressed as mL/revolution) was linear for individual animals in all experimental conditions and pump speeds [median (range) r^2 0.9999 (0.811 to 1.0)]. MSFP increased with increasing intensity of both treatments. For the doses used, the effect was more pronounced for *Volume Expansion* than for *Vasoconstriction*. The treatments led to haemodilution and haemoconcentration respectively. Blood lactate levels increased together with oxygen consumption (VO_2) throughout the experiment, despite maintenance of the target S_VO_2. Urine output was stable during both *Vasoconstriction* and *Volume Expansion* at 2.6 ± 1.1 *vs*. 2.7 ± 1.4 $mL \times kg^{-1} \times h^{-1}$ (p=0.832). Factors defining venous return (MSFP, maintenance Q_{ECMO}, rpm, RAP, VRdP, and RVR) were not different between *Euvolemia* and *Post Vasoconstriction*.

Maximum Q_{ECMO} increased with increasing intensity of both treatments. For the doses used, the maximum achievable Q_{ECMO} was higher following *Volume Expansion*, but due to concomitant haemodilution, this did not translate into higher DO_2 as compared to *Vasoconstriction*.

A total of 360 pump speed maneuvers were performed at the five pump speeds higher than zero. During offline analysis (performed independently by three investigators), signs of vascular collapse were seen in 17% of maneuvers, with equal distribution between treatments. There was a negative linear relation between changing Q_{ECMO} and RAP over all conditions [median (range) r^2 0.975 (0.626-1.000)]. Both treatments increased MSFP and flow, and the respective VR curves were shifted to the right (Figure 33). VRdP was not different between conditions and at maintenance speed. The response of RVR at different levels of vasoconstriction was highly variable, with an equal distribution of increasing, unchanged and decreasing values for individual animals. In contrast, *Volume Expansion* consistently and progressively lowered RVR.

The relation between generated pressure head (MAP-RAP) *vs*. Q_{ECMO} was highly linear in all conditions. The resistance needed to be overcome by the pump was lower in *Volume Expansion 3* than in *Euvolemia* and *Vasoconstriction 3*.

	Euvolemia	Vasoconstriction			Post Vasoconstr.	Volume Expansion			*p* values		
		Step 1	Step 2	Step 3		Step 1	Step 2	Step 3	treatment	intensity	interaction
MSFP: mmHg	7.1 ± 1.1	6.7 ± 0.6	7.4 ± 1.0	7.9 ± 0.6	6.5 ± 0.7	7.8 ± 0.7	8.6 ± 1.1	8.9 ± 1.1	0.023	<0.0005	<0.0005
									Vasoconstriction 0.021* Volume Expansion <0.0005*		
Q_{ECMO}; mL × min^{-1}	3382 ± 199	3454 ± 262	3515 ± 163	3606 ± 207	3144 ± 682	3887 ± 308	4237 ± 492	4317 ± 386	0.002	<0.0005	<0.0005
									Vasoconstriction 0.20* Volume Expansion 0.015*		
rpm: min^{-1}	2978 ± 164	3047 ± 296	3133 ± 218	3144 ± 213	2944 ± 403	3206 ± 248	3344 ± 292	3422 ± 327	0.017	0.004	0.079
SvO_2: %	54 ± 7	52 ± 3	54 ± 4	56 ± 5	46 ± 9	49 ± 5	52 ± 5	54 ± 5	0.027	0.047	0.376
VRdP: mmHg	5.1 ± 2	5.2 ± 1.4	4.8 ± 1.0	5.1 ± 1.1	4.7 ± 2.8	4.7 ± 0.8	4.5 ± 1.3	4.0 ± 1.5	0.209	0.524	0.663
MAP: mmHg	70 ± 15	82 ± 12	90 ± 22	76 ± 14	54 ± 10	60 ± 8	60 ± 11	59 ± 11	0.001	0.001	0.015
Hemoglobin: g × L^{-1}	94 ± 6	100 ± 7	106 ± 7	108 ± 7	108 ± 6	101 ± 5	97 ± 6	93 ± 7	0.079	0.818	<0.001
Lactate: mmol × L^{-1}	1.2 ± 0.8	1.6 ± 1.1	2.1 ± 1.3	3.2 ± 2.0	5.7 ± 3.3	6.2 ± 2.5	6.0 ± 4.5	6.0 ± 4.5	0.003	0.036	0.003

*Table 7 – Hemodynamics at maintenance pump speed. Data is mean ± SD. n=9. Two-way repeated measurements ANOVA, within-subject factors treatment modality and treatment intensity. *In case of significant interaction, simple main effect for intensity was assessed with repeated measurements ANOVA, within-subject factor treatment intensity. MSFP= mean systemic filling pressure; Q_{ECMO}= ECMO flow; rpm: revolutions per minute; VRdP= MSFP-RAP= venous return driving pressure; MAP= mean arterial pressure.*

	Euvolemia	Vasoconstriction			Post Vasoconstr.	Volume Expansion			*p* values		
		Step 1	Step 2	Step 3		Step 1	Step 2	Step 3	treatment	intensity	interaction
Q_{ECMO} max: mL × min^{-1}	4376 ± 887	4369 ± 802	4670 ± 746	4967 ± 977	3470 ± 902	4792 ± 677	5469 ± 982	5649±1040	0.127	<0.0005	0.003
									Vasoconstriction 0.012* Volume Expansion <0.0005*		
rpm max: min^{-1}	3756 ± 644	3744 ± 570	3972 ±603	4000 ± 634	3104 ± 585	3756 ± 413	4167 ± 608	4322 ± 626	0.663	<0.0005	<0.0005
									Vasoconstriction 0.064* Volume Expansion <0.0005*		
Pump efficiency: mL × revolution^{-1}	1.17 ± 0.16	1.16 ± 0.10	1.18 ± 0.12	1.23 ± 0.07	1.11 ± 0.12	1.27 ± 0.07	1.31 ± 0.10	1.30 ± 0.12	0.042	<0.0005	0.008
									Vasoconstriction 0.203* Volume Expansion <0.0005*		
DO_2 max: mL × min^{-1}	561 ± 112	597 ± 124	673 ± 133	734 ± 160	510 ± 140	661 ± 105	729 ± 161	726 ± 177	0.489	<0.0005	0.051

*Table 8 – Maximum ECMO flow. Data is mean ± SD. n=9. Two-way repeated measurements ANOVA, within-subject factors treatment modality and treatment intensity. *In case of significant interaction, simple main effect for intensity was assessed with repeated measurements ANOVA, within-subject factor treatment intensity. Q_{ECMO} max= maximum ECMO flow; rpm= pump speed giving Q_{ECMO} max; Pump efficiency= mL × revolution^{-1} at rpm max; DO_2 max = delivery of oxygen at maximum ECMO flow.*

	Euvolemia	Vasoconstriction			Post Vasoconstr.	Volume Expansion			*p* values		
		Step 1	Step 2	Step 3		Step 1	Step 2	Step 3	treatment	intensity	interaction
Q_{ECMO}: mL×min^{-1}	3828 ± 766	3858 ± 564	4139 ± 625	4103 ± 594	3093 ± 723	4415 ± 713	4891 ± 761	5078 ± 934	0.057	<0.0005	0.005
									Vasoconstriction 0.2* Volume Expansion <0.0005*		
VRdP : mmHg	5.76 ± 1.66	5.40 ± 1.27	5.54 ± 1.07	5.47 ± 1.12	5.35 ± 2.29	5.07 ± 1.68	5.34 ± 1.83	4.96 ± 2.04	0.558	0.583	0.960
RVR: mmHg/(mL×min^{-1})	1.59 ± 0.57	1.54 ± 0.40	1.44 ± 0.36	1.48 ± 0.25	2.00 ± 0.84	1.30 ± 0.25	1.19 ± 0.30	1.06 ± 0.31	0.348	0.007	0.041
									Vasoconstriction 0.445* Volume Expansion 0.014*		

Table 9 - Venous return function - closing conditions excluded. Data is mean ± SD. n=9. Statistical approach – see Table 8. Q_{ECMO} = highest ECMO flow in the per protocol data set (closing conditions excluded); VRdP highest= venous return driving pressure at highest Q_{ECMO}, calculated as MSFP-RAP; RVR= resistance to venous return calculated as inverse slope of individual animal RAP-Q_{ECMO} pairs

Vasoconstriction increased MSFP and decreased total blood volume, compared to *Euvolemia*, due to extravasation of plasma. *Volume Expansion* restored and increased the blood volume slightly over the baseline level of *Euvolemia* due to plasma expansion. *Vasoconstriction* increased vascular elastance compared to *Volume Expansion*. *Vasoconstriction* led to a leftward shift of the pressure-volume as unstressed volume was recruited into stressed volume. *Volume Expansion* shifted the pressure-volume plot back to the right with direct increases in both stressed and unstressed volumes (Figure 35).

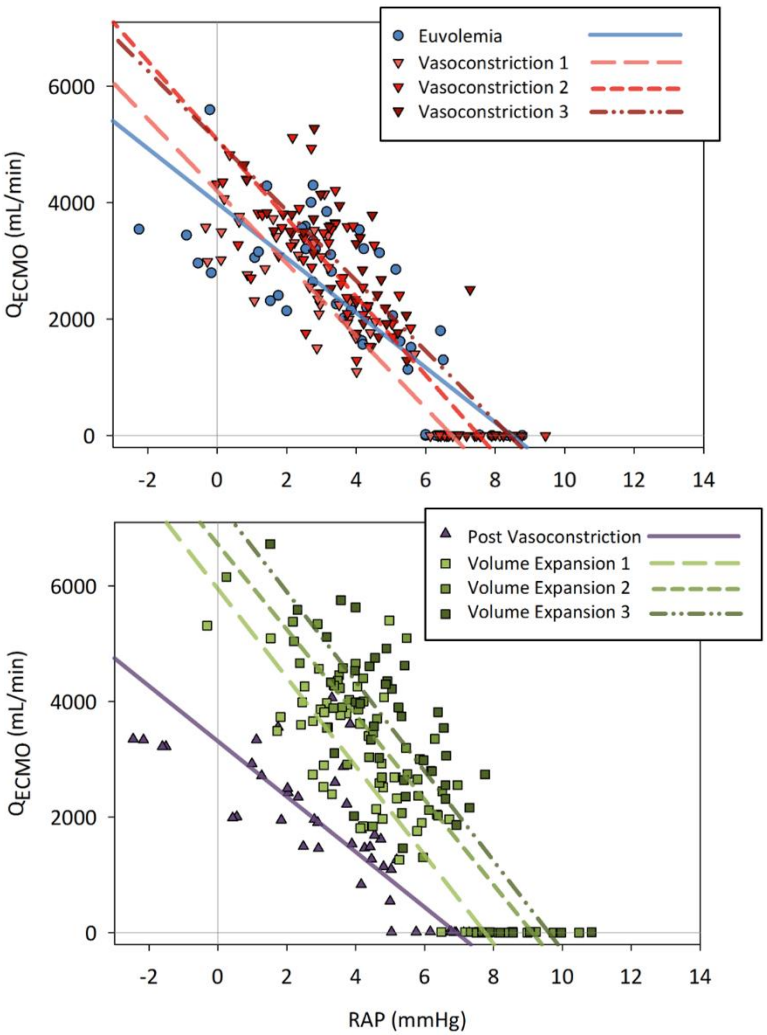

Figure 33 - Venous return curves after exclusion of closing conditions. Upper panel shows Euvolemia and Vasoconstriction 1-3, lower panel Post Vasoconstriction and Volume Expansion 1-3. Lines indicate the mean slopes from GEE.

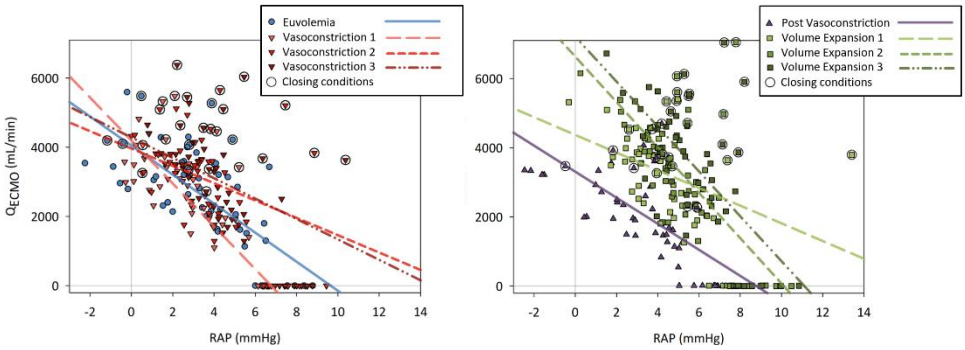

Figure 34 – Venous return curves per protocol (including closing conditions). Upper panel shows Euvolemia and Vasoconstriction 1-3, lower panel Post Vasoconstriction and Volume Expansion 1-3. Lines indicate the mean slopes from GEE. Data-points within circles were identified as closing conditions.

At the highest levels of *Vasoconstriction* and *Volume Expansion*, repeated measurements over 40 minutes showed a mean MSFP decay of 1.7 mmHg [equivalent to mean (CI) slope = -0.043 (-0.065 to – 0.021) mmHg×min^{-1}], with no difference between conditions. The changes in plasma volume were small, with no difference between conditions.

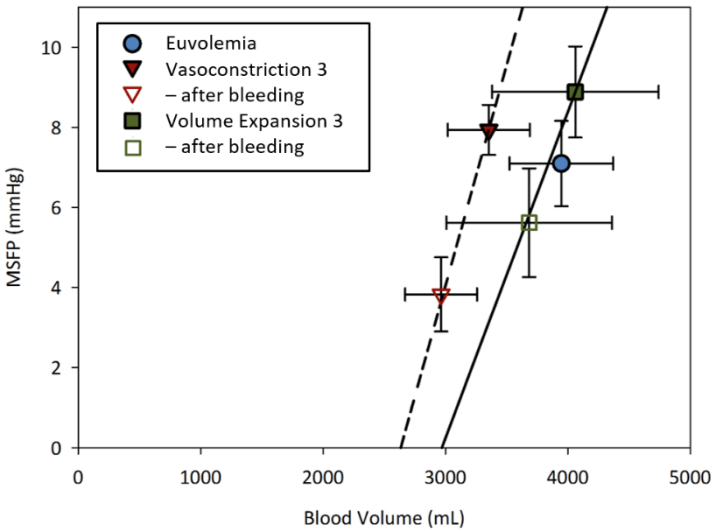

Figure 35 - Pressure-volume plots of vascular elastance derived from the rapid bleeding maneuvers in Vasoconstriction 3 (dashed line) and Volume Expansion 3 (solid line).

4.4 RESULTS – PAPER IV

Venous return driving pressure was 6.8 ± 2.4 mmHg in *Euvolemia* (n=9 in *Euvolemia*). The desired method agreement for changes in MSFP thereby corresponded to ≤0.7 mmHg. When all volume states were compared together, no difference was found between $MSFP_{inst\_VR}$ and $MSFP_{RAO}$, but $MSFP_{nadir\_hold}$ and $MSFP_a$ underestimated $MSFP_{RAO}$. The respective agreement between indirect estimates of MSFP and the reference method was influenced by the underlying volume state (method × volume state interaction $p \leq 0.020$) (Table 10). *Post hoc* paired methods comparison for separate volume states showed a trend of $MSFP_{inst\_VR}$ underestimating $MSFP_{RAO}$ in *Bleeding* only (see Paper IV: Table V).

	n	**Euvolemia:** mmHg	**Bleeding:** mmHg	**Hypervolemia:** mmHg	*p*
$MSFP_{RAO}$	8	13.0 ± 2.8	10.8 ± 2.2[a, b]	16.4 ± 3.0[c]	<0.0005
$MSFP_{inst\_VR}$	7	12.6 ± 1.3	8.7 ± 0.9[a, b]	18.5 ± 5.2	0.003
$MSFP_{nadir\_hold}$	7	11.6 ± 1.6	8.8 ± 1.6[a, b]	13.1 ± 1.4	<0.0005
$MSFP_a$	8	10.2 ± 1.8	8.6 ± 1.6[a, b]	12.9 ± 1.7[c]	<0.0005

Table 10 - MSFP with four methods over changing volume state. Data is mean ± SD. $MSFP_{RAO}$: see section 3.3.1; $MSFP_{inst\_VR}$: instantaneous VR - see section 3.4.3.; $MSFP_a$: dynamic analogue of static MSFP using mean values from 10 beats during tidal ventilation before RAO – see section 3.4.4. Repeated measurements ANOVA, within-subject factor volume state and pairwise comparisons with Bonferroni adjustment. Significant difference marked as [a] Bleeding vs. Euvolemia, [b] Bleeding vs. Hypervolemia, [c] Hypervolemia vs. Euvolemia.

	n	**Euvolemia:** mmHg	**Bleeding:** mmHg	**Hypervolemia:** mmHg	Method	Volume state	Inter-action
$MSFP_{inst\_VR}$	7	12.6 ± 1.3	8.7 ± 0.9	18.5 ± 5.2	0.396	0.001	0.020
$MSFP_{RAO}$		13.6 ± 2.3	11.4 ± 1.7	17.1 ± 2.4			
$MSFP_{nadir\_hold}$	7	11.6 ± 1.5	8.8 ± 1.6	13.1 ± 1.4	0.011	<0.0005	0.020
$MSFP_{RAO}$		13.3 ± 2.8	11.0 ± 2.4	16.7 ± 3.1			
$MSFP_a$	8	10.2 ± 1.8	8.6 ± 1.6	12.9 ± 1.7	0.013	<0.0005	0.008
$MSFP_{RAO}$		13.0 ± 2.8	10.8 ± 2.2	16.4 ± 3.0			

Table 11 - Data is mean ± SD. Two-way repeated measurements ANOVA, within-subject factors method and volume state.

Resistance to venous return calculated with the reference method did not change over volume states: RVR_{RAO} (n=8) 2.49 ± 0.60, 2.60 ± 0.58, and 2.50 ± 0.52 mmHg×min×L^{-1} in *Euvolemia*, *Bleeding*, and *Hypervolemia* respectively (p=0.489). However, RVR calculated from $MSFP_{inst\_VR}$ decreased in *Bleeding*: RVR_{inst_VR} (n=8) 2.25 ± 0.48, 1.46 ± 0.40, and 2.96 ± 1.28 mmHg×min×L^{-1} respectively (*p*=0.009; pairwise comparisons significant between *Bleeding-Euvolemia* at *p*=0.019 and *Bleeding-Hypervolemia* at *p*=0.031).

For absolute values, the lowest bias compared to the reference method $MSFP_{RAO}$ was seen for $MSFP_{inst\_VR}$ [bias (95% CI): -0.6 (-2.3 to 1.0) mmHg], with wide limits of agreement (LoA) and CIs (Table 12). Four-quadrant plots showed that all test methods tracked changes in the reference method concordantly with high correlation (see Paper IV; Figure 3). Bland-Altman analyses for changes in methods showed lowest bias between $\Delta MSFP_a$ *vs.* $\Delta MSFP_{RAO}$ [bias (95% CI): -0.4 (-0.7 to -0.0) mmHg]. The limits of agreement was -2.9 to 2.1 mmHg, exceeding the desired agreement of 10% VRdP in Euvolemia (0.7 mmHg) (Table 13).

The factor 'c' for $MSFP_a$ derived from SVR at Euvolemia was 0.78 ± 0.18 mmHg×min×L^{-1} (range 0.51-1.02). The corresponding values calculated anew from SVR at Bleeding and Hypervolemia were (n=8) 0.77 ± 0.22 and 0.63 ± 0.19 mmHg×min×L^{-1} respectively (main effect of volume state p=0.002; pairwise comparisons between Euvolemia-Hypervolemia and Bleeding-Hypervolemia significant at p≤0.017). The model assumption of a non-changing R_v resulted in an overestimation of the dynamic filling analogue by 0.48 mmHg, or 3.8 ± 2.3% in Hypervolemia.

	n (pairs)	Bias (95% CI): mmHg	LoA: mmHg	95% CI lower LoA: mmHg	95% CI upper LoA: mmHg	SD_{diff} ± SE: mmHg	ICC ± SE:
$MSFP_{inst\_VR}$ *vs.* $MSFP_{RAO}$	24	-0.6 (-2.3 to 1.0)	-6.7 to 5.5	-10.4 to -4.9	3.6 to 9.2	3.1 ± 0.5	0.15 ± 0.22
$MSFP_{nadir\_hold}$ *vs.* $MSFP_{RAO}$	23	-2.5 (-3.9 to -1.1)	-6.5 to 1.5	-9.9 to -5.0	0.0 to 4.9	2.1 ± 0.4	0.50 ± 0.19
$MSFP_a$ *vs.* $MSFP_{RAO}$	25	-2.7 (-4.5 to -0.8)	-7.5 to 2.2	-12.0 to -5.4	0.1 to 6.7	2.5 ± 0.6	0.87 ± 0.06

Table 12 - Comparison of methods, with CIs adjusted for repeated measurements over volume states. Bias: grand mean of test method – reference method; LoA: Limits of Agreement; SD_{diff}: standard deviation of differences with its standard error; ICC: intraclass correlation (ratio of between-subjects variance to total variance).

	n (pairs)	Bias (95% CI): mmHg	LoA: mmHg	95% CI lower LoA: mmHg	95% CI upper LoA: mmHg	SD_{diff} ± SE: mmHg	ICC ± SE:	r^2
$MSFP_{inst\_VR}$ *vs.* $MSFP_{RAO}$	14	1.5 (0.3 to 2.7)	-5.0 to 8.0	-10.8 to -3.0	6.0 to 13.8	3.3 ± 0.7	-0.68 ± 0.82	0.88
$MSFP_{nadir\_hold}$ *vs.* $MSFP_{RAO}$	15	-1.0 (-1.9 to -0.1)	-4.0 to 1.9	-6.5 to -2.9	0.9 to 4.5	1.5 ± 0.3	-0.19 ± 0.47	0.92
$MSFP_a$ *vs.* $MSFP_{RAO}$	16	-0.4 (-0.7 to -0.0)	-2.9 to 2.1	-5.1 to -2.1	1.4 to 4.3	1.3 ± 0.3	-0.80 ± 0.81	0.94

Table 13 - Assessment of method tracking ability, comparing Δ[test method] to Δ[reference method] between Euvolemia and Bleeding and Bleeding and Hypervolemia, with CIs adjusted for repeated measurements. Bias: grand mean of test method – reference method; LoA: Limits of Agreement; SD_{diff}: standard deviation of differences with its standard error; ICC: intraclass correlation (ratio of between-subjects variance to total variance); r^2: proportion of variance (Pearson correlation coefficient squared). As a reference, venous return driving pressure (VRdP) was 6.8 ± 2.4 mmHg in Euvolemia.

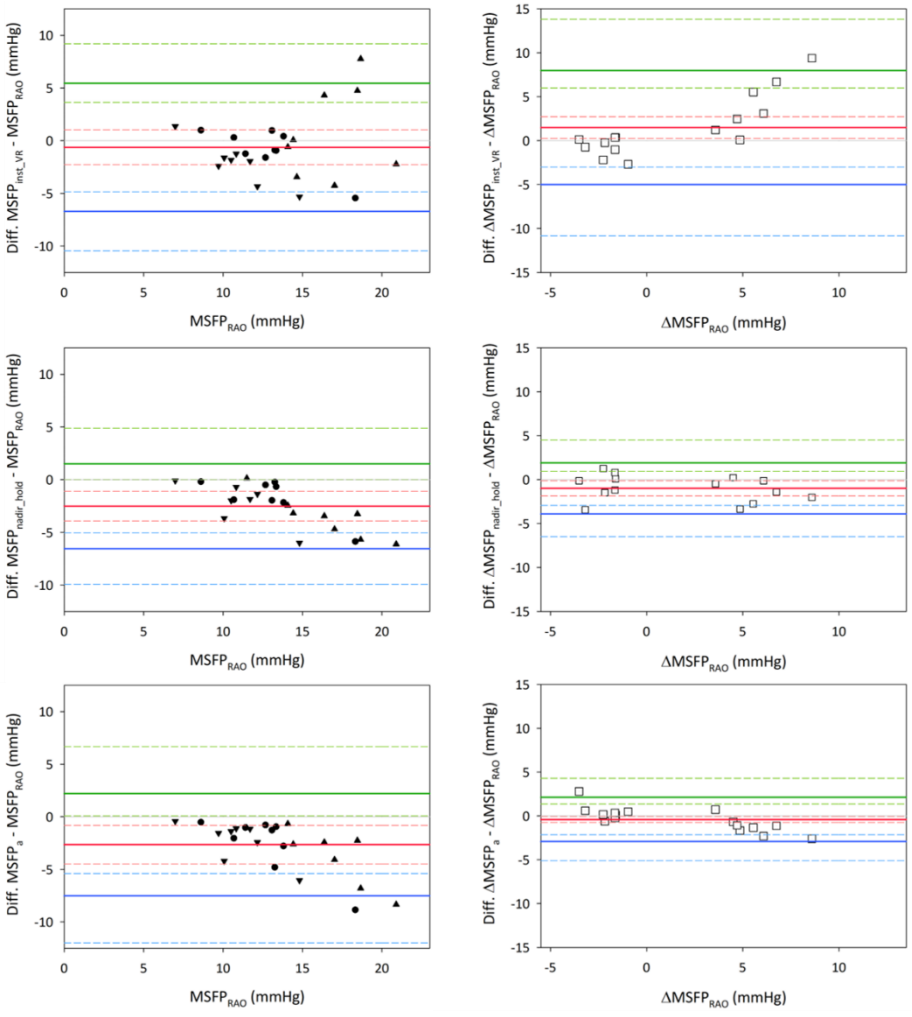

Figure 36 - Bland-Altman plots. Left hand panels represent [difference between test method and reference method] vs. absolute values of $MSFP_{RAO}$ (Euvolemia – circles; Bleeding – downward pointing triangles; Hypervolemia – upward pointing triangles). Right hand panels represent [difference between Δtest method and $\Delta MSFP_{RAO}$] vs. $\Delta MSFP_{RAO}$. Method bias in red, upper and lower LoA in green and blue, dashed lines CIs.

5 DISCUSSION

5.1 DISCUSSION - PAPER I

There were three main findings in Paper I: First, a moderate increase in PEEP level from 5 to 10 cmH_2O was associated with an increase in $MSFP_{RAO}$ that partly defended venous return. However, the VRdP decreased and RVR was unchanged. The steady state Q_{PA}, and therefore cardiac output, decreased slightly, but this change did not reach statistical significance. Second, changes in blood volume were associated with concordant changes in $MSFP_{RAO}$, RAP, and VRdP. Again, there were no changes in RVR. Third, inspiratory hold maneuvers shifted the VR curve to the right as compared to the reference curve of $MSFP_{RAO}$ in euvolemic conditions, but not in *Bleeding* or *Hypervolemia*. Consequently, $MSFP_{insp\_hold}$ overestimated $MSFP_{RAO}$ in euvolemic conditions.

To explore the right-shift of the VR curve, we examined flow dynamics of the caval veins and the pulmonary artery in the early and late phases of the inspiratory hold maneuver. We found that the patterns of decrease and recovery of blood flows differed between the IVC and the SVC in euvolemic conditions. The pattern of caval flow recovery therefore matched the pattern of right-shifted VR curve over the experimental conditions. The flow recovery occurred within heartbeats after initiation of the static hold maneuver, and seemed to be completed as flows reached new steady states well before nine seconds into the maneuver. Reflex activation within this period is unlikely. However, a vascular waterfall mechanism located in the splanchnic region, could offer a possible explanation for the observed difference over volume states (68, 80).

The vascular drainage of the liver has a vascular waterfall mechanism that can be overcome when the outflow pressure (RAP) exceeds ~5 mmHg. Above this pressure, the internal flow resistance of the liver decreases with passive distension of the venous system. In studies on isolated porcine livers, the distensibility appeared to be maximal at outflow pressures above 10 mmHg (8, 19, 68). As RAP is acutely increased by the inspiratory hold maneuver, the vascular waterfall is first overcome, followed by upstream distension in the liver, resulting in decreased flow resistance. This mechanism could defend the hepatosplanchnic and IVC venous return during acute increases in RAP.

In hypervolemia, the elevated RAP would already act as the true downstream pressure (having inactivated the waterfall) and a lesser reserve of decreased flow resistance from further vascular distension would remain as the

inspiratory hold maneuver began. In hypovolemia, the splanchnic reservoir would, to varying extent, already have been mobilized by passive and reflex mediated mechanisms. Once the vascular waterfall was opened by inspiratory hold, there would remain less splanchnic blood volume available for flow recovery. It is unknown to what extent the hepatic arterial buffer response could upregulate arterial inflow to the liver during the course of an inspiratory hold maneuver.

Fessler showed in dogs that vascular waterfalls can develop in both caval veins as a consequence of PEEP (28). If present also in pigs, this would further modulate the flow dynamics described above.

To summarize, in the early phase of increased airway pressure, upstream areas will be volume loaded and the inflow to the right atrium will underestimate the steady state venous return. In the later phase of a static increase in airway pressure, vascular waterfalls and modulation of hepatic flow resistance will be activated to an extent that is *dependent on the underlying volume state*. It is therefore impossible to know if the new steady state flow, present 10-20 seconds into the hold maneuver, is representative of the steady state VR or not. The degree of dynamic flow restoration will remain an unknown factor. Importantly, the agreement (or lack thereof) between an inspiratory hold estimation and a true zero-flow measure of MSFP will only become apparent when they are compared over *changing volume states*.

The *site* of flow measurement, be it the caval veins, the pulmonary artery or the aorta, will determine how much of the actual dynamic flow restoration that becomes apparent to the investigator. However, the choice of site does not obviate the need for method comparisons over changing volume states.

As we measured $MSFP_{RAO}$ only in expiratory hold, it is impossible from this study to answer whether true MSFP changes within the respiratory cycle, or if it changes with acutely increased airway pressure (as opposed to the "chronic" change in P_{AW} seen for example after one minute at a new PEEP level). Our VR reference curve connected data from 10 beats of expiratory hold with $MSFP_{RAO}$ measured in expiratory hold. The pressure-flow data-point representing mean values from 10 beats of tidal ventilation, plotted in the same graph, was shifted down and to the right, and fell slightly but significantly *to the right* of the reference curve. From the present experiment, it is not possible to deduce if true MSFP would have been shifted to the right, if there was a true isolated decrease in RVR, or even a combination of increased MSFP and increased RVR.

As discussed previously (section 3.3.1), since we did not actively transfer blood between arteries and veins, an arteriovenous pressure difference of ~10 mmHg remained at zero flow and time of best equilibrium. Compared to the results of Ogilvie (same technique and species) and Jellinek (ICD testing in patients), the zero-flow measurements from the present experiment likely represents a high degree of equilibration – albeit not total. This translates into a slight *underestimation* of MSFP. However, between the onset of right atrial balloon occlusion and the time of best equilibrium, the beating heart will transfer volume from the pulmonary compartment to the systemic compartment. This volume shift will theoretically *increase* the stressed volume in the systemic compartment, but since the overall compliance is high, the resulting increase in MSFP was estimated to around 1-2% (data not shown). Taken together, it is *unlikely* that our measure of $MSFP_{RAO}$ greatly *underestimates* the true MSFP.

In agreement with previous investigators, we report an increase in MSFP from increased PEEP. However, in contrast to the studies by Fessler and Nanas (29, 30, 71), we found that increasing PEEP level was associated with a *decrease* in VRdP and *unchanged* RVR. This is the same pattern of change that Chihara reported for rats in the transition from spontaneous to controlled positive pressure ventilation (both conditions under anaesthesia) (21). Compared to the previous studies, we used lower levels of PEEP and moderate tidal volumes, which may have less impact on the circulation. One of the afferent signals leading to a reflex adjustment of PEEP is a *decrease* in arterial blood pressure. With reflexes abolished, the PEEP-associated increase in MSFP was diminished (30). In the present study, as PEEP increased from 5 to 10 cmH_2O, Q_{PA} decreased slightly (but not significantly) and MAP was *unchanged*. This could mean that the afferent signal from the baroreceptors was weak, and that the observed PEEP-associated increase in MSFP was mainly an effect of central-to-peripheral volume shift, with less adjustment of vascular capacitance.

Upon publication, Paper I was accompanied by a Letter to the Editor written by Brengelmann (15), entitled “Why persist in the fallacy that mean systemic pressure drives venous return?”. We answered all questions in a point-by-point response, largely by citing ourselves and what we actually had written (11). It was obvious that we had entered a minefield and were assumed ‘guilty by association’ of numerous ideas previously advocated by ‘our side’. As an example, Brengelmann incorrectly ascribed to us the belief that MSFP “exists physically within some significant sub-compartment at the upstream end of the venous resistance”. It was also clear that the unresolved debate on ‘RAP as backpressure for venous return’ loomed over all issues related to venous return

physiology. This motivated us to design the protocol of Paper II, in order to address the backpressure issue comprehensively and using contemporary clinical ECMO equipment.

5.2 DISCUSSION - PAPER II

There were four main findings of this study: First, there was an inverse relationship between RAP and VR, present regardless of whether RAP was altered by means of airway pressure or pump speed. Second, changes in VR in response to changes in RAP were immediate, but transient. Any disturbance of the steady state of the system simultaneously initiated volume shifts and flow restoration. Third, the volume shifts changed both downstream, upstream and consequently the driving pressure for venous return. Fourth, increased airway pressure was associated with increased MSFP in *Euvolemia* only.

We conclude from the first three findings that RAP acts as backpressure for venous return. It also implies that VR driving pressure is dynamically changing in the transit between steady states, mainly due to changes in RAP. The study shows that RAP is *both a result* of the volume shifting work of the pump, *and a determinant* for venous return. It illustrates that RAP is the node of interaction between the systemic circuit and the cardiopulmonary circuit, and is in line with the earlier findings of Versprille and Pinsky (82, 97) with beating heart preparations as well as the original bypass experiments by Guyton (40, 41). The dual nature of RAP is well described by Parkin (77):

"Thus the right atrial pressure, often used as a preload measure, is in fact a complex signal dependent upon the intrathoracic and intrapericardial pressures and their determinants, atrial compliance and unstressed volume, biventricular performance and itself. Right atrial pressure only measures the volume state when the heart is stopped".

The linear decrease of RAP with increasing pump speed is a result of volume shift away from the right atrium, where increased pump speed is equivalent to improved cardiac function (13, 79). The proof of the backpressure role of RAP rests on the experimental setup, with independent control of RAP and pump function - and not in the subtleties of cross correlation analysis (the result of which obviously supports the conclusion). In the airway pressure maneuvers, the choice of controlled variable (*airway pressure*) and the chain of events (the sequence begins when the experimenter operates the ventilator) provide the frame for interpretation. This was already present in the experiments by Versprille and Jansen (and in our Paper I), where airway pressure maneuvers in the form of inspiratory holds elicited the now familiar acute decrease and restoration of VR. What this study provides in addition is an experimental setup where any possible effects that increased airway pressure may have on the right ventricle become irrelevant, since flow forward from the RA was strictly controlled by the ECMO.

The dynamic change in caval flow seen in the *airway pressure maneuvers*, occurred despite a constant aortic flow. This was confirmed in three animals where ECMO flow was monitored with a high-resolution flowprobe (data not shown). Therefore, the initial decrease in VR was a consequence of increased RAP from the inspiratory hold maneuver. In the zero PEEP maneuver, the initial increase in VR was a result of acutely decreased RAP. As venous return decreased in the inspiratory hold maneuvers, volume was shifted out from the RA by the constant pump flow. Conversely, in the zero PEEP maneuvers, volume was shifted into the RA by increased caval flow. These volume shifts are (at least partly) responsible for the return of RAP in spite of a sustained P_{AW} towards the level preceding the maneuver. The transient imbalance of decreased inflow and constant RA drainage, initiated by the inspiratory hold, will shift volume *within* the systemic compartment, from downstream to upstream areas. The reverse process is seen when airway pressure decreases and volume is shifted from upstream to downstream areas. These volume shifts will act to partially restore both RAP and the driving pressure for venous return, to the levels preceding the onset of imbalance. This constitutes a hydraulic, physical, self-regulating mechanism of the cardiovascular system, that is unrelated to any active homeostatic adaption.

Volume shifts caused by respiratory maneuvers are small, as reported by us in Paper I, and others (20, 96). The upstream pressure effect of the transient volume shifts by the end of the "early" phase of increased P_{AW} was <5% of MSFP (regardless of whether we used data for C_{vasc} from Ogilvie or from the present study). It was of a similar magnitude as the increase in MSFP seen during static inspiratory hold in *Euvolemia*. The overall high compliance of the systemic vasculature diminishes the upstream pressure effect on MSFP (64). The downstream pressure effect of the volume shift is larger, as seen by the return of RAP towards the level preceding the maneuver. The explanation is likely that the compliances of the RA and adjacent large veins are lower than the average vascular component of the systemic vasculature. Therefore, the predominant mechanism for restoring VRdP and VR is attributed to the restoration of RAP in the downstream area.

If Guyton's cardiovascular model should be applied to dynamic situations, the effect of transient volume shifts need to be acknowledged. In dynamically changing venous return following airway pressure maneuvers, we could show that the pressure effect in the systemic compartment was small, and the estimates of MSFP remain relatively robust.

The effect of acutely increased airway pressure on the zero-flow pressure has been demonstrated by Jellinek and Repessé, in patients at ICD testing and

immediately after death (46, 86). In the present study, MSFP was higher in inspiration than in expiration, regardless of shunt state – but only in *Euvolemia*. An example of a stop-flow maneuver with ongoing tidal ventilation can be seen in Figure 37 (unpublished data from experimental series II). Atrial and arterial pressures vary with airway pressure, and all flows oscillate around zero with a tide-and-ebb effect from respiration visible for caval flows.

The reported value for systemic vascular compliance was larger here than in the first experimental series, or in the study by Ogilvie (72): 4.3 ± 1.8 *vs*. 3.2 ± 0.7 *vs*. 3.5 ± 2.4 mL×mmHg^{-1}×kg^{-1}, respectively. As we did not measure plasma volume, we may have overestimated the true C_{vasc}, if part of the infused colloid was redistributed to the extravascular space and/or if *Hypervolemia* was associated with vasodilation. Leakage may have been enhanced due to systemic inflammation, but compliance may also have been increased by a vasoplegic state – both phenomena which are associated with extracorporeal circulation (88).

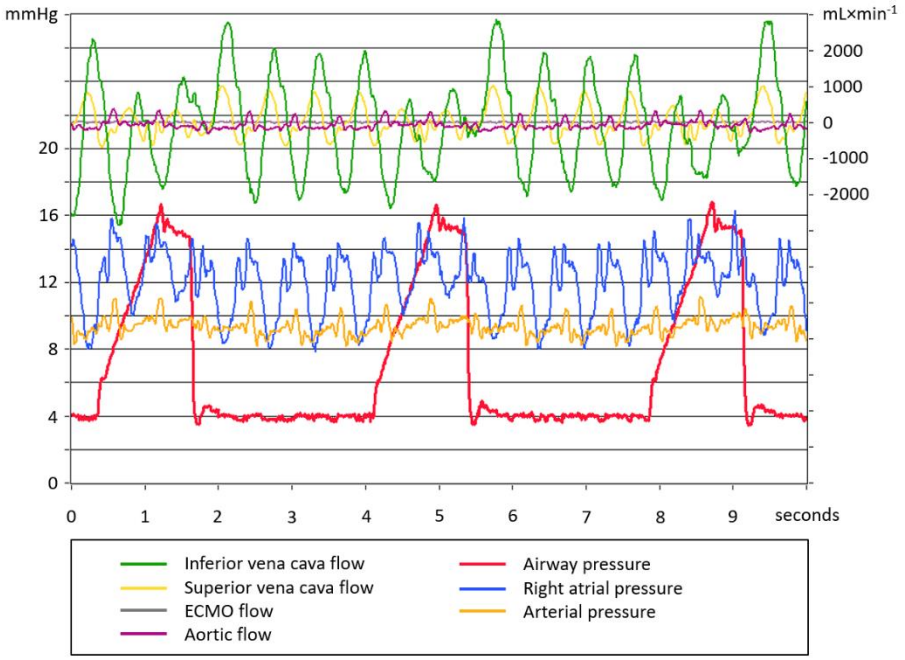

Figure 37 – Stop-flow maneuver caused by clamping the ECMO tubing with open shunt and tidal ventilation continued. Pulsatility is present, but the average flows over time are not different from zero. Atrial and arterial pressures vary with changing airway pressure. There is net retrograde caval flow on inspiration, with antegrade flow in expiration (tide-and-ebb effect). The caval flow profile is inversely proportional to RAP, as confirmed by cross correlation analysis during the airway pressure maneuvers.

Paper II was accompanied by an Editorial by Kamiya (47), discussing our results within the interesting context of the ‘extended Guyton model”, as formulated by Sunagawa (92). This model incorporates left arterial pressure and handles volume shifts between the cardiopulmonary and systemic compartments. Kamyia concludes that neither RAP nor venous return should be seen as a cause of the other. Instead, they are both determined by ’unmeasurable properties’ of the cardiovascular system, such as total stressed blood volume, pump function, and systemic arterial resistance. It is of course possible to include any number of higher-level hierarchies in a model. We chose to accept RAP as a reasonable surrogate for the stressed blood volume in the RA, and therefore conclude that RAP acts as backpressure for venous return. However, one can argue that in our experiment, this was in turn affected by the changing airway pressure, which was in turn affected by the ventilator, which was operated by the experimenter, *et cetera, et cetera in absurdum*.

5.3 DISCUSSION - PAPER III

The study was an application of the principles of venous return to modern venoarterial ECMO treatment. The main finding was that both *Vasoconstriction* with norepinephrine, and *Volume Expansion* with Ringer's lactate, increased MSFP and the maximum achievable ECMO flow, with similar effects on oxygen delivery. *Volume Expansion* had a larger effect on blood flow than *Vasoconstriction*. Since pump-performance was constant between treatments and intensities, our results represent solely changes in the properties of the vascular circuit.

The maximum ECMO flows were associated with imminent vascular collapse in all experimental conditions, which could not be observed clinically, but became evident in the offline analysis. The vascular waterfall that forms at collapse will dissociate the Q_{ECMO}-RAP relationship, as RAP no longer represents the downstream pressure for VR. Depending on the site of RAP measurement, data-points representing flow rates at or above closing conditions, can either move leftwards to increasingly negative pressures, or drift off to the right, if the pressure is measured in a position where drainage is partially obstructed by downstream cannula-vessel interaction. The latter was a more frequent observation in our experiment where data-points at closing conditions displayed increasing RAP (as seen in Figure 34). Closing conditions were recognized as the main limit to flow increase in the studies by Guyton (40, 41). The study endpoint of maximum achievable Q_{ECMO} is unrelated to whether closing conditions occurred or not – the highest flow that can be generated will be valid. However, in the clinical context, operating at or near maximum will carry risks of haemolysis, vascular damage and/or sudden loss of flow. When closing conditions were excluded, the VR plots were linear, as predicted by Guyton's cardiovascular model.

The study had a serial treatment design. Both *Vasoconstriction* and *Volume Expansion* increased MSFP, allowed for an increased maximum Q_{ECMO}, and thereby shifted the VR curves to the right. In addition, *Volume Expansion* decreased resistance to venous return for all animals in proportion to the treatment intensity. In contrast, the response of flow resistance to vasoconstriction was highly heterogeneous.

When compared to *Euvolemia*, *Vasoconstriction* led to a decrease in total blood volume (seen as a leftward shift of the pressure-volume curve) and an increase in MSFP from recruitment of unstressed into stressed volume. Vascular elastance was higher under norepinephrine in this study than during euvolemic conditions in studies I-II. Vascular elastance was not determined in

Euvolemia and we therefore cannot quantify the change, but increased values under vasoconstriction have been reported (4, 27). An increased elastance would increase MSFP for the given vascular capacitance (93). Compared to *Euvolemia*, as vascular capacitance decreased and stressed volume was recruited, approximately 20% of the plasma volume was lost. Plasma leakage may have been enhanced by inflammation associated with extracorporeal circulation (67). *Volume Expansion* shifted the pressure-volume curve to the right. Both stressed and unstressed volumes were increased, but to a lesser extent than expected from the large amount infused.

The individually variable response to norepinephrine has been reported earlier (57) and is of clinical importance when VA-ECMO is used to support a failing left ventricle, as increases in afterload may have negative effects. Recruitment of stressed volume via vasoconstriction can occur without increase in RVR (24, 26). This was reproduced in our study and the average slopes of the VR curves were unchanged between *Euvolemia* and *Vasoconstriction*. On a group level, increasing intensity of *Vasoconstriction* led to increased maximum Q_{ECMO}, without any measureable change in VRdP or RVR. One mechanism behind the increase in maximum flow could be decreased cannula tip-vessel wall interaction, via centralisation of blood volume from vasoconstriction. This explanation is supported by the parallel increase in RAP and MSFP with increasing treatment intensity, but it was not possible in the present study to determine whether RAP measured at the border of vascular collapse truly represented the downstream pressure for venous return. To strengthen the analysis and exclude possible artefacts from dissociated Q_{ECMO} and RAP, we also estimated the increase in Q_{ECMO} at standard levels of RAP for each condition, which confirmed the increase in flow and curve shifts.

The linear pump function over the range of pump speeds and afterload conditions studied, illustrates that flow/rpm will depend on the variables of the Hagen-Poiseuille equation. It states that flow is proportional to the pressure gradient and the fourth power of vessel radius, and inversely proportional to viscosity and tubing length (48). In *Volume Expansion*, the resulting pump pressure head (=MAP-RAP) and RVR would have been affected by all these factors, with the possible exception of tubing (or total vessel) length. As a physical result of plasma expansion, the average vessel radius increases, further modulated by baroreflex adjustments of vascular diameter in both arterial and venous compartments. As a consequence of volume expansion, the average vascular element will move downstream. Finally, haemodilution will lower viscosity. In our sequential treatment approach, weaning from norepinephrine, and progressive SIRS may also add to the vasodilation.

The sequential approach used was a pragmatic compromise in study design that does not allow the evaluation of treatment benefit of one approach over the other. The main determinants of venous return (RAP, MSFP, VRdP and RVR) were not different between the two baseline conditions *Euvolemia* and *Post Vasoconstriction*. We show that both volume expansion and vasoconstriction, used in moderate doses, increase the maximum achievable ECMO flow with similar effects on oxygen delivery. We conclude that ECMO flow is dependent on factors that determine venous return, i.e. closing conditions, stressed vascular volume, and elastic and resistive vascular properties.

5.4 DISCUSSION - PAPER IV

The main finding of this study was that the relationships between the indirect estimates and the reference method of $MSFP_{RAO}$ were influenced by the underlying volume state. All methods tracked changes in $MSFP_{RAO}$ concordantly. In this study, we have modified the inspiratory hold techniques in order to minimize the volume state related impact on venous return, but this effect could still not be eliminated. The effect was manifest as a significant *bias for changes* between the respective indirect method and the reference method. Poor tracking ability of changing volume state is problematic, since this is the context where access to a reliable measurement of MSFP would be clinically most useful. In a review of clinical studies using inspiratory hold maneuvers for the estimation of MSFP, values between 19-33 mmHg were reported (103). Even considering the increased values of RAP associated with volume loading, this is far above what can be expected from animal data. The developing theoretical and experimental framework for the inspiratory hold maneuver has been described in section 1.8. However, to the best of our knowledge, the methods have not been properly evaluated against a zero-flow measure *over changing volume state*, prior to our study. A comparison against the arm-occlusion technique is available, and both methods reported high values (58). As commented previously (section 1.12), the resulting venous return driving pressures were also very high, and suggestive of a grossly increased RVR, as the patients were not generally hyperdynamic. The high values of MSFP may therefore be related to the methods themselves.

$MSFP_{nadir\_hold}$ is conceptually unaffected by flow restoration. Although the pressure-flow data-pairs obtained at nadir flow should underestimate steady state VR, the accuracy *vs*. the reference method could potentially be constant over changing volume states. In this study, we showed that $MSFP_{nadir\_hold}$ underestimated $MSFP_{RAO}$, and with a significant bias and wide limits of agreement for changes: [bias (CI)] -1.0 (-1.9 to -0.1) mmHg, LoA -4.0 to 1.9 mmHg. The primary reason for the underestimation is likely due to upstream volume loading during increased airway pressure (Figure 38). Three additional mechanisms may contribute: First, if airway pressure led to vessel collapse upstream from the RA, this would dissociate the pressure-flow relationship and shift the zero-flow estimate to the left. Second, venous vessel distensibility and interaction with vascular waterfalls (as described in Paper I) could vary with changing volume state and in part explain that volume state changed the agreement *vs*. $MSFP_{RAO}$. Third, transmural RAP increased between the beat preceding nadir Q_{PA} beat, and the nadir beat, in 62 of 93 cases (67%) (data not shown). This suggests that inspiration increased right ventricular afterload (50,

98, 100) with possible distention, further adding to the discrepancy between measured flow and steady state VR.

$MSFP_{inst\_VR}$ integrates pressure-flow data-pairs from tidal ventilation. The absence of interventions (such as static hold maneuvers) has the benefit of not disturbing the system. The volume loaded in upstream vessels as a consequence of increasing RAP during inspiration will be released into the right atrium as vessels recoil during expiration (Paper II and (25)). In the data analysis of the present study, it became apparent that the effects of vessel

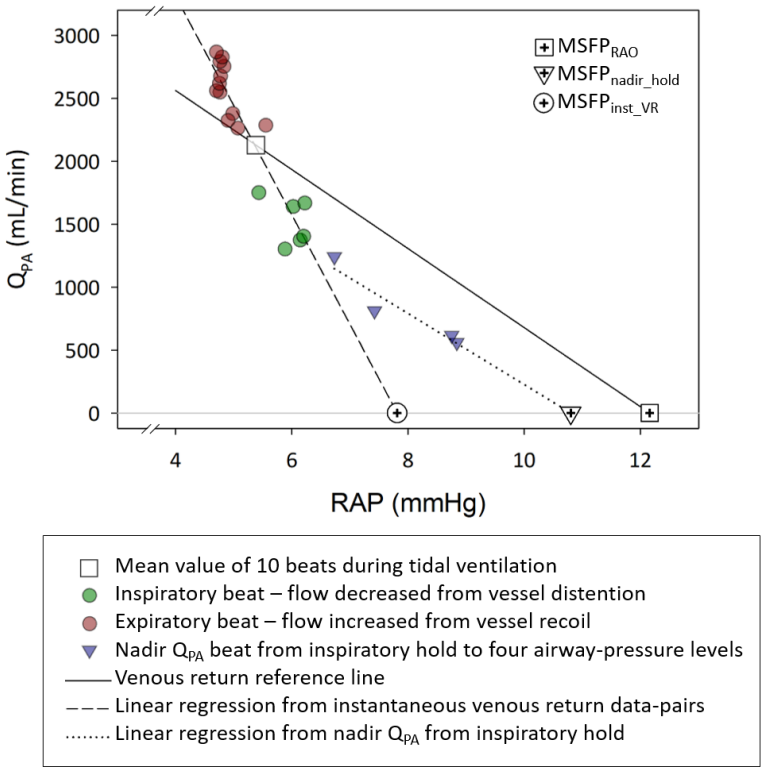

Figure 38 - Venous return plots for animal 5 in Bleeding. The VR reference line connects the RAP-Q_{PA} data-point (square; representing mean values of 10 beats during tidal ventilation before RA balloon occlusion) with $MSFP_{RAO}$. Filled circles represent individual beat mean Q_{PA} matched with mean RAP from the preceding beat, obtained during three respiratory cycles of tidal breathing. Green and red circle data-points, representing inspiration and expiration, are displaced downwards and upwards in respect to the reference VR line because of distention and recoil of compliant vessels upstream from the RA. The dashed regression line extrapolates to $MSFP_{inst\_VR}$. Blue triangle data-points represent the mean values of individual beat nadir Q_{PA}, matched with mean RAP from the preceding beat, caused by inspiratory hold to increasing levels of airway pressure. They are displaced downwards in respect to the reference VR line because of upstream vessel distention, and the dotted regression line extrapolates to $MSFP_{nadir\_hold}$.

distention and recoil on the zero-flow estimate do not cancel, *but act additively* (see Figure 38). Compared to a venous return plot unaffected by volume shifts, vessel distention will displace high RAP-low flow data-pairs from inspiration *downwards*, and vessel recoil will displace low RAP-high flow data-pairs from expiration *upwards*. The result is a *clockwise rotation* of the regression line, with a leftward shift of the zero-flow intercept.

The original study by Pinsky compared $MSFP_{inst\_VR}$ to MSFP at zero flow from ventricular fibrillation at baseline and after volume expansion, and reported no interaction between volume state and method (82). In contrast, we found that the accuracy of $MSFP_{inst\_VR}$ *vs*. $MSFP_{RAO}$ was influenced by the volume state, and $MSFP_{inst\_VR}$ showed a trend of underestimation $MSFP_{RAO}$ in *Bleeding*. Calculation of RVR using $MSFP_{inst\_VR}$ resulted in a reduced RVR in *Bleeding*, which is physiologically unlikely, and was not seen for RVR_{RAO}. The reason for $MSFP_{inst\_VR}$ underestimating $MSFP_{RAO}$ in *Bleeding* may be found among factors that enhance the rotation of the regression line. In hypovolemia, inspiration promotes transient vessel collapse (99), which dissociates the pressure-flow relationship and temporarily stores all venous inflow into distended vessels. When the vessels reopen, enhanced flow from recoil will displace pressure-flow data-points upwards and enhance the rotation and the leftward zero-flow shift.

The dynamic model analogue P_{msa}, here adapted for pigs as $MSFP_a$, also showed an agreement *vs*. $MSFP_{RAO}$ that was influenced by the underlying volume state. The clinical relevance of this cannot be judged with certainty, as $MSFP_a$ tracked changes in $MSFP_{RAO}$ with a low bias, albeit with wide limits of agreement – exceeding the desired 0.7 mmHg. As the within-method variability is unknown, we cannot assess the relative contributions of variance in $MSFP_{RAO}$ and $MSFP_a$, to the LoA. The dynamic model analogue is expected to differ from static zero-flow pressure if the actual venoarterial compliance and/or arteriovenous resistance ratios deviate from the assumptions (78). We chose not to set factor 'c' using an approach that deliberately adjusts the calculated model analogue to 7 mmHg (51). Instead, we believe that one of the advantages of the Parkin equation is its simplicity, and the transparent selection of physiologically reasonable VA compliance and AV resistance ratios. The effect of incorporating changing SVR and R_v in factor 'c' during the course of the experiment, became statistically significant only in *Hypervolemia*. The clinical impact would be moderate with the model assumption of a non-changing R_v overestimating the dynamic filling analogue by 0.48 mmHg or 3.8 ± 2.3% in *Hypervolemia*.

A derived variable like $MSFP_a$ is mathematically coupled to the precision of the entering signals RAP, MAP and CO. The accuracy of the ultrasonic flowprobes used in this study is reported as ± 10%. With the average flow in *Euvolemia*, this error was equal to ± 0.28 L/min. With the average value for 'c'= 0.78 ± 0.18 mmHg×min×L^{-1}, this translates into an error in the pressure signal of ± 0.2 mmHg in $MSFP_a$. A cardiac output monitor used in clinical practice and calibrated by thermodilution would have an accuracy in the range of 6-10 %. Nevertheless, the high tracking ability and non-interventional nature of the dynamic analogue $MSFP_a$ is favourable.

In the clinical setting, the absolute values of MSFP, regardless of method used, are likely to be less relevant than the tracking ability *vs.* changes in MSFP.

For all indirect methods, the accuracy *vs.* the reference method was dependent on the underlying volume state. For this reason, comparisons *between* the indirect methods were not performed. Instead, to assess the *relative* performances of the indirect methods, the most relevant information is the ability of each individual method to track changes in MSFP as measured with the reference method (Table 13). The bias of $MSFP_{inst\_VR}$ against $MSFP_{RAO}$ was higher (non-overlapping 95% confidence intervals) than the respective biases of $MSFP_{nadir\_hold}$ and $MSFP_a$. There were no statistical differences in bias or LoA in the performance between $MSFP_{nadir\_hold}$ and $MSFP_a$. The high tracking ability and non-interventional nature of the dynamic analogue $MSFP_a$ is favourable in the clinical context.

A serious limitation to this method comparison is the of lack repeated measurements for each method under conditions where the true value can be assumed to remain constant. Since the within-method variability (i.e. precision or repeatability) cannot be determined, the relative contributions of test and reference methods to the reported agreement remain unknown. In the end, the study protocol reflects a compromise to avoid excessive physiological stress and a potentially unstable preparation.

6 CONCLUSION

In this thesis, I have shown that RAP is *simultaneously* a function of volume redistribution *and* the backpressure determinant for venous return. In the dynamic transit between steady states, temporary imbalance between venous return and cardiac output is associated with volume shifts. In the intact circulation, these volume shifts will occur between the cardiopulmonary and systemic compartments, as well as within the systemic compartment. The related pressure effects are predominantly seen in the downstream area and will act to restore RAP and VRdP to the levels preceding the onset of imbalance. The is also a pressure effect in the upstream area, but due to the large compliance, it is small. If these pressure effects are accounted for, Guyton's cardiovascular model can be applied also to dynamic conditions. As indicated by almost forty years of debate, this is a major physiologic finding.

The maximum achievable ECMO flow can be increased by both vasoconstriction with norepinephrine, and volume expansion with Ringer's lactate. The two treatments increased stressed vascular volume and MSFP via different mechanisms. Increased flow between conditions was not associated with increased venous return driving pressure, as RAP and MSFP increased in parallel. Instead, with increasing levels of volume expansion, the resistance to venous return decreased. We speculate that the flow increase observed with vasoconstriction may be related to improved venous cannula-vessel wall interaction following centralisation of blood volume.

When moderate tidal volumes were used, an increase in PEEP from 5-10 cmH_2O was associated with an increase in MSFP that partially compensated for the increase in RAP. The decrease in pulmonary artery flow was small, and did not reach statistical significance. VRdP decreased and RVR was unchanged.

I present data from two separate porcine experiments, with intact circulation and using VA-ECMO, indicating that acutely changed airway pressure is translated to MSFP, probably from central-to-peripheral redistribution of stressed volume. This is supported by a recent study in critically ill patients examined just after death (86).

Airway pressure maneuvers provide valuable insights into the complex physiology of circuit-heart-lung-interactions. However, they are unsuitable for the estimation of MSFP, since the accuracy compared to zero-flow measurements is affected by the underlying volume state.

Zero-flow extrapolation using pressure-flow data-pairs early in the hold maneuver *underestimated* steady state VR and MSFP, due to upstream volume loading and vessel distention.

Zero-flow extrapolation using pressure-flow data-pairs 9-12 seconds into the hold maneuver *overestimated* steady state VR and MSFP in euvolemic conditions, due to flow restoration preferentially seen in the inferior vena cava. This mechanism may involve activation of vascular waterfalls in the splanchnic circulation.

Zero-flow extrapolation of instantaneous venous return using pressure-flow data-pairs from undisturbed tidal ventilation showed a trend of *underestimating* steady state VR and MSFP in hypovolemia, since flow decrease and flow restoration from vessel distension and recoil introduced a rotation of the regression line, as compared to steady state VR.

Although indirect estimates of MSFP from airway pressure maneuvers tracked changes in the reference method of $MSFP_{RAO}$ concordantly, the limits of agreement were too wide to detect a 10% change in VRdP at euvolemia.

The dynamic model analogue of static filling pressure was adapted to pigs ($MSFP_a$). The accuracy compared to $MSFP_{RAO}$ was influenced by the underlying volume state. The clinical relevance of this finding is uncertain, as $MSFP_a$ tracked changes in $MSFP_{RAO}$ with a low bias, but with limits of agreement exceeding 10% of VRdP at euvolemia.

7 FUTURE PERSPECTIVES

Instead of conducting further clinical studies using inspiratory hold maneuvers for the estimation of MSFP, researchers are encouraged to repeat our studies regarding the agreement between inspiratory hold estimates and zero-flow measurements of MSFP *over changing volume states*. The relevance of liver haemodynamics to the flow restoration should be explored further. A future study on the impact of acutely changing airway pressure on MSFP could institute zero flow at varying airway plateau pressures. There is need for data on the within-method precision, or repeatability, of $MSFP_{RAO}$. The theoretical framework and derived measures from the Parkin dynamic model analogue are indeed appealing. For a measure that is in itself non-invasive and non-interventional, the tracking ability of $MSFP_a$ for changes in $MSFP_{RAO}$ is impressive.

However, since no patient will ever *improve* from monitoring alone, it is now time to study the possible outcome benefits of hemodynamic management guided by applied venous return physiology, as compared to standard care.

ACKNOWLEDGEMENTS

I would like to express my deepest gratitude to Professor Jukka Takala - my co-supervisor for the thesis and Head of the Department of Intensive Care Medicine, Inselspital, Bern University Hospital, Switzerland. I was invited to work abroad despite an almost total lack of research experience. Senior colleagues were generous and confident enough to trust me with this opportunity. I think it turned out quite well.

Research is a team effort, involving multiple parallel and serial constellations. For me it was a privilege and joy to prepare and perform the animal experiments together with the fantastic staff of ESI. However, the majority of the work was done by a handful of individuals, each investing countless hours. During an intense year on-site in Bern we were united geographically, but over the following years the team was spread out over Europe. At times, we met over Skype, or reunited in Bern. Sometimes we met in Brussels, for food for thought, and for seafood.

I hit most of the 'eureka' moments while running. The remaining part of the runs were mentally downhill.

I would especially like to thank the following persons:

Olgica Beslac for exquisite craftsmanship and a good sense of humour.

Kay Nettelbeck for being the first person in the lab, but still the last one to leave. And for pastry and ECMO plumbing.

Michael Lensch for always being ultra-professional and helpful. If you ever take a vacation – drive north!

Ville Pettilä for sharing your experience and expertise, and for offering perspectives beyond the Department. You only smiled gently as I, eyes wide shut and with hands in the air, tried to visualize tidal waves of venous return, with cardiac contractions and respiratory variation superimposed.

Stefan Blöchlinger The best is yet to come. Except for all-you-can-eat sushi buffets, where we most likely have passed the summit.

Stephan Jakob for letting me into (and out of) the ESI, for generous employment, and for judicious co-authorship.

Jukka Takala Working with you has been an honor. Fascinating, frustrating and rewarding. Your devotion to the task definitely borders ruthlessness, but is also paired with generosity and warmth. Things do improve with each revision. Thank you for having us in Muri and Mörel. It is good to know that you spend more time there.

David Berger Colleague-who-turned friend - I am so glad that we met. We discovered some cool things together! I am impressed and grateful for your knowledge, comradeship, leadership, and hospitality. Continue to buy LEGO.

Søren Søndergaard Renaissance man: linguist, humanist, entrepreneur, engineer, physiologist, physician, and friend. It was your generosity and counselling that brought me to Switzerland in the first place.

Mattias Sköld My best friend. I may have showed you how to tie shoelaces, but you led by example the way to research, to skiing in the tracks of Karl Molitor, and generally shared your way of enjoying life.

Helena and **Eric Werner** For support and love in everyday life.

Gunilla and **Göran Möller** For life-long love, care, support, engagement and interest. For being clear. For sharing and building enthusiasm. For being there for us and for the children – also when I was working during holidays.

Otto and **Hedda** I will not pretend that this book was written for you. The truth is that it was a time-thief - but still it made me happy. You have both already written books of your own, and most likely more will follow in the future. In the meantime, let us continue working and playing *together*! I love you.

Anna Werner My love! The meaning of life - from Sävelången to Sense, and back again.

REFERENCES

1. Animal Research: Reporting In Vivo Experiments: The ARRIVE guidelines. *Journal of Physiology* 588: 2519-2521, 2010.
2. **Anderson RM**. *The Gross Physiology of the Cardiovascular System*. Racquet Press 1993, 1993, p. 114.
3. **Andrew P**. Rebuttal from Philip Andrew. *The Journal of physiology* 591: 5799-5799, 2013.
4. **Appleton CP, Lee RW, Martin GV, Olajos M, and Goldman S**. Alpha 1- and alpha 2-adrenoceptor stimulation: changes in venous capacitance in intact dogs. *The American journal of physiology* 250: H1071-1078, 1986.
5. **Aya HD, Rhodes A, Fletcher N, Grounds RM, and Cecconi M**. Transient stop-flow arm arterial-venous equilibrium pressure measurement: determination of precision of the technique. *Journal of clinical monitoring and computing* 30: 55-61, 2016.
6. **Bayliss WM, and Starling EH**. Observations on Venous Pressures and their Relationship to Capillary Pressures. *The Journal of physiology* 16: 159-318 157, 1894.
7. **Beard DA, and Feigl EO**. CrossTalk opposing view: Guyton's venous return curves should not be taught. *The Journal of physiology* 591: 5795-5797, 2013.
8. **Beloucif S, Brienza N, Andreoni K, Ayuse T, Takata M, O'Donnell CP, and Robotham JL**. Distinct behavior of portal venous and arterial vascular waterfalls in porcine liver. *Journal of critical care* 10: 104-114, 1995.
9. **Bender R, and Lange S**. Adjusting for multiple testing--when and how? *Journal of clinical epidemiology* 54: 343, 2001.
10. **Berger D, Bloechlinger S, Takala J, Sinderby C, and Brander L**. Heart-lung interactions during neurally adjusted ventilatory assist. *Critical care* 18: 499, 2014.
11. **Berger D, Moller PW, and Takala J**. Reply to “Letter to the editor: Why persist in the fallacy that mean systemic pressure drives venous return?”. *American Journal of Physiology - Heart and Circulatory Physiology* 311: H1336-H1337, 2016.
12. **Berger D, Moller PW, Weber A, Bloch A, Bloechlinger S, Haenggi M, Sondergaard S, Jakob SM, Magder S, and Takala J**. Effect of PEEP, blood volume, and inspiratory hold maneuvers on venous return. *American journal of physiology Heart and circulatory physiology* 311: H794-806, 2016.
13. **Berlin DA, and Bakker J**. Starling curves and central venous pressure. *Critical care* 19: 55, 2015.
14. **Braunwald TE, Binion LJ, Morgan JW, and Sarnoff JS**. Alterations in Central Blood Volume and Cardiac Output Induced by Positive

Pressure Breathing and Counteracted by Metaraminol (Aramine). *Circulation research* 5: 670-675, 1957.
15. **Brengelmann G**. Why persist in the fallacy that mean systemic pressure drives venous return? *American journal of physiology Heart and circulatory physiology* 2016.
16. **Brengelmann GL**. The classical Guyton view that mean systemic pressure, right atrial pressure, and venous resistance govern venous return is/is not correct. *Journal of applied physiology (Bethesda, Md : 1985)* 101: 1532, 2006.
17. **Brengelmann GL**. Counterpoint: the classical Guyton view that mean systemic pressure, right atrial pressure, and venous resistance govern venous return is not correct. *Journal of applied physiology (Bethesda, Md : 1985)* 101: 1525-1526; discussion 1526-1527, 2006.
18. **Brengelmann GL**. A critical analysis of the view that right atrial pressure determines venous return. *Journal of applied physiology (Bethesda, Md : 1985)* 94: 849-859, 2003.
19. **Brienza N, Ayuse T, O'Donnell CP, Permutt S, and Robotham JL**. Regional control of venous return: liver blood flow. *American journal of respiratory and critical care medicine* 152: 511-518, 1995.
20. **Brower R, Wise RA, Hassapoyannes C, Bromberger-Barnea B, and Permutt S**. Effect of lung inflation on lung blood volume and pulmonary venous flow. *Journal of applied physiology (Bethesda, Md : 1985)* 58: 954-963, 1985.
21. **Chihara E, Hashimoto S, Kinoshita T, Hirose M, Tanaka Y, and Morimoto T**. Elevated mean systemic filling pressure due to intermittent positive-pressure ventilation. *The American journal of physiology* 262: H1116-1121, 1992.
22. **Cowley AW, and Guyton AC**. Heart rate as a determinant of cardiac output in dogs with arteriovenous fistula. *The American journal of cardiology* 28: 321-325, 1971.
23. **Critchley LA, and Critchley JA**. A meta-analysis of studies using bias and precision statistics to compare cardiac output measurement techniques. *Journal of clinical monitoring and computing* 15: 85-91, 1999.
24. **Datta P, and Magder S**. Hemodynamic response to norepinephrine with and without inhibition of nitric oxide synthase in porcine endotoxemia. *American journal of respiratory and critical care medicine* 160: 1987, 1999.
25. **Den Hartog EA, Jansen JR, Moens GH, and Versprille A**. Systemic filling pressure in the intact circulation determined with a slow inflation procedure. *Pflugers Archiv : European journal of physiology* 431: 863-867, 1996.
26. **Deschamps A, and Magder S**. Baroreflex control of regional capacitance and blood flow distribution with or without alpha-adrenergic blockade. *American Journal of Physiology-Heart and Circulatory Physiology* 263: H1755-H1763, 1992.

27. **Drees JA, Rothe, and CF**. Reflex Venoconstriction and Capacity Vessel Pressure-Volume Relationships in Dogs. *Circulation research* 34: 360-373, 1974.
28. **Fessler HE, Brower RG, Shapiro EP, and Permutt S**. Effects of positive end-expiratory pressure and body position on pressure in the thoracic great veins. *The American review of respiratory disease* 148: 1657-1664, 1993.
29. **Fessler HE, Brower RG, Wise RA, and Permutt S**. Effects of positive end-expiratory pressure on the canine venous return curve. *The American review of respiratory disease* 146: 4-10, 1992.
30. **Fessler HE, Brower RG, Wise RA, and Permutt S**. Effects of positive end-expiratory pressure on the gradient for venous return. *The American review of respiratory disease* 143: 19-24, 1991.
31. **Funk DJ, Jacobsohn E, and Kumar A**. Role of the venous return in critical illness and shock: part II-shock and mechanical ventilation. *Critical care medicine* 41: 573-579, 2013.
32. **Funk DJ, Jacobsohn E, and Kumar A**. The role of venous return in critical illness and shock-part I: physiology. *Critical care medicine* 41: 255-262, 2013.
33. **Geerts BF, Maas J, de Wilde RB, Aarts LP, and Jansen JR**. Arm occlusion pressure is a useful predictor of an increase in cardiac output after fluid loading following cardiac surgery. *European journal of anaesthesiology* 28: 802-806, 2011.
34. **Geerts BF, Maas JJ, Aarts LP, Pinsky MR, and Jansen JR**. Partitioning the resistances along the vascular tree: effects of dobutamine and hypovolemia in piglets with an intact circulation. *Journal of clinical monitoring and computing* 24: 377-384, 2010.
35. **Green JF**. Pressure-flow and volume-flow relationships of the systemic circulation of the dog. *The American journal of physiology* 229: 761, 1975.
36. **Guerin C, and Richard JC**. Comparison of 2 correction methods for absolute values of esophageal pressure in subjects with acute hypoxemic respiratory failure, mechanically ventilated in the ICU. *Respiratory care* 57: 2045-2051, 2012.
37. **Gulati HG, Novero HA, Loring HS, and Talmor HD**. Pleural Pressure and Optimal Positive End-Expiratory Pressure Based on Esophageal Pressure Versus Chest Wall Elastance: Incompatible Results*. *Critical care medicine* 41: 1951-1957, 2013.
38. **Gupta K, Sondergaard S, Parkin G, Leaning M, and Aneman A**. Applying mean systemic filling pressure to assess the response to fluid boluses in cardiac post-surgical patients. *Intensive care medicine* 41: 265-272, 2015.
39. **Guyton AC**. Determination of cardiac output by equating venous return curves with cardiac response curves. *Physiological reviews* 35: 123-129, 1955.

40. **Guyton AC, Lindsey AW, Abernathy B, and Richardson T**. Venous return at various right atrial pressures and the normal venous return curve. *The American journal of physiology* 189: 609-615, 1957.
41. **Guyton AC, Lindsey AW, and Kaufmann BN**. Effect of mean circulatory filling pressure and other peripheral circulatory factors on cardiac output. *The American journal of physiology* 180: 1955.
42. **Guyton AC, Polizo D, and Armstrong GG**. Mean circulatory filling pressure measured immediately after cessation of heart pumping. *The American journal of physiology* 179: 261, 1954.
43. **Hannon JP, Bossone CA, and Wade CE**. Normal physiological values for conscious pigs used in biomedical research. *Laboratory animal science* 40: 293-298, 1990.
44. **Harrison MH**. Effects of thermal stress and exercise on blood volume in humans. 1985, p. 149-209.
45. **Jacob M, Conzen P, Finsterer U, Krafft A, Becker BF, and Rehm M**. Technical and physiological background of plasma volume measurement with indocyanine green: a clarification of misunderstandings. *Journal of applied physiology (Bethesda, Md : 1985)* 102: 1235-1242, 2007.
46. **Jellinek H, Krenn H, Oczenski W, Veit F, Schwarz S, and Fitzgerald RD**. Influence of positive airway pressure on the pressure gradient for venous return in humans. *Journal of applied physiology (Bethesda, Md : 1985)* 88: 926-932, 2000.
47. **Kamiya A, Hayama Y, Shimizu S, and Kawada T**. State-space representation of the extended Guyton's model. *American Journal of Physiology - Heart and Circulatory Physiology* 313: H320-H322, 2017.
48. **Kohler K, Valchanov K, Nias G, and Vuylsteke A**. ECMO cannula review. *Perfusion* 28: 114-124, 2013.
49. **Krogh A**. The Regulation of the Supply of Blood to the Right Heart. *Skandinavisches Archiv Für Physiologie* 27: 227-248, 1912.
50. **Lansdorp B, Hofhuizen C, van Lavieren M, van Swieten H, Lemson J, van Putten MJ, van der Hoeven JG, and Pickkers P**. Mechanical Ventilation-Induced Intrathoracic Pressure Distribution and Heart-Lung Interactions. *Critical care medicine* 2014.
51. **Lee JM, Ogundele O, Pike F, and Pinsky MR**. Effect of acute endotoxemia on analog estimates of mean systemic pressure. *Journal of critical care* 28: 880 e889-815, 2013.
52. **Levy MN**. The cardiac and vascular factors that determine systemic blood flow. *Circulation research* 44: 739-747, 1979.
53. **Maas JJ, de Wilde RB, Aarts LP, Pinsky MR, and Jansen JR**. Determination of vascular waterfall phenomenon by bedside measurement of mean systemic filling pressure and critical closing pressure in the intensive care unit. *Anesthesia and analgesia* 114: 803-810, 2012.
54. **Maas JJ, Geerts BF, and Jansen JR**. Evaluation of mean systemic filling pressure from pulse contour cardiac output and central venous pressure. *Journal of clinical monitoring and computing* 25: 193-201, 2011.

55. **Maas JJ, Geerts BF, van den Berg PC, Pinsky MR, and Jansen JR**. Assessment of venous return curve and mean systemic filling pressure in postoperative cardiac surgery patients. *Critical care medicine* 37: 912-918, 2009.
56. **Maas JJ, Pinsky MR, Aarts LP, and Jansen JR**. Bedside assessment of total systemic vascular compliance, stressed volume, and cardiac function curves in intensive care unit patients. *Anesthesia and analgesia* 115: 880-887, 2012.
57. **Maas JJ, Pinsky MR, de Wilde RB, de Jonge E, and Jansen JR**. Cardiac output response to norepinephrine in postoperative cardiac surgery patients: interpretation with venous return and cardiac function curves. *Critical care medicine* 41: 143-150, 2013.
58. **Maas JJ, Pinsky MR, Geerts BF, de Wilde RB, and Jansen JR**. Estimation of mean systemic filling pressure in postoperative cardiac surgery patients with three methods. *Intensive care medicine* 38: 1452-1460, 2012.
59. **Magder S**. The classical Guyton view that mean systemic pressure, right atrial pressure, and venous resistance govern venous return is/is not correct. *Journal of applied physiology (Bethesda, Md : 1985)* 101: 1533, 2006.
60. **Magder S**. How Does Volume Make the Blood Go Around? 2015: 327-338, 2015.
61. **Magder S**. How to use central venous pressure measurements. *Current opinion in critical care* 11: 264-270, 2005.
62. **Magder S**. Point: the classical Guyton view that mean systemic pressure, right atrial pressure, and venous resistance govern venous return is/is not correct. *Journal of applied physiology (Bethesda, Md : 1985)* 101: 1523-1525, 2006.
63. **Magder S**. Starling resistor versus compliance. Which explains the zero-flow pressure of a dynamic arterial pressure-flow relation? *Circulation research* 67: 209-220, 1990.
64. **Magder S**. Volume and its relationship to cardiac output and venous return. *Critical care* 20: 271, 2016.
65. **Magder S, and De Varennes B**. Clinical death and the measurement of stressed vascular volume. *Critical care medicine* 26: 1061-1064, 1998.
66. **Magder S, Veerassamy S, and Bates JH**. A further analysis of why pulmonary venous pressure rises after the onset of LV dysfunction. *Journal of applied physiology (Bethesda, Md : 1985)* 106: 81-90, 2009.
67. **Millar J, Fanning JP, McDonald C, McAuley D, and Fraser J**. The inflammatory response to extracorporeal membrane oxygenation (ECMO): a review of the pathophysiology. *Critical care* 20: 2016.
68. **Mitzner W**. Hepatic outflow resistance, sinusoid pressure, and the vascular waterfall. *The American journal of physiology* 227: 513-519, 1974.

69. **Moller P, Winkler B, Hurni S, Heinisch P, Bloch A, Sondergaard S, Jakob S, Takala J, and Berger D**. Right atrial pressure and venous return during cardiopulmonary bypass. *American Journal of Physiology* 313: H408, 2017.
70. **Morgan CJ**. Use of proper statistical techniques for research studies with small samples. *American Journal Of Physiology-Lung Cellular And Molecular Physiology* 313: L873-L877, 2017.
71. **Nanas S, and Magder S**. Adaptations of the peripheral circulation to PEEP. *The American review of respiratory disease* 146: 688-693, 1992.
72. **Ogilvie RI, Zborowska-Sluis D, and Tenaschuk B**. Measurement of mean circulatory filling pressure and vascular compliance in domestic pigs. *The American journal of physiology* 258: H1925-1932, 1990.
73. **Olofsen E, Dahan A, Borsboom G, and Drummond G**. Improvements in the application and reporting of advanced Bland-Altman methods of comparison. *Journal of clinical monitoring and computing* 29: 127-139, 2015.
74. **Pang CCY**. Measurement of body venous tone. *Journal of Pharmacological and Toxicological Methods* 44: 341-360, 2000.
75. **Parkin G, Wright C, Bellomo R, and Boyce N**. Use of a mean systemic filling pressure analogue during the closed-loop control of fluid replacement in continuous hemodiafiltration. *Journal of critical care* 9: 124-133, 1994.
76. **Parkin WG**. Volume state control - a new approach. *Critical care and resuscitation : journal of the Australasian Academy of Critical Care Medicine* 1: 311-321, 1999.
77. **Parkin WG, and Leaning MS**. Therapeutic control of the circulation. *Journal of clinical monitoring and computing* 22: 391-400, 2008.
78. **Parkin WG, and Wright CA**. Three dimensional closed loop control of the human circulation. *International journal of clinical monitoring and computing* 8: 35-42, 1991.
79. **Patterson SW, and Starling EH**. On the mechanical factors which determine the output of the ventricles. *The Journal of physiology* 48: 357-379, 1914.
80. **Permutt S, and Riley RL**. Hemodynamics of Collapsible Vessels with Tone: The Vascular Waterfall. *Journal of applied physiology: respiratory, environmental and exercise physiology* 18: 924-932, 1963.
81. **Pinsky MR**. Determinants of pulmonary arterial flow variation during respiration. *Journal of applied physiology: respiratory, environmental and exercise physiology* 56: 1237-1245, 1984.
82. **Pinsky MR**. Instantaneous venous return curves in an intact canine preparation. *J Appl Physiol Respir Environ Exerc Physiol* 56: 765-771, 1984.

83. **Pinsky MR**. My paper 20 years later: Effect of positive end-expiratory pressure on right ventricular function in humans. *Intensive care medicine* 40: 935-941, 2014.
84. **Pinsky MR**. Why knowing the effects of positive-pressure ventilation on venous, pleural, and pericardial pressures is important to the bedside clinician?*. *Critical care medicine* 42: 2129-2131, 2014.
85. **Pinsky MR, Desmet JM, and Vincent JL**. Effect of positive end-expiratory pressure on right ventricular function in humans. *The American review of respiratory disease* 146: 681-687, 1992.
86. **Repessé X, Charron C, Geri G, Aubry A, Paternot A, Maizel J, Slama M, and Vieillard-Baron A**. Impact of positive pressure ventilation on mean systemic filling pressure in critically ill patients after death. *Journal of applied physiology (Bethesda, Md : 1985)* 122: 1373, 2017.
87. **Rothe CF**. Mean circulatory filling pressure: its meaning and measurement. *Journal of applied physiology (Bethesda, Md : 1985)* 74: 499-509, 1993.
88. **Sakamoto K, Saku K, Kishi T, Kakino T, Tanaka A, Sakamoto T, Ide T, and Sunagawa K**. Prediction of the impact of venoarterial extracorporeal membrane oxygenation on hemodynamics. *American journal of physiology Heart and circulatory physiology* 308: H921-930, 2015.
89. **Scher AM, and Young AC**. Servoanalysis of carotid sinus reflex effects on peripheral resistance. *Circulation research* 12: 152-162, 1963.
90. **Schipke JD, Heusch G, Sanii AP, Gams E, and Winter J**. Static filling pressure in patients during induced ventricular fibrillation. *American journal of physiology Heart and circulatory physiology* 285: H2510-2515, 2003.
91. **Stabling E**. The Arris and Bale Lectures ON SOME POINTS IN THE PATHOLOGY OF HEART DISEASE. *The Lancet* 149: 652-655, 1897.
92. **Sunagawa K, Sagawa K, and Maughan W**. Ventricular interaction with the loading system. *Annals of biomedical engineering* 12: 163-189, 1984.
93. **Trippodo NC**. Total circulatory capacity in the rat. Effects of epinephrine and vasopressin on compliance and unstressed volume. *Circulation research* 49: 923-931, 1981.
94. **Tyberg JV**. How changes in venous capacitance modulate cardiac output. *Pflugers Archiv : European journal of physiology* 445: 10-17, 2002.
95. **Van Belle G, and Fisher L**. *Biostatistics : a methodology for the health sciences*. Chichester: Chichester : Wiley-Interscience, 2004.
96. **Versprille A, and Jansen J**. Tidal variation of pulmonary blood flow and blood volume in piglets during mechanical ventilation during hyper-, normo- and hypovolaemia. *Pflügers Archiv* 424: 255-265, 1993.

97. **Versprille A, Jansen J, Drop A, and Hulsmann A**. Mean systemic filling pressure as a characteristic pressure for venous return. *Pflügers Archiv* 405: 226-233, 1985.
98. **Versprille A, Jansen JRC, Frietman RC, Hulsmann AR, and Klauw MMVD**. Negative effect of insufflation on cardiac output and pulmonary blood volume. *Acta anaesthesiologica Scandinavica* 34: 607-615, 1990.
99. **Vieillard-Baron A, Augarde R, Prin S, Page B, Beauchet A, and Jardin F**. Influence of superior vena caval zone condition on cyclic changes in right ventricular outflow during respiratory support. *Anesthesiology* 95: 1083-1088, 2001.
100. **Vieillard-Baron A, Repesse X, and Charron C**. Heart-lung interactions: have a look on the superior vena cava and on the changes in right ventricular afterload. *Critical care medicine* 43: e52, 2015.
101. **Weber E**. Über die Anwendung der Wellenlehre auf die Lehre vom Kreislauf des Blutes und Insbesondere auf die Pulslehre. *Arch Anat Physiol* 18: 497-501, 1851.
102. **Wenger RK, Bavaria JE, Ratcliffe MB, Bogen D, and Edmunds LH, Jr.** Flow dynamics of peripheral venous catheters during extracorporeal membrane oxygenation with a centrifugal pump. *The Journal of thoracic and cardiovascular surgery* 96: 478-484, 1988.
103. **Wijnberge M, Sindhunata DP, Pinsky MR, Vlaar AP, Ouweneel E, Jansen JR, Veelo DP, and Geerts BF**. Estimating mean circulatory filling pressure in clinical practice: a systematic review comparing three bedside methods in the critically ill. *Annals of intensive care* 8: 73, 2018.